

**STUDY ON THE PERFORMANCE OF CFRP
STRENGTHENED CORRODED STEEL MEMBERS**

U.N.D.Perera

168045 K

Degree of Master of Philosophy

Department of Civil Engineering

University of Moratuwa

Sri Lanka

May 2020

**STUDY ON THE PERFORMANCE OF CFRP
STRENGTHENED CORRODED STEEL MEMBERS**

Ushettige Nirosha Dilrangi Perera

168045K

Thesis submitted in partial fulfilment of the requirements for the degree Master of Philosophy

Department of Civil Engineering

University of Moratuwa

Sri Lanka

May 2020

DECLARATION

I declare that this is my own work and this thesis does not incorporate without acknowledgement any material previously submitted for a Degree or Diploma in any other University or institute of higher learning and to the best of my knowledge and belief it does not contain any material previously published or written by another person except where the acknowledgement is made in the text.

Also, I hereby grant to University of Moratuwa the non-exclusive right to reproduce and distribute my thesis, in whole or in part in print, electronic or other medium. I retain the right to use this content in whole or part in future works (such as articles or books).

Signature: ***UOM Verified Signature***

Date: 05.27.2020

The above candidate has carried out research for the MPhil thesis under my supervision.

Signature of the supervisor:

Date: 05.27.2020

ACKNOWLEDGEMENT

Throughout my years of study, I had many opportunities to explore knowledge and gather skills in research. Many parties contributed to the success of this project in many ways. I hereby acknowledge all of them and extend my heartfelt gratitude.

Foremost, I would like to express my sincere gratitude to my supervisor, Dr. J.C.P.H. Gamage, Senior Lecturer at the Department of Civil Engineering, the University of Moratuwa for her valuable guidance, instructions and patience to make this project a reality. As a woman in the Civil Engineering industry, her expertise in balancing professional life with family life has influenced me throughout and beyond.

My special thanks go to the Senate Research Grant of the University of Moratuwa (Grant no: SRC/LT/2016/19) for creating this opportunity for me by providing financial support during this research study.

I would like to convey my sincere gratitude to Prof. S.M.A. Nanayakkara and Prof. J.M.S. Bandara, former Heads of the Department, Department of Civil Engineering and Prof. S.A.S Kulathilake, Head of the Department, Department of Civil Engineering, University of Moratuwa.

I would like to thank Professor Ranjith Dissanayake, Senior Lecturer at the Department of Civil Engineering, University of Peradeniya, for the guidance provided to me as the chairperson of the progress review committee. I am grateful to Dr. Lesly Ekanayake, Senior Lecturer at the Department of Civil Engineering, University of Moratuwa, Mr. V. Sivahar, Professor of Materials Science and Engineering for the advice and support given. I am also thankful to Prof. A.A.D.A.J Perera and Prof. R.U. Halwatura, former research coordinators of Department of Civil Engineering, University of Moratuwa, for their support throughout the period.

Professional assistance was also provided by a variety of academic staff at the Department of Civil Engineering and was essential in refining our research on numerous occasions during the progress of this study. Hence my heartfelt gratitude is conveyed unto them for their sustained interest and wilful advice.

The laboratory staff of the Departments of Civil Engineering, Mechanical Engineering and Materials Science Engineering, University of Moratuwa, is also acknowledged.

Specially, Ms. C.T. Amila Perera, H.P.U. Madushan and D.M.N.L. Dissanayake are acknowledged for their kind and selfless assistance in my academic work.

I am extremely thankful for all my fellow research students, namely, Kanishka Chandrathilaka and Indunil Erandi who gave me huge support during the specimen casting and testing. Also, my fellow bachelor colleagues Erandi Ariyachandra and Manasi Wijerathne are heartfully thanked for their friendly assistance.

Airow Solutions (Pvt) Ltd is greatly appreciated for providing CFRP materials and importing the adhesive materials on time. Mr. François Petiteau, the Sales Engineer at Digital Surf, is also acknowledged for his guidance given on using MountainsMap software.

Finally, I would like to thank my husband, Hareendra Herath, for his understanding, unfailing support and the encouragement throughout. Also, my mother, father and sister who always stood by the side with me and my friends for their kind assistance, blessings and encouragement when it was most required.

ABSTRACT

Most of the metallic structures such as offshore platforms and railway bridges are now in the need of retrofitting due to corrosion. One of the efficient ways of strengthening these structures is by using (Carbon Fibre Reinforced Polymer) CFRP materials. Since the weakest link in this system is the bond between the adherends, the effect of pre-corrosion level of the steel elements on the bond characteristics and durability performance of the strengthened units should be properly evaluated. Even though there are many research studies on bond durability none of them has used corroded steel plates for bond strength evaluation and considered the inherent surface characteristics of the corroded steel surfaces. Therefore, this study aimed at investigating the bond performance of CFRP bonded corroded steel plates which are subjected to different ageing conditions and surface roughness characteristics.

A total of one hundred and twenty-eight conditioned and non-conditioned double strap joint specimens were tested. Both corroded and non-corroded steel plates and two different surface preparation methods were used to witness the importance of the surface texture properties. Scanning Electronic Microscopic (SEM) analysis was carried out to determine the surface characteristic properties of the corroded/non-corroded steel plates. The short-term bond performance was evaluated along with different bonding configurations. In the long-term analysis, six different environmental exposures; seawater, wet/dry cycles, open tropical environment, and distilled water at three different temperature levels, 25 °C -30 °C, 40 °C and 3 °C were considered for conditioning. Residual bond strengths of the conditioned test specimens were evaluated after 6- and 12-month exposure periods at ambient temperature. A numerical model was developed to estimate the stress-strain variation of CFRP/steel specimens along the bond line. Bond-slip curves were evaluated to estimate the interfacial fracture energy of CFRP/steel composites. Moreover, experimental results were compared with the analytical results obtained from Hart-Smith model and a theoretical relationship between the failure modes was derived.

Test results indicated a major influence of surface roughness on the long-term performance of CFRP/steel joints. CFRP strengthened corroded steel joints showed a residual bond capacity of about 90% in seawater immersion and 111% in tropical environmental condition suggesting its suitability to adopt CFRP technique in these exposures. After 12 months of exposure duration, a similar bond degradation was observed of about 31% in distilled water immersed specimens at ambient temperature and about 60% in dry/wet cyclic condition irrespective of the pre-corrosion level. During an exposure period of 12 months, the rate of bond degradation was found to be less than 20% for cold water immersed specimens with non-corroded steel plates. The interfacial fracture energy of CFRP/steel composites exposed to hot humid environments indicated a significant reduction of 78% compared to control test specimens.

Keywords: *CFRP/Steel, Double strap joints, Corroded steel, Bond performance, Environmental durability*

TABLE OF CONTENTS

	Page
DECLARATION	i
ACKNOWLEDGEMENT	ii
ABSTRACT	iv
TABLE OF CONTENTS	v
LIST OF FIGURES	x
LIST OF TABLES	xv
LIST OF ABBREVIATIONS	xvii
1 INTRODUCTION	1
1.1 Background	1
1.2 The aim and objectives	3
1.3 Layout of the Thesis	4
2 LITERATURE REVIEW	7
2.1 General	7
2.2 Strengthening steel structures using CFRP	7
2.2.1 Material Characteristics	8
2.2.2 Available Codes and Guidelines	11
2.2.3 Real World Applications	11
2.2.4 Bonding Techniques	14
2.2.5 Limitations in CFRP application in steel structures	16
2.3 Strengthening steel elements subjected to corrosion using CFRP	16
2.3.1 Introduction to corrosion	16
2.3.2 Galvanic Corrosion	17
2.3.3 Application of CFRP in corroded steel elements	18
2.4 Bond Performance of Steel/CFRP Joints	21
2.4.1 Force Transfer between the metal substrate, CFRP and adhesive	21
2.4.2 Failure Modes	21
2.4.3 Durability of the Bond	23
2.4.4 Evaluation of Bond Strength	29
2.4.5 Bond Testing Methods	33

2.5	Research Gap and Summary	35
3	MATERIAL PROPERTIES	37
3.1	Introduction	37
3.2	CFRP Wrap	38
3.2.1	General	38
3.2.2	Manufacturer Specified Properties	38
3.2.3	Measured Properties	38
3.3	Adhesive	42
3.3.1	General	42
3.3.2	Manufacturer Specified Properties	42
3.3.3	Measured Properties	43
3.4	Steel	45
3.4.1	General	45
3.4.2	Measured Properties	45
3.5	Summary	48
4	SEM ANALYSIS ON THE SURFACE MORPHOLOGY OF CORRODED STEEL SURFACES	49
4.1	Introduction	49
4.2	Surface Morphology	51
4.2.1	SEM stereo – imaging	51
4.2.2	Acquisition of the roughness parameters using 3D reconstruction	52
4.2.2.1	Evaluating the surface roughness parameters	52
4.2.2.2	Evaluating the profile roughness parameters	57
4.3	Surface Metrology	58
4.3.1	General	58
4.3.2	Profile and aerial field parameters	58
4.4	Summary	60
5	EXPERIMENTAL PROGRAMME	61
5.1	Introduction	61
5.2	Specimen Preparation and Instrumentation	61
5.2.1	General	62
5.2.2	Surface Preparation	63

5.2.3	Preparation of Double Strap Joints	63
5.3	Preliminary Investigation	65
5.3.1	Effective Bond Length	65
5.4	Detailed Investigation	67
5.5	Summary	68
6	SHORT TERM BOND PERFORMANCE OF CFRP STRENGTHENED CORRODED STEEL PLATES	69
6.1	Introduction	69
6.2	Materials, experimental programme and test set up	69
6.2.1	Materials	69
6.2.2	Specimen preparation, instrumentation and testing	70
6.2.3	Profile roughness parameters	70
6.3	Test Results	71
6.3.1	Ultimate bond strength	71
6.3.2	The effect of surface roughness properties	73
6.3.3	Stain variation along the CFRP bonded length	76
6.3.4	Failure modes	77
6.4	Summary	78
7	EFFECTS OF BONDING TECHNIQUES OF CFRP STRENGTHENED CORRODED STEEL PLATES ON SHORT TERM PERFORMANCE	80
7.1	Introduction	80
7.2	Materials, experimental programme and test set up	81
7.2.1	Materials	81
7.2.2	Specimen preparation	81
7.2.3	Bonding configurations	83
7.3	Test results	84
7.3.1	Ultimate bond strength	84
7.3.2	Strain variation along the CFRP bonded length	86
7.3.3	The effect of surface roughness parameters	86
7.3.4	Failure modes	87
7.4	Summary	88

8	LONG TERM BOND PERFORMANCE OF CFRP STRENGTHENED CORRODED STEEL PLATES	90
8.1	Introduction	90
8.2	Materials	90
8.3	Experimental Programme and test set up	91
8.3.1	Specimen Preparation	91
8.3.2	Environmental Conditioning	91
8.4	Test Results	95
8.4.1	Behaviour in sea water	95
8.4.2	Behaviour in distilled water under different temperatures	98
8.4.3	Behaviour in tropical environmental exposure	100
8.4.4	Behaviour in dry/wet conditions	101
8.4.5	Failure modes	102
8.4.6	The effect of surface roughness parameters	105
8.4.7	Comparison to existing guidelines and literature	107
8.5	Summary	109
9	THEORETICAL/NUMERICAL MODELLING	111
9.1	Introduction	111
9.2	Theoretical modelling	111
9.2.1	Short-term bond performance – Joint strength degradation	111
9.2.2	Long-term bond performance – seawater and distilled water immersed conditions at ambient temperature	114
9.2.2.1	Material degradation	114
9.2.2.2	The time-dependent effective bond length	116
9.2.2.3	The joint strength degradation	118
9.3	Numerical analysis	121
9.3.1	Validation of the model	123
9.3.2	Bond slip relationships	123
9.3.3	Interfacial fracture energy	127
9.4	Summary	128
10	CONCLUSIONS AND RECOMMENDATIONS	129
10.1	Research Summary	129

10.2	Conclusions and recommendations	129
10.3	Limitations	133
10.4	Future research	133
	REFERENCES	134
	APPENDIX A – LIST OF PUBLICATIONS	144

LIST OF FIGURES

	Page
Figure 1.1: Layout of the thesis	04
Figure 2.1: Different forms of CFRP (a) Fabric (b) Rods (c) Strip	08
Figure 2.2: Mechanical Properties of different materials (a) Elastic Modulus (b) Stress–strain behaviour	09
Figure 2.3: Typical location of corrosion on a steel girder bridge	19
Figure 2.4: Failure modes of an FRP strengthened steel member	22
Figure 2.5: types of debonding in FRP strengthened steel members	23
Figure 2.6: Geometric discontinuities causing stress concentrations	29
Figure 2.7: Bond Slip Relationship by Xia and Teng	32
Figure 2.8: Bond Slip Model by Dehgani et al (2012)	32
Figure 2.9: Four-Point Bending Testing Arrangement	33
Figure 2.10: (a) Single lap joint (b) Double lap joint	34
Figure 2.11: Double Strap Joint (a) Side view (b) Plan view	34
Figure 2.12: (a) Butt – Joint test specimen and (b) Pull – off test specimen	34
Figure 3.1: The general procedure of the material testing programme	37
Figure 3.2: Schematic diagram of a CFRP coupon test specimen (a) Plan view (b) side view	39
Figure 3.3: Test setup of a CFRP test coupon specimen	39
Figure 3.4: Failure mode (Edge Delamination in the Middle Gauge area) of CFRP coupon test specimens	40
Figure 3.5: Stress – strain curves of CFRP test samples	41

Figure 3.6: Araldite 420A/B (resin/hardener) adhesive	42
Figure 3.7: Dimensions of an adhesive coupon specimen	43
Figure 3.8 (a): Adhesive test sample with attached strain gauges	44
Figure 3.8 (b): Test setup of an adhesive coupon	44
Figure 3.9: The failure mode of an adhesive coupon	45
Figure 3.10: Scanning Electron Microscopic (SEM) Images of Rust Levels (i) A (ii) B (iii) C and (iv) D	46
Figure 3.11: (a) A Steel Coupon (Schematic diagram, not in scale) (b) A prepared steel coupon with strain gauges attached in the middle	46
Figure 3.12: Failure mode of steel coupons	47
Figure 3.13: Stress – Strain curves obtained from steel samples of Corrosion level A, B, C and D	47
Figure 4.1: sampling wavelength (a) Profile roughness parameters (b) Area roughness parameters	50
Figure 4.2: Scanning Electronic Microscope	52
Figure 4.3: The scale operator	53
Figure 4.4: 3D stereoscopic reconstruction	54
Figure 4.5: A 3D reconstructed image (a) Pseudo-colour view (b) 3D view	54
Figure 4.6: Levelling the surface using the Least Square Method	55
Figure 4.7: Form removal	55
Figure 4.8: Using the standard filter (Gaussian filter, cut-off length = 0.8 mm)	56
Figure 4.9: Extracted profile curve obtained for a corroded steel plate (Corrosion level (B)) before surface preparation	57
Figure 4.10: Variation of Sa with respect to the level of corrosion	58

Figure 4.11: Variation of Sa with respect to the level of corrosion	59
Figure 4.12: The effect of surface preparation by M-01 method (a) Non – corroded steel (b) Corroded steel	60
Figure 5.1: Summary of the experimental programme	61
Figure 5.2: Visual images of Rust Levels (i) A (ii) B (iii) C and (iv) D	62
Figure 5.3: Scanning Electron Microscopic (SEM) Images of Rust Levels (i) A (ii) B (iii) C and (iv) D	62
Figure 5.4: Corrosion level (C) samples after the surface preparation (a) M – 01 (b) M – 02	63
Figure 5.5: X – Wrap Primer (X – Calibur Structural Systems) (i) Base (ii) Hardener	64
Figure 5.6: Schematic diagram of a double strap joint	64
Figure 5.7: Prepared test specimen of a double strap joint	64
Figure 5.8: Universal Testing Machine	65
Figure 5.9: Double strap joints with unequal bond lengths	66
Figure 5.10: Average load at failure Vs. CFRP bond length	67
Figure 5.11: Flowchart of the programme for the detail investigation	67
Figure 6.1: Variation of joint strength with the level of corrosion	73
Figure 6.2: Variation of surface roughness measures with respect to the corrosion level	74
Fig 6.3: Variation of Joint strength with the Ra	75
Fig 6.4: Variation of Joint strength with the Sa	75
Figure 6.5: Schematic view of a double strap joint and the locations of the strain gauges	76

Figure 6.6: Strain variation in CFRP/Steel joint a)35 mm b)90 mm away from the joint	77
Figure 6.7: Failure modes observed for the specimens	78
Figure 7.1: Schematic diagram of a double strap joint and the location of strain gauges	82
Figure 7.2: (a & b) corroded plate before and after surface preparation, (c & d) relevant SEM images, respectively	82
Figure 7.3: Bonding Configurations	83
Figure 7.4: Samples prepared with (a) “P” type, (b) “PC” type, (c) “G” type and (d) “GC” type bonding configurations	84
Figure 7.5: Stain variation of double strap joints	86
Figure 7.6: Failure modes observed for bonding configurations; (a1,2) “P” type, (b) “C” type, (c) “PC” type, (d) “G” type, (e) “GC” type and (f) “GCG” type	88
Figure 8.1: Specimens immersed in simulated sea water condition	92
Figure 8.2: Samples immersed in distilled water at room temperature (25 °C - 30 °C)	93
Figure 8.3: Samples immersed in distilled water at 40 °C	93
Figure 8.4: Samples immersed in distilled water at 3 °C	93
Figure 8.5: Samples exposed to tropical environmental condition	94
Figure 8.6: Samples subjected to dry/wet condition – in a 5% NaCl solution (Wet condition)	94
Figure 8.7: Variation of average joint strength with the exposure condition	96
Figure 8.8: Normalized joint strength of DW samples	99
Figure 8.9: Normalized joint strength of DW - CW samples	99

Figure 8.10: Joint strength variation of conditioned samples immersed in distilled water after 6 months	100
Figure 8.11 Failed specimens of all exposure conditions after 6 months	105
Figure 8.12: Joint strength variation with the quality of substrate (6 months)	106
Figure 9.1: Comparison of the experimental and the theoretical model results	114
Fig. 9.2 Normalized degradation behaviour of mechanical properties of adhesive in sea water and distilled water at ambient temperature (a) Tensile Strength (ft,a) (b) Elastic modulus (Ea)	115
Figure 9.3 Variation of effective bond length over time in DW and SW conditions	117
Figure 9.4 Comparison of experimental and model predicted joint strength degradation over time (a) DW condition (b) SW condition	120
Figure 9.5: (a) Boundary conditions and (b) FE mesh used in the numerical analysis	121
Figure 9.6: The behavioural variation in adhesive properties with respect to the type of conditioning and the exposure duration	122
Figure 9.7 Comparison of numerical and experimental failure loads	123
Figure 9.8. Bi-linear bond-slip curve	124
Fig. 9.9 Bond-slip curves of specimens with steel (a) NDM1 (b) NDM2 (c) DM1 (d) DM2	126
Fig. 9.10. (a) Determination of fracture energy using bond-slip curves (b) Estimated fracture energies of the test specimens	127

LIST OF TABLES

	Page
Table 2.1: Moduli of Elasticity of CFRP (Perera & Gamage, 2016)	09
Table 2.2: Advantages/Disadvantages of CFRP	10
Table 2.3: Typical values of measured material properties of adhesives in tension (X.-L. Zhao, 2013)	10
Table 2.4 : Available codes/guidelines/state-of-the-art-reviews	12
Table 3.1: Laboratory test data provided by the manufacturer (X-Calibur Construction Chemistry Inc.)	38
Table 3.2: Measured material properties of CFRP coupons	41
Table 3.3: Manufacturer (Huntsman Advanced Materials) specified material properties	43
Table 3.4: Mechanical properties of steel samples	48
Table 4.1: Parameters table obtained according to ISO 25178	56
Table 4.2: Parameters table obtained according to ISO 4287	57
Table 4.3: Profile Parameters (ISO 4287)	58
Table 4.4: Areal Field Parameters (ISO 25178)	59
Table 5.1: Test results obtained for effective bond length investigation	66
Table 6.1: Test configuration of the experimental programme	71
Table 6.2: Short term bond testing results	72
Table 7.1: Material Properties	81
Table 7.2: Bond strength results	85
Table 8.1: Water quality properties of distilled water	92

Table 8.2: Weather summary in Colombo (data taken from timeanddate.com	95
Table 8.3: Long term test results	97
Table 8.4: Failure modes of samples exposed for 6 months duration	102
Table 8.5: Proposed Environmental durability design factors (based on the strength results obtained after 12 months exposure duration)	109
Table 9.1: Table of Data	112
Table 9.2: Layer thicknesses in the CFRP / Steel joint	113

LIST OF ABBREVIATIONS

Abbreviation	Description
ACI	American Concrete Institute
ASTM	American Society for Testing and Materials
CFRP	Carbon Fibre Reinforced Polymer
CL(A)	Corrosion Level (A)
CL(B)	Corrosion Level (A)
CL(C)	Corrosion Level (A)
CL(D)	Corrosion Level (A)
DM1	Deteriorated steel surface prepared with M-01
DM2	Deteriorated steel surface prepared with M-02
DW	Distilled water immersion at ambient temperature
DW-CW	Distilled water immersion at cold weather
DW-HW	Distilled water immersion at hot weather
FE	Finite Element
FEA	Finite Element Analysis
FEM	Finite Element Modelling
FRP	Fibre Reinforced Polymer
GFRP	Glass Fibre Reinforced Polymer
HDT	Heat Distortion Temperature
HM	High Modulus
LEFM	Linear Elastic Fracture Mechanics
LM	Low Modulus
LVDT	Linear Variable Differential Transformers
NDM1	Non-deteriorated steel surface prepared with M-01
NDM2	Non-deteriorated steel surface prepared with M-01
NM	Normal Modulus
UHM	Ultra-High Modulus
SEM	Scanning Electronic Microscope
SERR	Strain Energy Release Rate
SET	Surface Exposure Time

CHAPTER 01

INTRODUCTION

1.1 Background

The need for retrofitting/rehabilitating metallic structures such as offshore platforms and railway/highway bridges has been a major concern nowadays as most of them are either exceeding or close to their design lifetime. There are numerous serviceability issues encountered in these types of structures in Sri Lanka as well as in the whole parts of the world like Europe, Japan, Australia, USA etc. (Bocciarelli, Colombi, Fava, & Poggi, 2009b). Being exposed to various environmental conditions like corrosive atmosphere, increased loading conditions than they have been designed, poor workmanship in construction, poor maintenance, deficiencies in the structural design stage, vehicular impacts and cyclic load variations, have caused these structures to worsen their structural degradation (Bocciarelli, Colombi, Fava, & Poggi, 2009a; Hollaway & Cadei, 2002). Among the various reasons mentioned above, repairing corroded steel structures has become one of the major concerns in the field (Rahgozar, 2009). Bridges with adverse environmental exposure, offshore platforms and marine structures often find corrosion as one of the major hindrances for their structural integrity. Corrosion tends to lose the operational quality of these structures with the reduced stiffness and the member capacities and it always puts public safety into risk by being unable to predict the life expectancy of the structure (Elchalakani, 2016).

The most common remedy for corroded steel structures is to replace the whole/part of the structure. However, strengthening can be chosen over partial/complete reconstruction due to the less cost, time and space involved and minimum functional disturbances. Apart from that, some of these old structures are national icons and bear historical importance in which the demolition is prohibited. The most common traditional techniques of retrofitting used to be external post-tensioning, replacing the damaged structural elements and attachment of steel plates into the required metallic substrate by the methods of welding, bolting or clamping (Al-Mosawe, Al-Mahaidi, & Zhao, 2013). These methods discover several drawbacks such as difficulties in transportation and installation of heavy steel plates, more time engaged, the

requirement of falsework/formwork, corrosion and additional weight introduced to the structure, etc. (Hollaway & Cadei, 2002; Tavakkolizadeh & Saadatmanesh, 2001). Hence, it has become a major requirement to develop an effective solution in adopting an efficient strengthening system.

Nowadays, Carbon Fibre Reinforced Polymer (CFRP) materials are known to be one of the efficient means of strengthening deteriorated structures. Because of its favourable physical and mechanical properties like high strength/weight proportion, superior resistant capacities to corrosion, fatigue and weathering and flexibility in different structural forms, etc., CFRP can be found as the best available alternative to get rid of the aforementioned drawbacks of the conventional methods.

Although usage of CFRP composites in steel structures has not been advanced much yet, this has been successfully used in retrofitting concrete structures for some time with the developed standards and regulations (ACI Committee, 2008). Direct substitution of these results is not applicable for retrofitting steel structures because of the disparate failure scenarios of steel compared to concrete. According to the literature, the dominant failure mode of FRP – Concrete composite system is the cohesive failure of the concrete substrate while it is mostly the failure of the adhesive-steel interface in the FRP – Steel system (Perera & Gamage, 2016). Therefore, the reliability of this technique adopted in the FRP - Steel system is highly dependent on the bond behaviour between the steel substrate and the CFRP fibre composite. Therefore, the research studies on evaluation of bond performance has become an interesting topic among the studies based on CFRP strengthening technique.

Since the corrosion can heavily damage the substrate properties of the steel substrate, proper awareness of optimum surface characteristics is a must to ensure a durable bond capacity in the CFRP strengthened corroded steel system. The majority of the research studies conducted on the assessment of durability performance of the CFRP/Steel system used CFRP strengthened non - corroded steel plates. Attention on the substrate properties on bond characteristics is also less. The consequences of strengthening already corroded members with CFRP materials may be different from the behaviour of the CFRP strengthened non – corroded steel members due to the presence of increased surface irregularities in the corroded steel surface. Usage of a notch or

reducing the thickness of the plate to simulate the corrosion effect (Deng, Jia, & Zheng, 2016) may not reflect the real performance.

1.2 The aim and objectives

The study aimed to is to evaluate the effectiveness of using CFRP composite patches in corroded steel structural elements by examining the bonding effects of CFRP/Steel joints. The preferred application should be able to prevent further progression of corrosion, increase the life cycle of the structure and decrease the maintenance cost required in its operational stage. Hence, determining the characteristics of corroded steel substrate surfaces and level of surface preparation required to enhance the bonding strength, identifying the most appropriate bonding technique to be adopted and the effects of different environmental exposures on bond strength degradation, and developing a theoretical / analytical model to predict the bond performance are the key aspects to be addressed in this project. The main objectives of the current research project are summarized below.

1. Understanding the effects of corrosion on service performance and bond characteristics between CFRP and steel. In order to assess the bond performance of a CFRP strengthened steel substrate, it is essential to study the possible corrosion levels and its consequences on structural members, surface energy remained and available analysis methods to enhance the bond performance.
2. Experimental study on the bond performance between CFRP and corroded metallic surfaces, taking into account the parameters such as level of corrosion, level of surface preparation, bonding technique and long-term durability performance under accelerated corroded nature, natural outside environment, water immersed conditions and marine conditions.
3. Theoretical study and developing an energy/fracture mechanics-based model to predict bond performance of CFRP/steel composites. The existing models which have been developed in bond strength evaluation have considered only defects free steel surfaces. The potential surface energy reductions and the adhesion strength decrements due to corroded steel surfaces are to be taken into consider in improving the current theoretical models. Further, bond-slip models to identify the fracture load of the strengthening system are to be advanced when the substrates are defected.

4. Proposing design recommendations on strengthening corroded steel structures using CFRP.

1.3 Layout of the thesis

This thesis is written to remark the investigation carried out in determining the bond characteristics of CFRP composites bonded with deteriorated steel members. This has been spread out of 10 chapters and its layout is summarized in the following organizational chart (Figure 1.1).

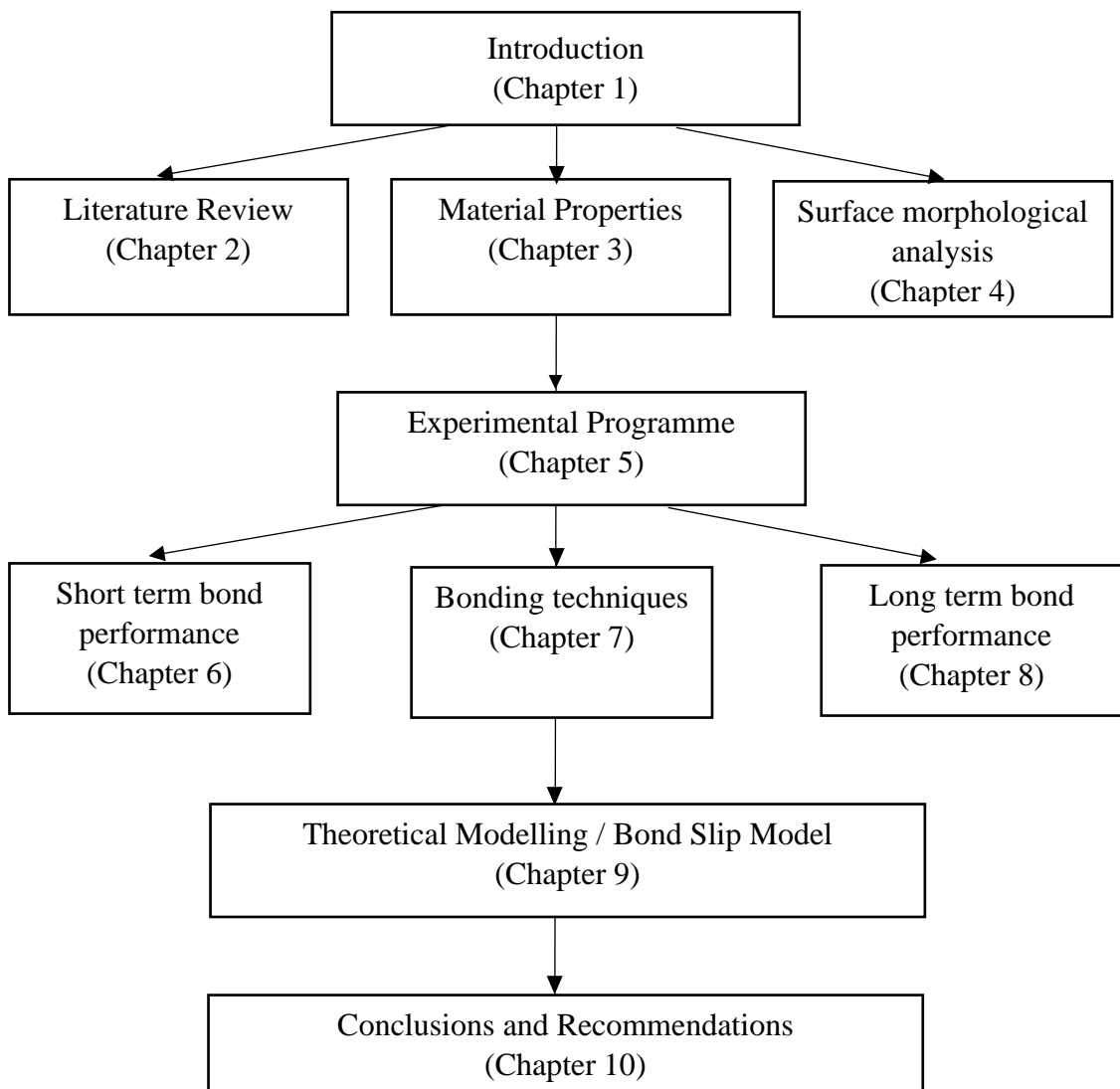


Figure 1.1: Layout of the thesis

As an introduction, a brief background study about the related research area is presented in this first chapter. Then the objectives of the study are specified along with the problem statement.

In the second chapter, a thorough knowledge of the CFRP/ steel strengthening system is summarized based on the literature reviewed by the author. The focus is mainly on the application of the CFRP composites in corroded steel surfaces. Thus, concise information on general forms of corrosion is provided. Moreover, the current knowledge acquired on the bond performance of CFRP/steel is described. The attention is given on how the force is transferred between the metal substrate and the CFRP layer and between the metal substrate and the adhesive, the failure modes of CFRP/Steel joints, bond durability when subjected to various environmental and loading conditions and the available methods of bond strength evaluation. Finally, the research gap identified in the present study is noted.

Chapter 3 is about the materials used in the experimental program of the present study. A brief about the material's physical/mechanical characteristics are pictured on each matter. Both measured and manufacturer specified material properties, identified by tensile coupon tests are described.

CHAPTER 4 describes the scanning electronic microscopic analysis carried out to identify the surface roughness properties of the corroded steel substrates. The concept of surface morphological analysis, instrumentation, steps taken in the quantitative analysis and the obtained roughness measures are detailed in this chapter.

Chapter 5 presents the experimental programme carried out on bond performance evaluation of CFRP/steel metallic joints. The test series is divided into two sections as preliminary and detailed investigation. For both investigations, double strap joint specimens were used, and its method of preparation is described hereby. During the preliminary investigation, the effective bond length is determined. Under the detailed investigation, how the test series is designed to determine the short term and long-term bond performance is introduced. Each test data is presented more informatively in the next chapters for clarity.

CHAPTER 6 explains about the test series, which evaluates the short-term bond performance of the CFRP strengthened corroded steel plates. Material usage, test setup and the procedure are briefly described. Test results are elaborated based on the ultimate bond strength, strain variation along the CFRP bonded length, effects of surface roughness properties and the failure modes.

CHAPTER 7 is about the experimental series carried out to determine the effects of bonding techniques of CFRP strengthened corroded steel plates on short term bonding performance. Usage of the materials, test setup and the different bonding configurations chosen to assess the short-term bond performance are described. Discussion of the results is presented comparing the ultimate bond strengths, strain variation, effects of surface roughness and the failure modes of each bond configuration.

CHAPTER 8 thoroughly describes the bond testing series adapted in long-term bond performance evaluation of CFRP/Steel joints under various environmental conditions. Six conditioning variations were adopted, and the bond strengths were obtained after 6 and 12 months of exposure durations. Bond behavioural variations under all conditioning types are well-discussed along with the strain variation, failure modes and the influence of the surface roughness characteristics. Finally, a comparison has been made on the proposed durability factors with the factors introduced in the existing guidelines/literature.

CHAPTER 9 includes the investigation carried out through theoretical modelling and the numerical modelling. One of the existing theoretical models was used to justify the results obtained in the experimental study. A numerical analysis also had been carried using a Finite Element Modelling software and the bond behaviour was studied.

CHAPTER 10 summarizes the conclusions and the recommendations based on the results obtained from the experimental, numerical and the theoretical studies.

CHAPTER 2

LITERATURE REVIEW

2.1 General

The use of advanced composite materials goes its way back to World War II and is being used successfully in structural applications for more than 60 years. CFRP (Carbon Fibre Reinforced Polymer) is proven to be very effective in the strengthening process which has been widely used in other areas like military, aerospace, and naval industries. Most of its structural applications are limited to reinforced concrete constructions and the present day interest is being arisen to find out the applicability of the CFRP materials in strengthening steel structures (Fawzia, 2007).

The literature available in this extent of CFRP strengthened steel structures can be categorized into several sections as follows.

- Evaluating bond performance between CFRP and metallic surface
- The influence of different loading conditions [static (tension, compression, etc.) and dynamic (fatigue/impact/earthquake loading etc.)] on CFRP strengthened steel substrates
- The influence of different environmental conditions / Durability performance evaluation (exposed temperature variations, humidity and moisture variations, marine conditions, effect of Ultraviolet radiation etc.): short term and long-term influence
- Design guidelines and state-of-the-art-review papers in the area

2.2 Strengthening steel structures using CFRP

The need for strengthening steel structures like offshore platforms, bridges and buildings has become more important at the present time. There is plenty of evidence available in many countries showing that most of these structures are required to be retrofitted / repaired. A recent survey carried out in the Europe has identified that more than 70% of the metallic bridges in their countries have exceeded 50 years of age. Federal Highway Administration (FHWA) of the US Department of Transportation has estimated the number of metallic highway bridges in need of repair is about 40%. (Bocciarelli, Colombi, Fava, & Poggi, 2009b). The other countries like Canada, Japan and Australia etc. are also experiencing the same circumstances.

Restoration of the damaged steel infrastructures is required because of several reasons like

to increase the load capacity and stiffness of the structure, re-gain strength due to loss of materials as a result of corrosion/ impact loadings and/or material degradation, extend the fatigue life and rectify design/construction errors (Stratford, T; Cadei, J; Hollaway, 2004). In order to overcome the drawbacks encountered in the conventional strengthening methods, the use of CFRP composite is adopted considering its excellent physical and mechanical characteristics. Generally, the joint between the CFRP and the strengthening substrate is attained by adhesive/epoxy bonding these two different materials. Bolting is not preferred as it contributes for the crack initiation when steel is subjected to cyclic/fatigue loads and susceptible for crevice corrosion. Likewise, adhesive bonded joints are chosen over other mechanical fastening methods to achieve a uniform stress distribution throughout the area and eliminate local stress concentrations.

2.2.1 Material Characteristics

CFRP (Carbon Fibre Reinforced Polymer)

ACI 440.2R-8 defines CFRP as a composite material which is made of a polymer matrix reinforced with carbon fibre (ACI Committee, 2008). Fibres are the load bearing portion of the composite while the matrix protects against effects such as abrasion and environmental corrosion to bind the fibres together and distribute the load. Thus, the physical properties of FRP depend on the resin or polymer and the mechanical strength of the composite is provided by the reinforcement. To improve the properties of the FRP material, fillers and additives can be used as the performance aids.



Figure 2.1: Different forms of CFRP (a) Fabric (b) Rods (c) Strips

CFRP sheets/fabric, laminates/strips and rods/bars (Figure 2.1) are the frequently used FRP forms in the strengthening process of steel. CFRP materials can be categorized based on the modulus of the elasticity (Table 2.1). Figure 2.2 compares the mechanical properties of CFRP material with the other available structural materials. Advantages and disadvantages of using CFRP are summarized in the Table 2.2.

Table 2.1: Moduli of Elasticity of CFRP (Perera & Gamage, 2016)

Form of CFRP	Modulus of Elasticity (GPa)	
CFRP Sheets (230–640 GPa) (X. L. Zhao & Zhang, 2007)	Low Modulus (LM) CFRP:	< 100 GPa ($E_{cfpr} < 0.5 E_{steel}$)
	Normal Modulus (NM) CFRP	100 – 200 GPa ($0.5 E_{steel} < E_{cfpr} < E_{steel}$)
	High Modulus (HM) CFRP	200 – 400 GPa ($E_{steel} < E_{cfpr} < 2 E_{steel}$)
	Ultra – High Modulus (UHM) CFRP	≥ 400 GPa ($\geq 2 E_{steel}$)
CFRP laminates (Ghafoori, Motavalli, Zhao, Nussbaumer, & Fontana, 2015)	Normal Modulus (NM) CFRP	100 – 250 GPa
	High Modulus (HM) CFRP	> 250 GPa

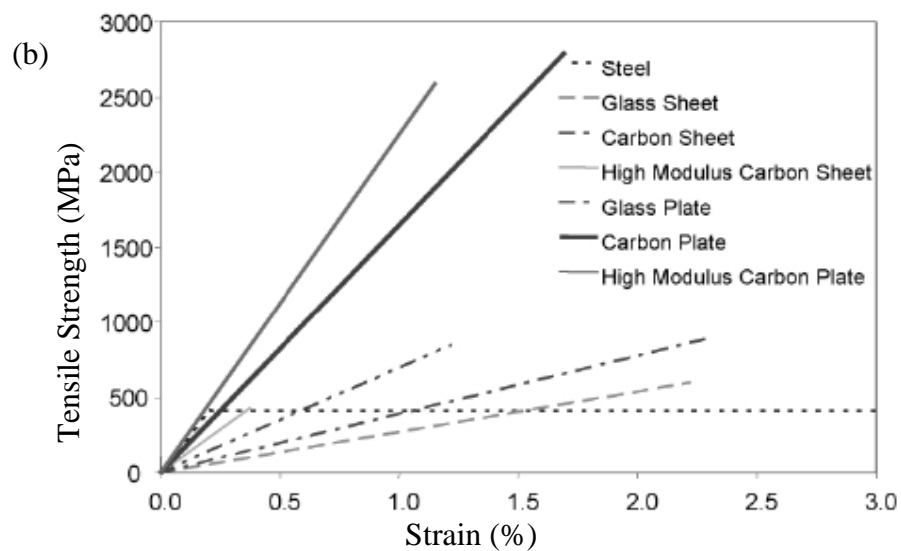
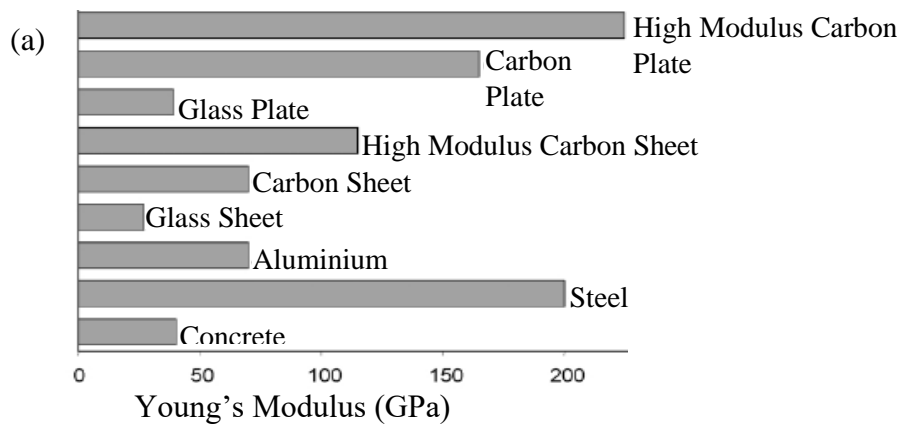


Figure 2.2: Mechanical Properties of different materials (a) Elastic Modulus (b) Stress – strain behaviour (Buyukozturk, O.; Gunes, O.; Karaca, 2004)

Table 2.2: Advantages/Disadvantages of CFRP

Advantages	Disadvantages
<ul style="list-style-type: none"> • High strength/stiffness ratio • Flexibility in different shapes • High wear resistant capacity • High corrosion resistant capacity • High fatigue resistant capacity • Ease of handling 	<ul style="list-style-type: none"> • High initial cost • Advanced design procedure • Lack of design guidelines • Complicated load paths • Brittle failure • Difficulties in damage evaluation

Adhesive

Depending on the molecular behaviour of the polymers, adhesives can be categorized into 2 groups; Thermosetting type (most common) or Thermoplastic type. Most of the field applications are based on thermosetting type adhesives. For this type of resins, heat distortion temperature (HDT) and the glass transition temperature (T_g) are the important measures which can identify adhesive softening. Epoxies are the most common thermoset resin type used in FRP application. Other than the epoxies, the other available thermoset resin types are unsaturated polyesters, vinyl esters and phenolic.

Table 2.3: Measured material properties of different adhesives types in tension

(X.-L. Zhao, 2013)

Adhesive	Modulus of Elasticity (MPa)	Ultimate tensile strength (MPa)	Ultimate tensile strain (%)	Reference
Araldite 2015	1,750	14.7	1.51	(Fernando, Yu, Teng, & Zhao, 2009)
Araldite 420	1,828	21.15	2.89	
FIFE - Tyfo	3,975	40.7	1.11	
Sikadur 30	11,250	22.3	0.30	(Fawzia, 2007)
Sikadur 330	4,820	31.3	0.75	
Araldite 420	1,901	28.6	2.40	
Sikadur 30	9,282	24.0	0.30	

The main purpose of adhesive is to provide a shear load path between the strengthening substrate and the composite material so that the full composite action may develop in the end product. Thus, it is essential to be concerned about the quality control during the installation process for the service and strength performance. Understanding the important adhesive material properties such as modulus of elasticity and ultimate tensile strain etc. is

also essential. The following Table 2.3 summarizes the material properties of some of the generally used adhesive types, in practice (X.-L. Zhao, 2013).

2.2.2 Available Codes and Guidelines

Even though there are reasonable amounts of design codes and guidelines available with respect to the design of CFRP/concrete strengthening, it is quite a few amounts for CFRP / Steel joints. Several researchers have published state-of-the-art-review papers summarizing all the scattered information published throughout (Table 2.4).

2.2.3 Real World Applications

Even though using CFRP composites in strengthening steel structures is not so widespread, there are some of its real-world applications cited for bridge structures. In 2001, two case studies were published by Dr. Sam Luke to address strengthening of two metallic bridges in the UK; Hythe bridge in Oxford (a cast iron bridge) and Slattocks Canal bridge in Rochdale (an early rolled steel bridge), using CFRP plates. Both structures were having historically important features and its location restricted them by demolishing and replacing. The latter was externally reinforced with CFRP strips while the former was strengthened with CFRP strips which were pre-stressed (Luke, 2001).

Another two numbers of existing steel girder bridges were strengthened utilizing CFRP composite materials in the USA. One was a steel girder-bridge (number 3903.0S 141) in Guthrie County, Iowa, on State Highway 141, USA and post-tensioned CFRP strands were used as the strengthening material. The other steel bridge was a continuous I-beam girder bridge (number 7838.5S092) in Pottawattamie County, Iowa, on State Highway 92, USA where CFRP strips were used (Phares, Wipf, Klaiber, Abu-Hawash, & Lee, 2003). Similarly, the Action Bridge, a steel bridge on the London underground, which has also been strengthened using Ultra High Modulus CFRP plates and it was able to confirm that this method is an effective and a predictable approach (Moy & Bloodworth, 2007).

Table 2.4 : Available codes/guidelines/state-of-the-art-reviews

Title of the Code/ Guideline/ Review paper	Author(s)/Year	Published in	Significance
• “ICE design and practice guide FRP composites”	S S J Moy (2001)	ICE (Institution of Civil Engineers, UK)	Consists analysis process, composite ad structural design and implementation of the strengthening system
• “Progress in the technique of upgrading metallic structures with advanced polymer composites”	L C Hollaway, J Cadei (2002)	Progress in Structural Engineering Materials	Reviews the problems encountered in bonding plates into metallic structures
• “Durability Gap Analysis for fiber – reinforced polymer composites in civil infrastructure”	V M Karbhari, W Chin, Hunston, B Benmokrane, T Juska, R Morgan, J J Lesko, U Sorathia, Reynaud (2003)	Journal of Composites for Construction	Focuses on the use of FRP in internal reinforcement, external strengthening, seismic retrofit etc. in various environmental conditions.
• “CIRIA Design Guide, C 595 - Strengthening metallic structures using externally bonded fiber-reinforced polymers”	JMC Cadei, TJ Stratford, C Hollaway (2004)	CIRIA (Construction Industry Research and Information Association)	Covers the main aspects of a strengthening scheme covering the processes of procurement, design, installation and inspection.
• “Retrofit of steel structures using Fiber - Reinforced Polymers (FRP): State-of-the-art”	A Shaat, D Schnerch, A Fam, S Rizalla (2004)	Transportation Research Board (TRB) Annual Meeting	

•“Guidelines for strengthening of steel – concrete composite beams with high modulus CFRP materials”	D Schnerch, M Dawood, E Sumner, Rizkalla (2007)		Provide guidelines on analysis of composite beams, design and installation of CFRP/steel systems
•“Guidelines for the design and construction of externally bonded FRP systems for strengthening”	Italian National Research Council	CNR – DT 202/2005	Conversion factors introduced for various types of FRP and exposure conditions
•“State-of-the-art review on FRP strengthened steel structures”	Xiao-Ling Zhao, Lei Zhang (2007)	Engineering Structures	Reviews areas on the bond between steel and FRP, strengthening of steel hollow sections and fatigue crack propagation
•“Proposed design guidelines for strengthening of steel bridges with FRP materials”	D Schnerch, M Dawood, Rizkalla, E Sumner (2007)	Construction and Building Materials	Proposes guidelines and installation techniques and presents a worked example to illustrate the design approach
•“A review on steel/CFRP strengthening systems focusing environmental performance”	M Gholami, ARM Sam, AM Yatim, MM Tahir (2013)	Construction and Building Materials	Summarizes the literature review on bonding and loading, environmental durability and gives recommendations
•“Effect of dynamic loading and environmental conditions on the bond between CFRP and Steel: State-of-the-art review”	XL Zhao, Y Bai, Riadh Al-Mahaidi, S Rizkalla (2014)	Journal of Composites for Construction	Reviews the effects of dynamic loading and environmental conditions on the bond between CFRP and steel
•“Environmental durability of adhesively bonded FRP/Steel joints in Civil Engineering applications”	M Heshmati, R Haghani, M Al-Emrani (2015)	Composites: Part B	Discusses factors affecting durability of adhesive bonded joints and different damage mechanisms.
•“A review on environmental durability of CFRP strengthened system”	S Fawzia, Md H Kabir (2016)		Reviews on durability of CFRP strengthened concrete and steel structures and identifies the future research topics.

2.2.4 Bonding Techniques

Surface Preparation

Adopting a proper surface preparation method is important as the maximum joint strength and the durability are dependent on the quality of the bond system (Hollaway & Cadei, 2002; Schnerch, D; Stanford, K; Sumner, E; Rizkalla, 2005). Poor surface treatment can end up with adhesive/adherend interface failure. Teng et al (2010) has recently proposed that cohesion failure within the adhesive should be promoted so that the de-bonding failures can be addressed based on the adhesive properties. A stable surface is free from contaminants, chemically active and capable of resisting environmental degradation.

Basic steps to carry out in the passive treatment process of steel surfaces are summarized below and the prevailing standard guidelines are BS 7079, ASTM D 2651 and ASTM D 2093 (Perera & Gamage, 2016).

i. Degreasing – removing contaminants like oil, grease and water.

- Solvent cleaning (excess solvent application is effective as the contamination may deposit when the solvent evaporates). One of the benefits of this method is the least effect on the surface properties of the steel substrate.
- Brushing, ultrasonic degreasing and vapour degreasing have found to be efficient (Schnerch, D; Stanford, K; Sumner, E; Rizkalla, 2005)

ii. Mechanical abrasion – roughening the surface and remove the weak, chemically inactive oxide layer

- Grit blasting is found to be more effective. Sufficiently finer grit should be chosen (e.g: 0.25 mm (Teng, Fernando, Yu, & Zhao, 2010).
- Other tools – sandpapers, wire brushes, abrasive pads and wheels, needle guns etc.

iii. Removing fine abrasive dust before adhesion bonding – for grit blasted/ hand ground specimens.

- By dry wipe or vacuum head
- Solvent cleaning is not suggested because in case of insufficient application, effectiveness of the surface can be reduced.

When the surface preparation process has been completed, the bonding is done. In some cases, it will not be possible to apply the adhesive soon after the surface preparation process

and the substrates may need to be stored for some time before bonding. The maximum allowable time between these two processes; surface preparation and bonding, depends on the nature of the substrate surface to alter with the exposed environment and the bond strength of the subsequent reformed surface into the base material. For an example, the maximum safe surface exposure time (SET) interval for a sand blasted steel surface is about 4 hours (Fawzia, 2007). In case of prolonged storage is necessary, keeping the specimens in a safe and clean environment or application of a primer should be adopted.

Application of a primer

Before applying the adhesive/resin into the substrate, it is better to adopt a prior coating of a primer in order to improve the bond strength as well as the durability. A primer can change the effective surface energy of a steel surface and improve the wettability; the ability of a liquid to maintain a good contact with a metal surface, protects the surface after cleaning prior to the bonding process, acts as an inhibitor between the steel/CFRP substrates and confers a good bond stability to the adhesive in the presence of moisture.

Adhesive bonding

The installation technique in the process of strengthening should be given a much care in order to achieve an economical and safe design. Selection of an installation process may depend on many aspects such as size, shape, complexity, type, level of reinforcement required and number of parts to be fabricated etc. Some of the available processes used in the industry are wet lay-up, spray up, injection moulding, compression moulding, autoclave moulding, filament winding, pultrusion and liquid moulding. Among all, the wet lay-up is the most common method used in applications.

Wet lay-up method

In this method, adhesive is applied on both FRP composite material and the substrate in layers by the means of pouring, brushing, rolling or spraying. Then the composite material is pressed on to the required surface and any entrapped air in the bond layer is removed by pressing the sheet using a rib-roller in the direction of which the fibres are oriented. As the composite material is uniformly impregnated, an optimum performance of this technique can be achieved with low viscosity resins.

Flow Chart: Surface preparation → Application of primer → Application of the resin in wet lay-up method → Curing

2.2.5 Limitations in CFRP application in steel structures

I. Some of the old bridges which are needed to strengthen are riveted bridges which are made out of cast iron or wrought iron. Application of CFRP fabric/sheets for an uneven surface like this would not be possible as it can cause peeling of the composite away from the substrate surface.

Recent research carried out by Ghafoori et al at Swiss Federal Materials Testing and Research Laboratories (EMPA) in Switzerland has developed a Pre-stressed Un-bonded Reinforcement (PUR) system as a solution for these types of structures (Ghafoori & Motavalli, 2015).

II. The risk of having a brittle failure mode.

III. High material cost: Even though the material cost is high, when the installation cost (transportation, erection, labour cost, time etc.) of other strengthening methods are compared with the CFRP strengthening system, an overall cost savings of about 20% is recorded (Hollaway & Cadei, 2002).

IV. Not availability of enough valid standards and codes

2.3 Strengthening steel elements subjected to corrosion

2.3.1 Introduction to corrosion

According to the definition interpreted in DIN EN ISO 8044, corrosion is the physical interaction between a metal and its environment which results in changes of the metal's properties which may lead to significant functional impairment of the metal, the environment or the technical system of which they form a part. The corrosion resistance of a material is affected by various factors like physical/chemical, thermodynamic, metallurgical, and electrochemical causes.

In order for corrosion to occur, there should be two electrochemical reactions to be present which are anodic and cathodic reactions where the oxidation and reduction are happened respectively. This can be understood by following basic equations formed when Zinc is attacked by hydrochloric acid.

- Anodic reaction : $\text{Zn} \rightarrow \text{Zn}^{2+} + 2\text{e}$
- Cathodic reaction : $2\text{H}^+ + 2\text{e} \rightarrow \text{H}_2$

There are several forms of corrosion taking place based on the type of the metal and the severity of the exposed environment. They are Uniform/General corrosion, Galvanic (two

– metal) corrosion, Crevice corrosion, Pitting corrosion, Inter-granular corrosion, Erosion corrosion, Stress corrosion and selective leaching/parting (Fontana, 1987). From all of these, General/uniform attack, pitting and at times the crevice corrosion is the most relevant types of corrosion to be taken care of in steel structures. General corrosion uniformly spreads over the entire exposed surface or over a large area. This type of corrosion is the most common corrosion form of all and can be destructive since it leads to gradual thinning of members in steel bridges.

Pitting corrosion is viable to occur as a localized attack and it would be difficult to detect for its small size or when covered with corrosion products. The pits formed will act as stress concentrations, reducing the metal's fatigue capacity. It will also increase the sensitivity to cracking. Almost all the places affected by pitting corrosion are susceptible to crevice corrosion and the latter is associated with the surface deposits and the crevices under bolt and rivet heads (Rahgozar, 2009).

2.3.2 Galvanic corrosion

Galvanic corrosion or two-metal corrosion is bound to happen when two dissimilar metals with a potential difference are immersed in a corrosive atmosphere. The four main requirements to be fulfilled for this form of corrosion are the anode (the less resistant metal), cathode (the more resistant metal), electrolyte and electrical connection. Corrosion of the metal is happening at the anode and the cathode usually corrodes very little or not at all. Electrolyte should be having enough conductivity to transfer ions and this solution can be generated by the presence of sea water, chemicals like fertilizer, acid or a combustion product. The anode and the cathode should be physically contacted to form an electrical connection.

In order to prevent the occurrence of galvanic corrosion in a CFRP strengthened joint, these two dissimilar metals should be isolated by not allowing for any possible physical contact. The studies presented, focusing on this matter have come up with several ideas to overcome this problem. In 1958, Evans and Rance have tried to insulate these two metals by coating with a water-resistant sealant. In 2001, Tavakkolizadeh and Saadatmanesh thoroughly examined this matter by comparing corrosion rates of samples, in which the CFRP had been washed in 3 different solvents; Acetone, isopropyl alcohol and carbontetrahydrochloride, tested in 2 different electrolytes. It has been observed acetone as

the most effective solvent and the galvanic corrosion rate is directly related to the adhesive thickness. Results show that applying a thick adhesive layer can influence to decrease the rate of corrosion. At the end, it suggests to use a non – conductive fabric layer (GFRP) in between CFRP and the metal substrate, an isolating epoxy film on the steel surface and a moisture barrier (Tavakkolizadeh & Saadatmanesh, 2001). This has been again confirmed by West in 2001 (Schnerch, D; Stanford, K; Sumner, E; Rizkalla, 2005).

2.3.3 Application of CFRP in corroded steel elements

Most of the steel bridges required to be strengthened are subjected to either fatigue, corrosion or both. Most of the time the reasons are the lack of inspection and the maintenance. The consequences of fatigue like crack initiation and propagation have been considered as a major concern and it has been identified that the results can be much worse if the structure/structural members are corroded. Further, CFRP can be used effectively in fatigue sensitive details to reduce stress intensity factors at the vicinity of the crack, produce crack closure effect (by the application of pre-stressed CFRP patches) and increase the stiffness of the cracked steel section (Bocciarelli, Colombi, Fava, & Poggi, 2009a). However, the usage of CFRP in corrosion damaged structures has not been studied much due to the uncertainty and the complex nature of the structural behaviour.

Corrosion tends to attack not only the structural performance but also makes it difficult to predict. The possible effects of corrosion can be identified as follows (Kayser & Nowak, 1989; Rahgozar, 2009).

- The members of the structure getting thinner due to the loss of material. Therefore, corrosion will lead to the loss of material strength and reduce load carrying capacity due to the decreased sectional properties of the elements.
- Accumulated corrosion products/rust on the surface will promote further corrosion for retained moisture and the “pack rust” can develop a considerable pressure on the surface, especially at connections.
- The possibility of occurring crevice corrosion in bolted joints which can become a huge disaster with the lost area of bolts.
- When the material is lost, the Class of the section (whether the section is compact/semi-compact/plastic) can also be changed which will increase the unreliability of the structural design.

- Increase of stress. When the material is lost and the structural elements are getting thinner, the overall stress levels can be increased for a given load. Moreover, when there are pits formed by further corrosion, stress concentrations at those points are prone to fatigue.

The study by Kayser and Nowak (1989) has studied the corrosion pattern of an I – beam and concluded that the most critical places to get affected by corrosion are the top part of the bottom flange and the bottom part of the web where water and other contaminants can get accumulated the most (Figure 2.3). Effect for the rest of the surface is comparatively low unless there is a hazardous situation like a chemical attack. It is also said that the corrosion penetration takes place everywhere in a uniform nature when the corrosion is in its initial stage. But, in the locations near to the supports, the surface loss can be expected over the entire web section.

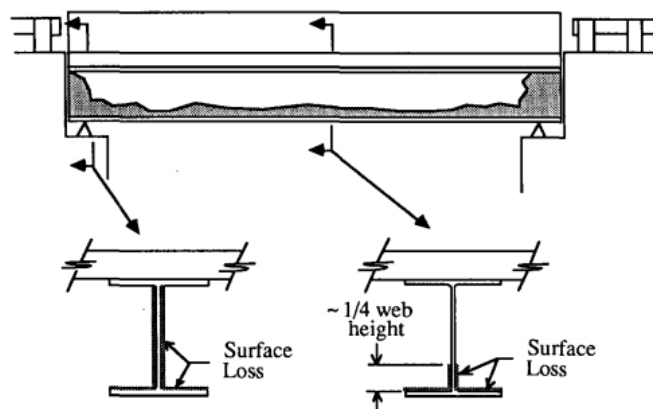


Figure 2.3: Typical location of corrosion on a steel girder bridge

When the direct structural effects are concerned, the failure modes of a corroded steel beam can be web shear failure or bearing failure, steel yielding and lateral torsional buckling. This can be summarized as follows (Kayser & Nowak, 1989; Rahgozar, 2009).

- Material loss in the flanges → Loss of area to resist bending → increase deflection → reduction of ultimate bending strength → reduction in maximum carrying capacity.
- Material loss in the web → reduction in bearing and shear resistance

There are only a few studies being done to evaluate the performance of CFRP strengthened corroded steel infrastructures.

Photiou et al, 2006 presented the experimental results of the investigation which was programmed to identify the effectiveness of using CFRP composites in artificially degraded

steel beams. In order to simulate the effect of general corrosion for a steel beam with a rectangular hollow section, the tension flange was machined to half of its thickness and the corners for about 5 mm of radius. Two types of CFRP pre-pegs; U shaped CFRP pre-peg unit and pre-peg flat plate unit, and both High Modulus (HM) and Ultra High Modulus (UHM) CFRP composites were used in four beams, tested under four-point loading and the effectiveness of the adopted systems were analysed. In addition, a layer of GFRP (Glass Fibre Reinforced Polymer) was placed in between the adhesive and the CFRP layer with the intention of preventing the effect of galvanic corrosion. According to the results, all beams reached the plastic collapse load of the original undamaged beam. The failure mode of UHM CFRP was Carbon fibre breakage and the HM CFRP indicated a ductile behaviour than the former. Also, the U – shaped system is recognized to be more effective than the flat plate system in increasing the stiffness while containing the failure.

While the Photiou et al addressed the effects of uniform/general corrosion, Ahn et al, 2013 discussed about the localized corrosion impacts on a plate girder bridge. They proposed that the regions near to the supports are more vulnerable to experience severe corrosion because of the high moisture level occurring due to bad air circulation, sediments and depositions accumulated, rainwater and anti-freeze penetration. Most importantly, they came up with a method of application to repair a corroded plate girder bridge and performed an FE analysis to evaluate the residual bearing strength of the girder. The repair method proposed by Ahn et al, 2013 can be summarized as follows.

01. Cleaning the surface of the corroded surface from rust and other contaminants with blast cleaning.
02. Making the corroded surface an even surface, by adopting a primer coating (epoxy resin) and corner shaping.
03. Attachment of carbon fibre sheets using epoxy resin and then the Aramid fibre sheets to protect the CFRP sheet.
04. Curing and painting.

In order to assess the effectiveness of the CFRP repair, a truck loading test was performed, and the strains were measured in both before and after the CFRP application. The study affirms that this technique can improve the sectional reinforcement effect and preventing the corrosion being progressed. It also recommends for further research to determine and

assess the effect of CFRP repair on the corroded steel substrates more accurately with new repair methods.

2.4 Bond Performance of Steel/CFRP joints

The adhesive joint being the weakest link between the strengthening system, evaluation of the bond strength of the CFRP/Steel joint is essential to increase the effectiveness of the system. Therefore, many of the research studies have tried to focus on evaluating the bond performance through both experimental and numerical investigations. The commercially available epoxy adhesives such as Sikadur-330, Sikadur 30, Araldite 420, Araldite it K138, have been used and tested to find out the most efficient adhesive type in different loading cases like static and dynamic and environmental conditions. The optimum adhesive thickness, failure modes, number of CFRP layers, the effect of the modulus of CFRP (NM, HM, UHM), different CFRP forms (sheet/laminate) have been used as the parameters of the studies.

2.4.1 Force Transfer between the metal substrate, CFRP and the adhesive

To design an efficient strengthening system, one may need to have a thorough knowledge on how the forces are being transferred between the metallic/CFRP substrates. This is important to understand the rate of force transfer, equivalent effective bond length (development length) which are needed to decide the required strengthening material length and the position. Hence, this is a wide subject which needs to be studied in detail. The idea of an effective bond length is, if the bond length of CFRP sheet/laminate is greater than the effective bond length or the development length, it can be assumed that the load is fully transferred and thus the debonding is minimized.

The research experiments carried out by Miller, 2000 have discovered that force transfer length is a function of geometric and material properties of the 3 components; steel substrate, CFRP plate and the adhesive. Also, they have seen that the transfer rate is most sensitive to the adhesive thickness and the CFRP plate thickness. Finally, they have concluded that the 98% of the force transfer is occurred within the 100 mm from the end of the cover plate.

2.4.2 Failure modes

The Failure modes of an FRP strengthened steel member subjected to a tensile force

Failure modes which are possible in a CFRP bonded steel system subjected to a tensile force include the following failure modes and the Figure (2.4) shows a schematic view of failure modes (X.-L. Zhao, 2013).

1. Failure in the interface between steel and adhesive
2. Cohesive Failure (adhesive layer failure)
3. Failure in the interface between FRP and adhesive
4. FRP delamination (separation of some carbon fibres from the resin matrix)
5. FRP rupture
6. Steel yielding

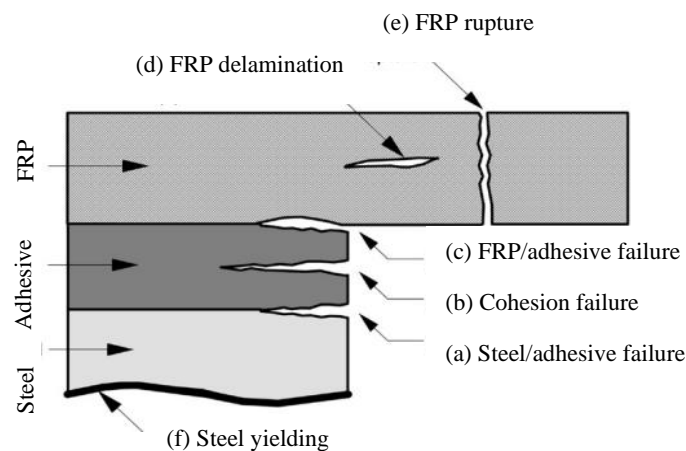


Figure 2.4: Failure modes of an FRP strengthened steel member (X. L. Zhao & Zhang, 2007)

Key parameters affecting failure modes:

It is found that the failure mode of CFRP sheet is mainly dependant on the tensile strength of the CFRP sheets (Normal Modulus CFRP sheet has higher tensile strength than the High Modulus CFRP sheet) while it depends on the adhesive thickness and the material properties for the CFRP laminates. A research study carried out by Xia and Teng (2005) to study the bond performance of CFRP/Steel joint using CFRP plates, found that the failure mode becomes the mode 2 (Cohesive failure) for thin adhesives whereas it changes to CFRP delamination (mode 4) for thick adhesives. From the results, Mode 4 is found to be more brittle than the Failure Mode 2. Failure modes 1 and 3 have not been observed which implies a strong bond of the adhesive to the steel substrate and the FRP plate surfaces. The failure mode 5 (CFRP rupture) can be expected for High Modulus CFRP composites

and the Mode 6 (Steel yielding) is often avoided in the testing by adopting a suitable steel plate thickness.

The Failure modes of an FRP strengthened flexural steel member (Buyukozturk, O.; Gunes, O.; Karaca, 2004)

1. Top flange buckling in compression
2. Web buckling in shear
3. FRP rupture
4. FRP de-bonding

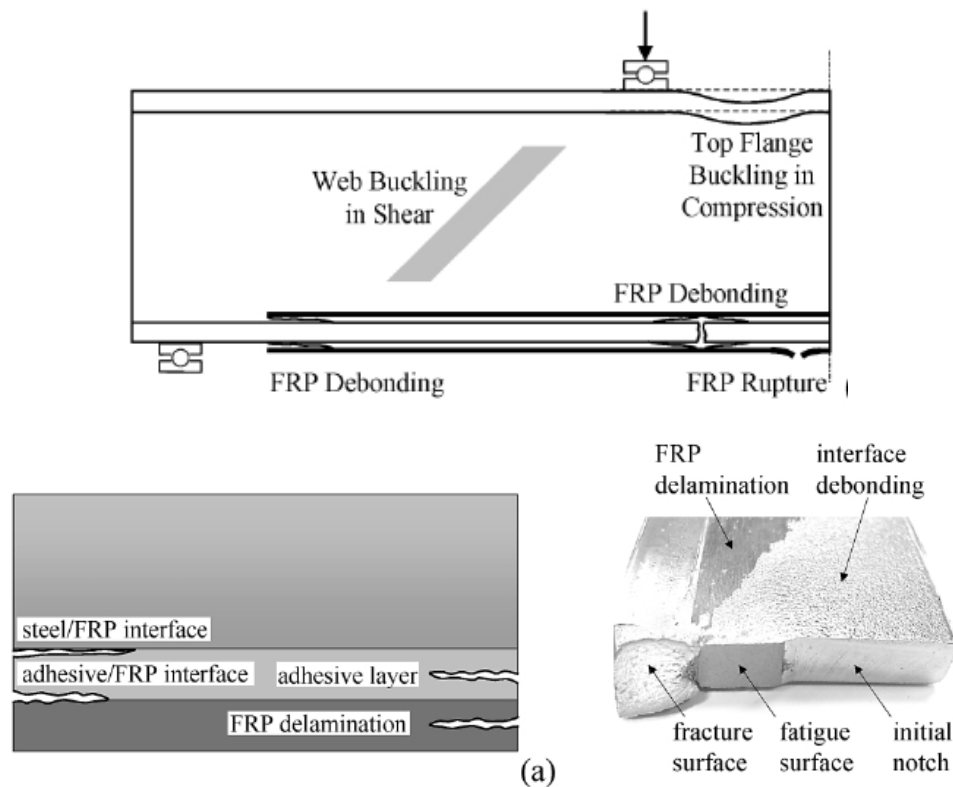


Figure 2.5: types of debonding in FRP strengthened steel members (Buyukozturk, O.; Gunes, O.; Karaca, 2004)

2.4.3 Durability of the bond

One of the advantages of using CFRP composites in retrofitting structures is the possibility to expect long structural life and low maintenance for its high capability to resist corrosion and weathering. Literature shows negligible degradation of CFRP materials in strength and stiffness (Nguyen, Bai, Zhao, & Al-Mahaidi, 2012a). Though, when the long-term effects are concerned, the adhesive joint can be weakened with the exposure to various environmental conditions like humidity, liquid-water, high temperatures, etc.

Environmental Effects

- **Moisture and Humidity effects**

Presence of moisture can affect a CFRP/steel bonded system by weakening the material properties of either the epoxy adhesive or the FRP matrix resin. Moisture ingress to a strengthened system can be occurred due to diffusion through inorganic adhesives/adherends, wicking along the interfaces, capillary action and absorption through porous adherent (Bowditch, 1996; Gholami, Sam, Yatim, & Tahir, 2013; Heshmati, Haghani, & Al-Emrani, 2016; Karbhari et al., 2003). Most critically it reduces the strength of the CFRP/steel joint. However, some studies have shown that when the water concentration is high, the weakening of the bonded joint is happening only after some point and until that critical water content, the joint is stable as the stress concentrations are reduced (Bowditch, 1996; Nguyen et al., 2012a).

The effects of moisture can be adverse with the presence of ions/salts, higher/lower temperature and sustained stress levels (Bowditch, 1996; Karbhari et al., 2003). Studies suggest to use adhesive promoters as Silane to minimize the effects of moisture, increase the bond durability and increase the curing temperature higher than the T_g (Schnerch, D; Stanford, K; Sumner, E; Rizkalla, 2005)

- **Alkali Effects**

Alkaline solutions are a threatening media to the degradation of fibers in FRP composites. Even though the resin of the composite material can protect the fibers from an alkaline attack, it contributes for an accelerated degradation of the FRP bond. Hence, the studies recommend to choose suitable epoxies with an appropriate thickness as the resin material and proper curing of both FRP composite and the resin. This exposure condition is likely to occur when FRP composites are exposed to alkaline chemicals, soil and concrete. Available research studies are mostly carried out on degradation of glass fibers and influence of concrete pore water solution (Karbhari et al., 2003).

- **Saltwater**

Bond performance of CFRP strengthened steel joints exposed to saltwater conditions such as marine environment and de-icing salts may differ from the effects causing due to moisture alone. Saltwater can act as an electrolyte which creates direct contact between the steel and CFRP material and cause galvanic corrosion. Tests carried out on tensile butt

joints immersed in sea water at room temperature have shown a gradual increment of failure stress with time and then to an asymptotic stress value after about 8 years (Bowditch, 1996). However, the elastic modulus and the tensile strength of the adhesive decrease in a slower rate and to a lesser degree for salt water than for distilled water (Heshmati et al., 2016; Nguyen et al., 2012a) concluded that the remained strength of CFRP/Steel joints immersed in sea water is about 85 % in 20°C. Studies have also shown that embedding a GFRP layer in between the steel substrate and the CFRP layer can enhance the ultimate strength of the saline water conditioned beams (Kabir, Fawzia, Chan, & Badawi, 2016)

- Thermal Effects

The possible thermal exposure conditions which can be experienced by CFRP strengthened units are elevated temperatures; temperatures above the glass transition temperature (T_g) of FRP composite matrix resin/adhesive, freezing /sub-zero temperatures and thermal cycles. When the operating temperature is close to the T_g , both the FRP resin and the adhesive can get softened and increase the viscoelastic properties (Karbhari et al., 2003; Nguyen, Bai, Zhao, & Al-Mahaidi, 2011). Since the thermal expansion coefficients of the matrix resin, adhesive and the fibers are different from each other, premature debonding of the FRP/adhesive or fiber/matrix interface can be occurred (Heshmati, Haghani, & Al-Emrani, 2015). The investigation results have shown that the strength and stiffness of the bonded joints are totally dependent on the thermo – mechanical behaviour of the adhesive (Nguyen et al., 2011). This is attributed to the fact of having a lower range of T_g value for adhesive (Usually in between 40°C – 65°C) than for the FRP resin matrix (65°C – 120°C). Hence, the design guidelines recommend to choose an adhesive with a T_g of 15°C greater than the operating temperature (Heshmati et al., 2015).

Nguyen et al, 2011 observed 15%, 50% and 80% joint strength degradation in CFRP/steel adhesively bonded double strap joints when the temperature is increased 0°C, 10°C and 20°C above T_g , respectively. The effect of high temperatures on FRP bonded joints vary not only based on the temperature difference between the T_g and the exposed temperature, but also on the exposure duration and the sustained stress level (Nguyen et al., 2012a). Further, the high temperatures cause to increase the bond slip of the joints as well as the effective bond length (Heshmati et al., 2015; Nguyen

et al., 2011).

Sub – zero/ freezing temperatures cause the deterioration of the FRP material initiating matrix hardening, matrix micro-cracking and fiber – matrix bond degradation (Karbhari et al., 2003). The effects of cold temperature conditions vary based on whether it is a sub – zero exposure in cyclic conditions (freeze/thaw condition) or noncyclic conditions. Cyclic condition has been identified as the most adverse condition. The influence on the bond strength by non – cyclic conditions is negligible when a compatible adhesive is chosen (Al-Shawaf, Al-Mahaidi, & Zhao, 2008; Heshmati et al., 2015; Karbhari et al., 2003)

- UV Radiation

Since most of the CFRP strengthened units are exposed to direct sunlight, the influence of UV radiation on the durability of the CFRP / Steel joint is needed to be considered. This becomes a matter of concern due to the fact that the wavelength of ultraviolet light being similar to the polymer bond dissociation energies, i.e. 290 – 400 nm (Karbhari et al., 2003; Nguyen, Bai, Zhao, & Al-Mahaidi, 2012b). Even though the depth of degradation may be limited only for few microns, the pits formed can be acted as stress concentrators which will accelerate the fracture initiation. Further, the effects can be worsened with the association of other environmental factors like, temperature, moisture and freeze-thaw conditions etc. However, according to the experimental results obtained by Nguyen et al 2012 (b), a similar degradation of strength and stiffness was observed when CFRP/steel double strap joints were exposed to temperature alone of 40°C and UV exposure with an associated temperature of 40°C.

Loading Effects

- Fatigue loading

In the recent past, various studies have been carried out to determine the fatigue performance of steel members when they are strengthened with externally bonded CFRP composites. The need of fatigue strengthening has rapidly increased mostly for the steel bridges and infrastructures in all over the world due to the increased traffic volume, progressive aging, improved safety requirements and deterioration caused by environmental effects (Ex. Corrosion). Study results have shown a superior fatigue performance of CFRP patches by extending fatigue life remarkably and restraining crack

growth. Thus, the effect of fatigue loading on the bonding is an important matter to be considered for the evaluation of effectiveness and reliability.

Liu et al. (Liu & Zhao, 2010) had performed a series of tests with double strap joints to investigate the effect on failure modes and bond strength caused by fatigue loading. Observations conclude that the failure modes under both static and fatigue loading are quite similar for Normal modulus CFRP sheets and the reduction in bond strength is about 20% for load ratios 0.2-0.3. For High modulus CFRP sheets, only an insignificant reduction of bond strength was observed even for the highest load ratio and the highest fatigue cycle. Another series of tests were carried out using CFRP strips to determine the fatigue performance of tensile steel/CFRP double-strap joints by Colombi et al. (Colombi & Fava, 2012). The stress concentration zones were found to be the CFRP strip ends and the gaps, from where the debonding gets started and have the highest adhesive peel and shear stresses. This identifies the requirement of having an evenly spread adhesive layer and the importance of interfacial stress parameters to predict the fatigue life. The paper also considers the bridging effect which reduces the stress at the gap by partially filling it with excess adhesive in the specimen. Related literature by Wu et al, 2013 has conducted a similar procedure with series of static and fatigue tests yet using UHM (Ultra – High Modulus) CFRP plates, which have a modulus of elasticity of 460 GPa. A similar fatigue behaviour was concluded for both UHM CFRP plates and HM CFRP sheets.

Few studies had been published on combined effect of fatigue loading and environmental conditions over the last couple of years. Borrie et al. (Borrie, Liu, Zhao, Raman, & Bai, 2015) tried to investigate the combined effects of fatigue loading and the marine environment on the bond behaviour of double lap joints. Specimens were tested for both with and without sea water exposure conditions at three different elevated temperatures (20, 40 and 50 °C), using HM CFRP sheets and NM CFRP laminates. It concludes that the worst environmental conditions are met, when the exposure durations are extended and in high temperatures. Borrie et al. (Borrie, Zhao, Raman, & Bai, 2016) further extended the study by taking in to account the pre-cracked steel plates, different CFRP sheet configurations in addition to the fatigue loading and severe environmental exposure. Silane treatment was introduced to investigate its capability to enhance the durability of the steel-CFRP bonds in exposed

conditions.

- Impact/ Dynamic loading (Perera & Gamage, 2016)

Impact loading behaviour is simulated in the laboratory by using different strain rates/loading rates on the CFRP strengthened steel joints. Double strap joints and Pull – off tests are being carried out in the experiments with the adoption of the drop mass technique. The obtained results are then compared with the results attained for quasi-static loading and the influence of impact loading on the bond behaviour is evaluated. Experiments carried out by (Al-Mosawe & Al-Mahaidi, 2014, 2015; Al-Mosawe, Al-Mahaidi, & Zhao, 2016, 2013; Al-Zubaidy, Al-Mahaidi, & Zhao, 2012; Al-Zubaidy, Zhao, & Al-Mahaidi, 2013) with quasi static loading rate of 3.34×10^{-4} m/s (quasi-static) and dynamic loading rates of 3.35 m/s, 4.43 m/s and 5 m/s can be summarized as below.

With NM CFRP sheets (CF 130): Bond performance (Bond strength, failure modes) can be expressively different based on the mechanical properties of the adhesive type used. It has been realized that dynamic bond strength is increased when 3 CFRP overlays are used instead of 1 CFRP layer with Araldite 420 adhesive. However, the number of CFRP layers did not affect the bond strength with the adhesive type MBrace saturant. Further, after the dynamic loading rate of 3.35 m/s, bond strength was slightly increased for Araldite 420 and for MBrace saturant, it decreased. This can be attributed to the elasto-plastic behaviour of Araldite 420 and elastic – brittle nature of MBrace saturant [26]. In addition, the effective bond length seemed to be independent of the loading rate and general trend of the strain distribution which is decreasing away from the joint is not changed with the number of CFRP sheets adopted at the joint.

With CFRP laminates: The increment in the ultimate bond strength for both LM CFRP and NM CFRP was similar, and it was comparatively less for UHM CFRP laminates. The reason can be understood as the low tensile strength and ultimate strain values of UHM CFRP plates. A similar trend of strain distribution for both LM and NM laminates could be observed. Ultimate strain values of UHM laminates are 2/3 times lower than for the LM/NM laminates and Increment of ultimate strain under dynamic loadings over static loading is about 15%.

2.4.4 Evaluation of bond strength

There are several approaches to evaluate the bond strength of a CFRP strengthened steel system. These approaches can be identified as, 1) Strength/stress distribution approach, 2) Fracture mechanics-based approach and 3) Bond-slip relationships. The first method calculates the bond stress distribution in the strengthened member based on the elastic material properties. The second method reflects the fatigue crack propagation and evaluates both analytical and finite element methods. Extensive research work is present, progressed in Aerospace Engineering.

Stress Distribution Approach

The stress transformation of a composite strengthening unit is happening as a combination of shear stresses and peel stresses. Shear stresses are the stresses parallel to the joint and the peel stresses are the stresses normal to the joint. The shear and peel stress distribution along the strengthened composite can be predicted by a stress distribution approach and be compared with the limiting strength of the adhesive joint.

The previous work carried out in assessing the intermediate adhesive stresses, has identified by both experimentally and theoretically that the stress concentrations which govern the adhesive joint strength, occur due to the varying strains within the adhesive layer. Strains are varied where the geometric discontinuities are present like bond defects, steps in the strengthening plates or at the end of a plate (Figure 2.6) (Stratford & Cadei, 2006).

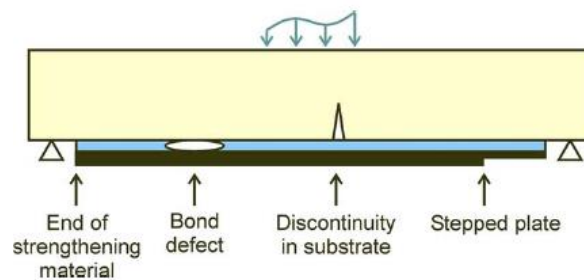


Figure 2.6: Geometric discontinuities causing stress concentrations (Stratford & Cadei, 2006)

Stratford and Cadei, 2006 has experimentally found, that the maximum shear and peel stresses are expected to be obtained in the vicinity of the plate ends. Therefore, to reduce the stresses trapped across the adhesive joint, several methods are suggested. One is to keep the strengthening plate end at a region of low moment and the others are to use a tapered

section to have a reduced section at the end or mechanical clamps.

Fracture Mechanics Based Approach

Fracture mechanics concepts deal with the idea of material failures caused by crack initiation and propagation. Hence, this approach has been a common area of study in the Aircraft industry in evaluating the service life of fatigue damaged structures. Yet, the study techniques are not directly applicable into the Structural Engineering applications for the discrepancies in load applications and the material thicknesses.

Basically, there are two main approaches in fracture mechanics. They are Stress intensity factor criterion (local) and energy balance criterion (global) (Janssen, Zuidema, & Wanhill, 2006). The first concept analyses the crack tip stress and displacement fields and identifies the parameters governing near tip stresses and displacements. First the stress intensity factor (K) for the given load and crack/part geometry is calculated and the fracture toughness is measured. Then, the maximum allowable load to cause zero crack growth for a given crack length is determined.

$$K_I = K_{Ic}$$

Where, K_I – stress intensity factor (stress at the crack tip)

K_{Ic} – fracture toughness (a material property)

Meanwhile, the energy concept considers the global energy balance during crack extension and compares between the Strain Energy Release Rate (SERR) which is a function of applied load and the material characteristic critical value (G). As the debonding process is always brittle in nature, it has been identified that energy approach is more effective than the stress-based failure criteria as the latter is more suitable for gradual and ductile failures (Carpinteri, A; Cornetti, P; Pugno, n.d.). Moreover, as energy concept is universal, non-linear effects can be accounted. Both fracture mechanics concepts are based on LEFM (Linear Elastic Fracture Mechanics) theory where the cracked solid is treated as a linear elastic medium and non-linear effects are assumed to be either minimal or ignored.

$$G = - d\pi / da$$

Where; G = Energy Release Rate

π = potential energy

a = crack length

- $d\pi / da$ = decrease in potential energy per unit crack extension under constant load

Most of the experimental research studies carried out have observed that the de-bonding of a CFRP strengthened joint is occurred due to either steel-adhesive interface failure or adhesive layer failure (cohesive failure). Bocciarelli et al. (Bocciarelli et al., 2009b) has performed an experimental study and proposed an analytical expression to predict the failure load based on fracture mechanics approach. It has been observed that both the experimental and analytical results are in good agreement with each other if SERR is assumed to be a function of the adhesive thickness.

Some research studies argue that the LEFM based methods are restricted to predict fracture toughness of an adhesive joint only for the estimation of the initiation fracture toughness (Sarrado, C; Turon, A; Costa, J; Renart, 2015). The results have shown that the fracture process zone and the bond configuration can significantly affect the LEFM methods. Most importantly, it has been observed that the adherend and the bond line thicknesses have a significant impact on the fracture toughness.

Fracture mechanics criteria often deal with the crack propagation where cracks are artificially placed prior to the modelling so that the crack initiation is simulated. To overcome this matter, cohesive zone models can be used for its benefits in simulating both crack initiation and propagation without any need of pre-crack formed.

Bond- Slip Relationship

Bond – slip relationships can be used to predict the ultimate load values which can be independent by the bonded joint as well as the effective bond lengths. These relationships are dependent on the properties of the adhesive (Elastic modulus, Tensile strength, Strain capacity) and interfacial fracture energy, G_f .

In 2005, Xia and Teng performed a series of Pull-off tests in order to identify the factors governing for the behaviour of an FRP bonded joint. Shear bond stress – slip curves were developed at different distances from the loaded end for specimens using two different adhesives. Finally, a simple bond – slip model and an analytical model were introduced so that the ultimate loads and effective bond lengths can be predicted (Figure 2.7).

Another bond-slip model was developed considering several parameters which are CFRP bond length, adhesive maximum strain and adhesive layer thickness by Sabrina et al, 2010 and both the experimental and numerical results showed that the maximum slip is directly dependent on the adhesive maximum strain and its effects on the maximum shear stress

and the initial slip are negligible. It also concludes that there is a significant effect causing from the adhesive thickness on both the initial and maximum slip.

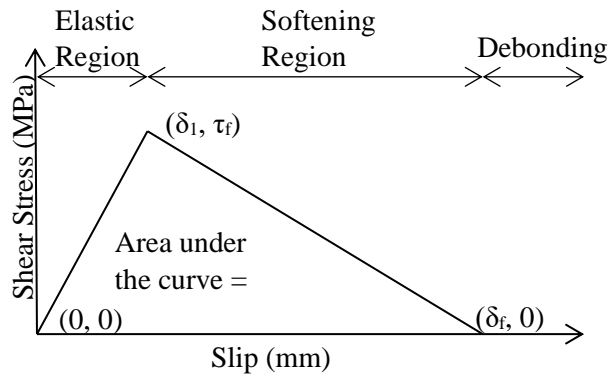


Figure 2.7: Bond Slip Relationship by Xia and Teng, where δ_1 – initial bond slip, δ_f – final bond slip, τ_f – Peak shear stress and G_f – Interfacial fracture energy

Dehghani et al, 2012 adopted a new approach to simulate the CFRP/steel bonded connection by considering a series of equivalent discrete springs. The advantages of this method can be identified as the possibility to analyse complicated steel connections and use of FE methods for the analysis. Above all, this method can be applied in analysing any pre-defined bond-slip model and add the plastic part into it so that the nonlinear properties of the adhesive can be taken into account. Unlike the results obtained in some previous research studies, it shows that the ultimate de-bonding load is independent from the adhesive thickness and it depends on the adhesive type and the axial stiffness of the bonded plate.

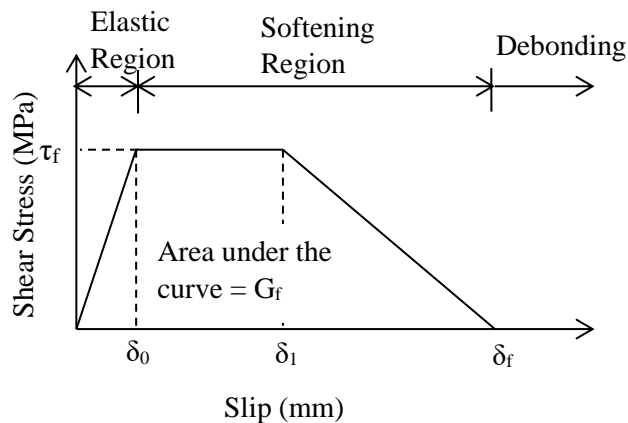


Figure 2.8: Bond Slip Model by Dehghani et al (2012)

The most common observations in all of these bond-slip model studies are that the shear stress is maximum at the loaded end and it gradually moves to the unloaded end when the debonding proceeds.

2.4.5 Bond Testing Methods

Three-point bending tests or four-point bending tests are performed to detect the adhesive shear stresses and peel stresses of the bonded joint when subjected to flexural loads. The load is indirectly applied to the FRP and these tests are generally used for steel members with I sections (Figure 2.9). For other types of loading (Static tension, dynamic loading, etc.) adhesive joint test methods are performed. Adhesive joint tests can be categorized as overlap and shear joint tests, Peel tests and Pull – off tests (Duncan , B; Crocker, 2001)



Figure 2.9: Four-Point Bending Testing Arrangement

Mostly used shear joint tests are Single – Lap joints (Figure 2.10 a), Double – Lap joints (Figure 2.10 b) and Double Strap joints (Figure 2.11 a, b). Lap joint tests are carried out by applying tensile force directly to the FRP layer. Single lap shear joints are capable of detailed monitoring and inspection of the failure mechanism. On the other hand, eccentricities may develop, FRP layer may bend and the bonded region may rotate. To eliminate the above situations by a symmetric arrangement, double lap shear joints are introduced. The applicability of these tests to CFRP sheets may be difficult as gripping is an issue. Stresses at the joints can be minimized by selecting a suitable adhesive type, modified shapes of joint ends and geometries of adhesive fillets (Duncan , B; Crocker, 2001). Double strap joints are formed by direct application of loading to the steel element. This test is very popular in the literature and the concern of uncertainty in the de-bonding location can be overcome by using unequal bond lengths, mechanical clamping and transverse CFRP strengthening (X. L. Zhao & Zhang, 2007).

T-Peel tests are suitable for flexible adherends and can be used to evaluate the resistance of the adhesive system to the normal force peel loading. The suitability of the test results in generating design data is yet uncertain. To assess the adhesive bond strength of the adhesive, pull – off and Butt joint tension tests (Figure 2.12) can be used. Possible

misalignments of the specimen or the applied load should be minimized for accurate results

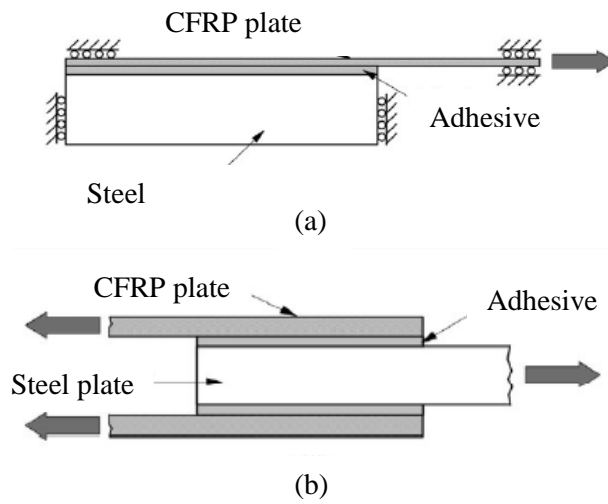


Figure 2.10: (a) Single lap joint (b) Double lap joint

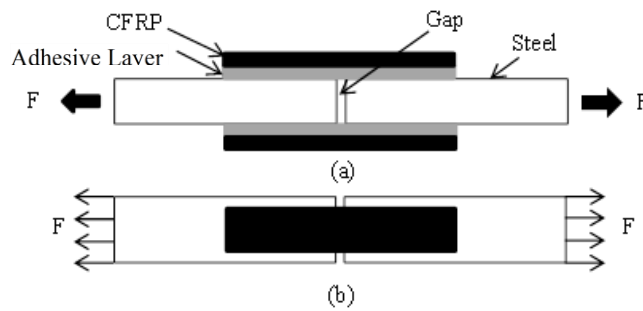


Figure 2.11: Double Strap Joint (a) Side view (b) Plan view

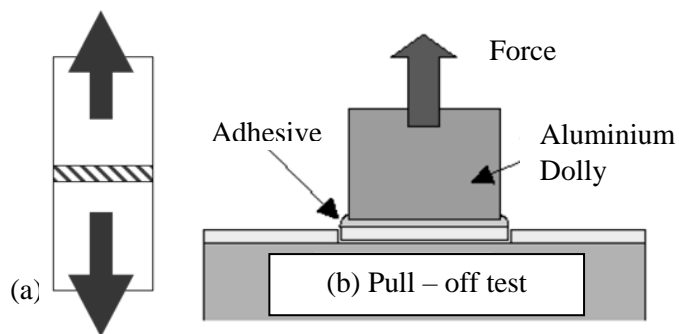


Figure 2.12: (a) Butt – Joint test specimen and (b) Pull – off test specimen

2.5 Research Gap and Summary

Although there are some real – world applications available in all over the world, this technique is not yet widely spread to use in metallic structures for several reasons, especially in Sri Lanka.

- ✓ Less research work available on the long-term durability performance of the strengthening system.
- ✓ Lack of knowledge on the performance of Steel/CFRP joints under combined environmental conditions like hygro-thermal exposure (combination of moisture and temperature)
- ✓ Literature has identified that the weakest link in a CFRP strengthened steel substrate is the adhesive bond between these two adherends. Hence, identifying the bond performance is vital for the development of this technique.
- ✓ Non availability of codes and standards.

When steel structures are deteriorated mainly due to corrosion, it increases the uncertainty of the structural behaviour. The major effect of corrosion on steel structural members is the thinning of member sections which result reduced carrying capacity of the structure. Therefore, the strengthening method should be capable of restoring the lost strength and stiffness of the structure/structural member, preventing corrosion progress, increasing its service life and decreasing the maintenance cost.

In general, CFRP applications can be effectively used in corroded steel structures with a proper understanding of the deterioration process. Corrosion badly effects on the substrate properties which will reduce the durability of the bond between CFRP and steel. Most of the research studies conducted to evaluate the long-term performance of the CFRP/Steel system has been focused on pure steel plates strengthened with CFRP. Attention on the substrate properties on bond characteristics is also less. The consequences of strengthening already corroded members with CFRP materials may be different from the behaviour of the CFRP strengthened non – corroded steel members due to the presence of increased surface irregularities in the corroded steel surface. Usage of a notch or reducing the thickness of the plate to simulate the

corrosion effect may not reflect the real performance. This research study is focused on the naturally corroded and non-corroded steel members strengthened with CFRP. Influence of varying surface texture on long term and short-term performance of the CFRP/Steel composites is one of the focus of this study.

CHAPTER 3

MATERIAL PROPERTIES

3.1 Introduction

The experimental programme for the study was designed to carry out on Carbon Fibre Reinforced Polymer (CFRP) bonded steel plates. Hence, three different materials can be identified in the proposed strengthening scheme, namely; CFRP sheet/wrap, adhesive material and structural steel. It is vital to understand the behaviour of each of these materials since the physical/mechanical properties of the composite system utterly dependent on them. The properties like ultimate tensile strength, ultimate strain and the elastic modulus were experimentally obtained according to the standard testing procedures. Even though the manufacturer specified material properties are available for CFRP and the adhesive material, the study relied on the experimental results for several reasons such as possible variations in testing and environmental conditions. The following flowchart (Figure 3.1) summarizes the general procedure of the material testing programme.

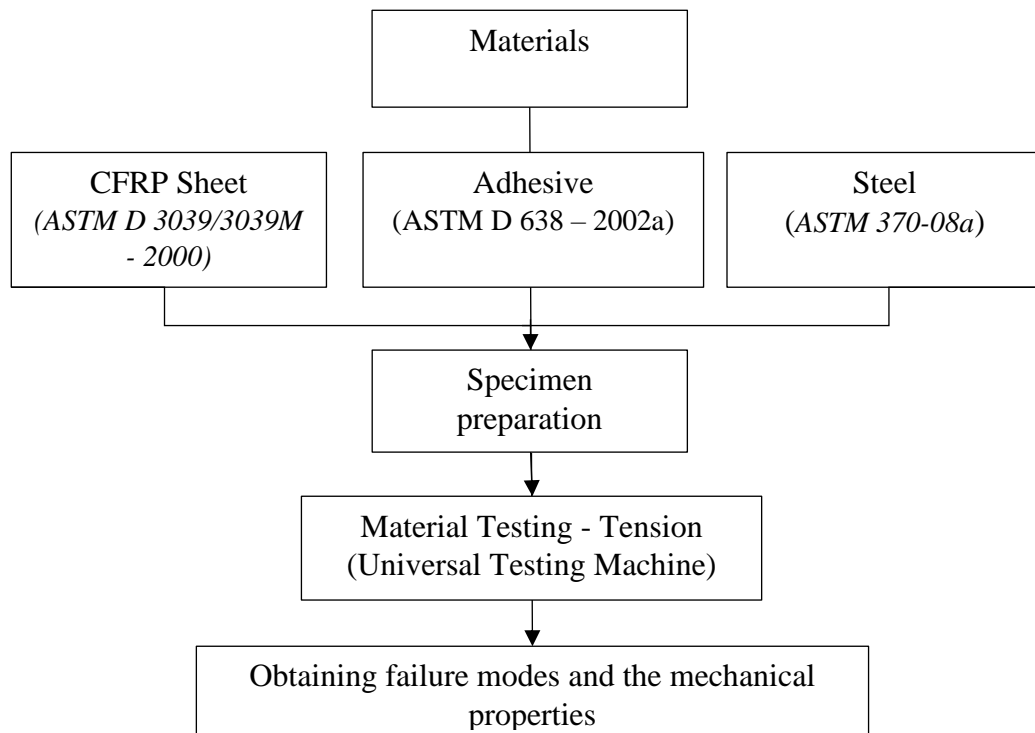


Figure 3.1: The general procedure of the material testing programme.

3.2 CFRP Wrap

3.2.1 General

Normal Modulus CFRP sheets were used for the specimen preparation. Material characteristics along with the advantages and disadvantages of using the Carbon Fibre Reinforced Polymer material are briefly described in the previous chapter, i.e. Chapter 02.

3.2.2 Manufacturer specified properties

High strength carbon fibre uni-directional fabric product, X – Wrap C 300 was used for the strengthening. As an extra advantage, the product data sheet (“X-Wrap C300 High strength carbon fiber fabric,” n.d.) highlights its capability to use in conjunction with the pultruded plates for combined strengthening and reinforcement. The manufacturer provided material properties are summarized in Table 3.1.

Table 3.1: Laboratory test data provided by the manufacturer (X-Calibur Construction Chemistry Inc.)

Sheet weight	300 g/m ²
Carbon content	95 %
Nett effective thickness	0.166 mm
Modulus of elasticity	240 GPa
Tensile strength	4000 MPa
Elongation at break	2%

3.2.3 Measured Properties

Tensile properties of the CFRP sheet were tested in accordance with the ASTM D 3039/3039M – 2000 (*ASTM D 3039/D 3039M - 00 Standard Test Method for Tensile Properties of Polymer Matrix Composite Materials*, 2000).

Preparation of coupon test specimens and test set – up

Five coupon specimens were made as recommended in the ASTM standard. The test specimen was made by attaching 2 dry fibre sheets together by gluing them with Araldite 420 epoxy. The adhesive thickness is so thin that only the thickness of the fabric layers was considered in the calculation of CFRP stress (Al-Zubaidy, Zhao, & Al-Mahaidi, 2013). A large panel was made and cut into five separate coupons after a

curing period of 7 days. Each coupon extremity was attached to an end grip of 56 mm long and 1.5 mm thick on both sides, in order to minimize the stress concentration and avoid gripping damage. These tabs were also bonded to the laminate using Araldite 420 epoxy and kept curing for minimum 7 days to prevent any slipping/sliding. In order to measure the strain readings and calculate the modulus of the CFRP material, two strain gauges had been attached at the centre of both sides of a specimen. Then the coupons were tested using a 1000 kN Universal Testing Machine at a displacement rate of 2mm/min. Figure 3.2 and Figure 3.3 show the schematic diagram of a CFRP coupon test specimen, and the test setup of the CFRP sample respectively.

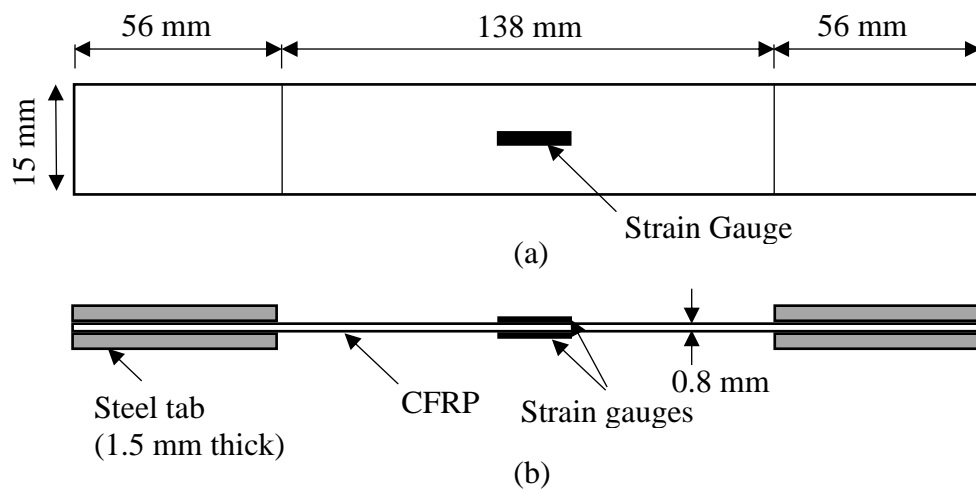


Figure 3.2: Schematic diagram of a CFRP coupon test specimen (a) Plan view
(b) side view



Figure 3.3: Test setup of a CFRP test coupon specimen

Failure modes and test results

The failure mode of four numbers of CFRP test samples was observed as edge delamination occurred in the middle gauge area (Figure 3.4) while the other failed at the grip/tab. However, the sample failed due to the failure of grip was not considered in calculating the average material properties for CFRP.



Figure 3.4: Failure mode (Edge Delamination in the Middle Gauge area) of CFRP coupon test specimens

Figure 3.5 shows the measured stress–strain variation of CFRP samples and a similar behaviour was identified in all the tested samples and the Table 3.2 summarizes the test results obtained for all five coupon samples. Results indicate an average modulus of elasticity of 175.6 GPa, average ultimate tensile strength of 1575 MPa and an average ultimate strain of 8980.6 $\mu\epsilon$. The maximum modulus value obtained from the test specimens is 184.5 GPa while the manufacturer provided modulus value is 240 GPa. The maximum measured ultimate tensile strength 1867 MPa and it is only slightly lesser than the half of the manufacturer specified value, 4000 MPa. This shows

the discrepancies between the manufacturer’s specified material properties and the measured properties and encourages to perform material testing as available standards/guidelines.

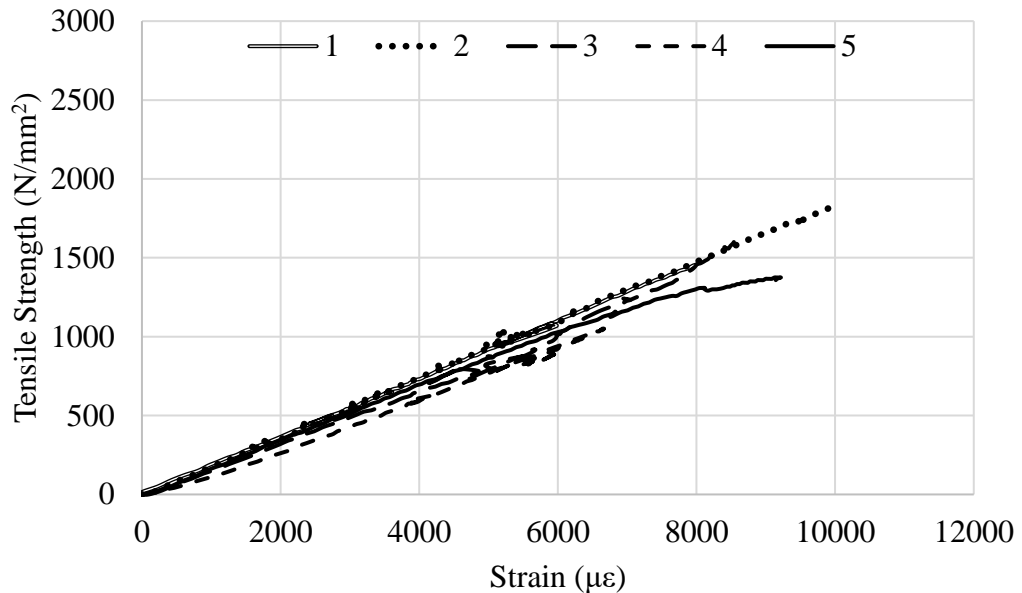


Figure 3.5: Stress – strain curves of CFRP test samples

Table 3.2: Measured material properties of CFRP coupons

Sample No.	Modulus of Elasticity (GPa)	Ultimate Tensile Strength (MPa)	Ultimate Strain (µε)	Typical Failure Mode
1	183.2	1458.3	8006.4	Edge Delamination in the Middle Gauge area (EGM)
2	184.5	1866.7	10196.1	
3	173.2	1600.0	8539.3	
4	152.0	1050.0	6046.2	At grip/tab
5	161.6	1375.0	9180.6	Edge Delamination in the Middle Gauge area (EGM)
Average (Measured)	175.6	1575.0	8980.6	
Standard Deviation	215.51	939.7	10.6	

3.3 Adhesive

3.3.1 General

A two-part epoxy adhesive was used for the testing. The benefit of using a two – part epoxy adhesive is the simple curing cycle required (approx. 16 – 24 hours) under ambient conditions, not like single component adhesives which require high temperatures as the curing conditions (Fawzia, 2007). A brief introduction is given about the purpose of using a suitable adhesive for the strengthening system in the Chapter 2.

The adhesive system used for the testing is Araldite 420 A/B. This epoxy adhesive paste cures under room temperature and has high strength and toughness. The material is easy to work with for its less viscosity. Araldite 420 A/B had been used and recommended by many a research studies carried out on strengthening metallic members using CFRP composites (Borrie, Zhao, Raman, & Bai, 2016; Fawzia, 2007). Borrie et al. (Borrie et al., 2016) has also concluded that Araldite 420 is capable of creating a more durable and effective CFRP composite system with a pro-longed fatigue life.

3.3.2 Manufacturer specified properties

The material properties given in the product data sheet (“Araldite 420 A/B Epoxy Adhesive,” n.d.) provided by the manufacturer, Huntsman Advanced Materials, are summarized in the Table 3.3. Pot life is mentioned as 60 minutes at 25°C.



Figure 3.6: Araldite 420A/B (resin/hardener) adhesive

Table 3.3: Manufacturer (Huntsman Advanced Materials) specified material properties

Tensile Strength	29 MPa
E – Modulus	1495 MPa
Elongation at Break	4.6 %
Shear Modulus	730 MPa

3.3.3 Measured Properties

Adhesive test samples were prepared and tested using a 1000 kN Universal Testing Machine to determine the mechanical properties in accordance with ASTM D 638 – 2002a (ASTM, 2003).

Preparation of coupon test specimens and test set – up

Five numbers of dumb – bell shaped adhesive test specimens were prepared. The geometry and the dimensions were decided according to the ASTM standard and its schematic view is shown in Figure 3.7. A 7mm thick mould has been prepared using a thin Aluminium sheet and it is removed after 2/3 days when the adhesive sample is fully hardened. All the specimens were kept to cure for 7 – 14 days as the manufacturer specified. Foil strain gauges were glued at the centre of both sides of each sample in order to measure the true strain. Figure 3.8 (a/b) shows a ready – to – test adhesive sample and the instrumentation.

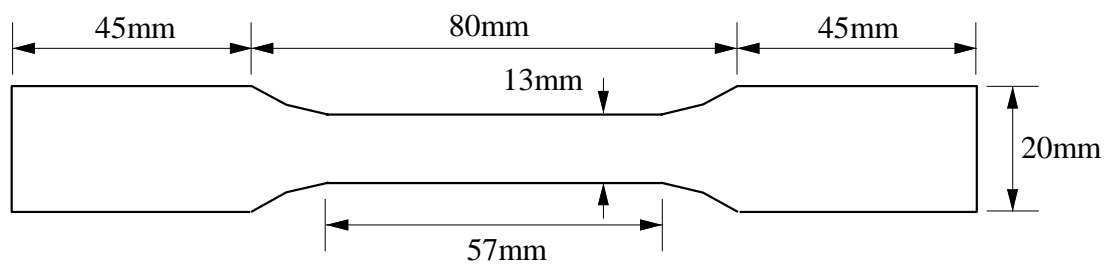


Figure 3.7: Dimensions of an adhesive coupon specimen

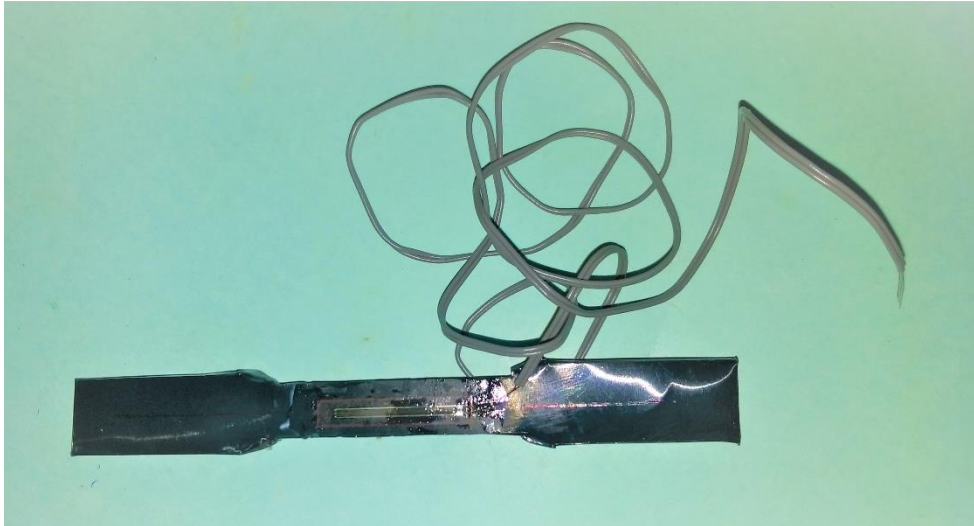


Figure 3.8 (a): Adhesive test sample with attached strain gauges



Figure 3.8 (b): Test setup of an adhesive coupon

Failure modes and test results

All specimens indicated a brittle failure mode as shown in Figure 3.9. The measured average tensile strength and its standard deviation were 30.13 MPa and 16.7 MPa, respectively.



Figure 3.9: The failure mode of an adhesive coupon

Long-term behaviour of the adhesive material is discussed in Chapter 09 along with the analytical/numerical analysis.

3.4 Steel

3.4.1 General

In the present study, naturally corroded steel specimens with four different corrosion levels; A) almost no rust, B) visible rust and flaking mill scale C) visible of pits and rusted mill scale and D) more pits with large in size, have been used. Steel plates which had been exposed to the open environment were chosen so that the different rust levels were represented. Initial material properties and the corrosion process of these plates are unknown and not monitored which is true for some deteriorated structures encountered. The rust level was identified by both visually and Scanning Electron Microscopic (SEM) images (Figure 3.10). An image analysing software was used to obtain the surface roughness characteristics of the steel plates by transforming the SEM images into 3D images (Chapter 04).

Measured Properties

The measured thickness of these rusted steel plates was about 5 mm. The steel coupon test was carried out for the steel plates subjected to different corrosion levels in accordance with ASTM 370-08a (ASTM, 2008) to determine the mechanical properties.

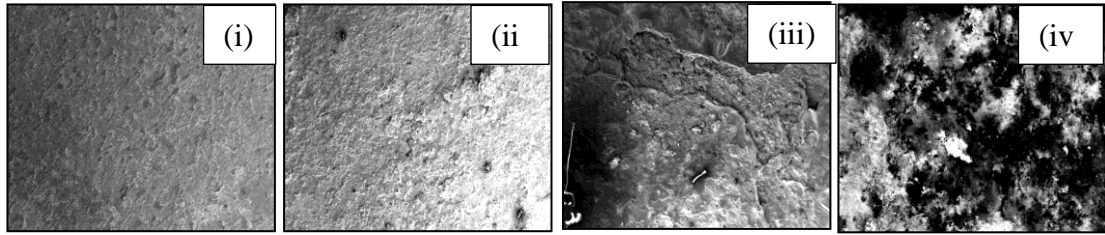


Figure 3.10: Scanning Electron Microscopic (SEM) Images of Rust Levels
(i) A (ii) B (iii) C and (iv) D

Preparation of coupon test specimens and test set – up

Dimensions of the rectangular steel tension test specimens were chosen as shown in Figure 3.11. Two steel coupons from each corrosion level, a total of eight steel coupons, were tested. Strain gauges were attached at the centre of each steel sample and strain readings were measured.

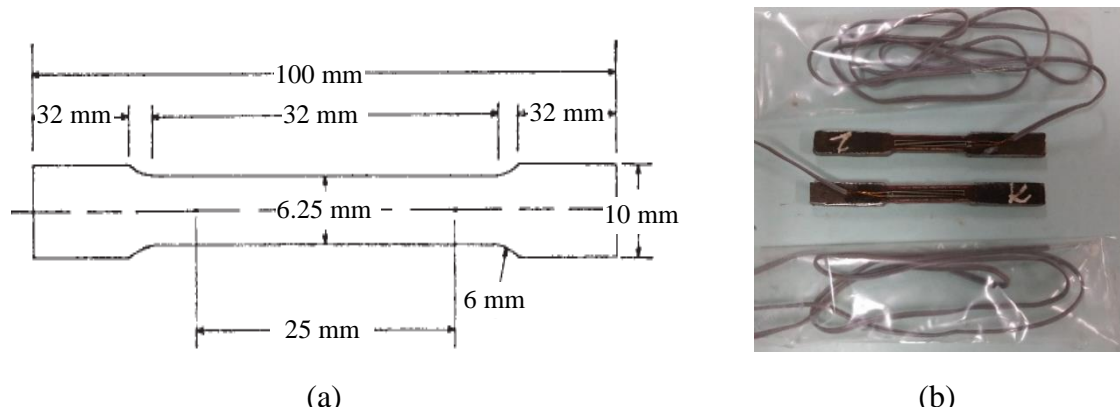


Figure 3.11: (a) A Steel Coupon (Schematic diagram, not in scale) (b) A prepared steel coupon with strain gauges attached in the middle

Failure modes and test results

The failure mode of a steel coupon specimen and the stress–strain relationship for all eight samples are shown in Figure 3.12 and Figure 3.13, respectively. The failure had occurred in between the gauge length of the coupon sample, yet closer to a one end. This must be due to the facts of smaller length of the steel coupon and the gripping system of the testing machine. However, when the figures 3.12 and 3.13 are explored, it can be deduced that the ductility of the steel has been somewhat reduced due to the corrosion. Elastic region of the stress–strain curves corresponding to all the steel plates

is seemed similar to each other. Hence, either secant modulus, or the tangent modulus of steel plates has not been changed with the severity of corrosion. However, there is a significant reduction in the ultimate strength with the corrosion level. The measured average ultimate tensile strength and the elastic modulus of these samples are listed in Table 3.4.

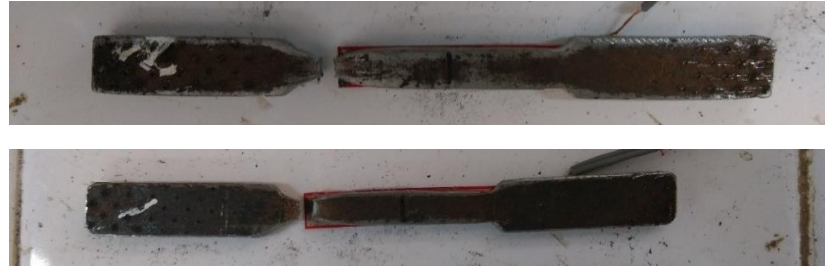


Figure 3.12: Failure mode of steel coupons

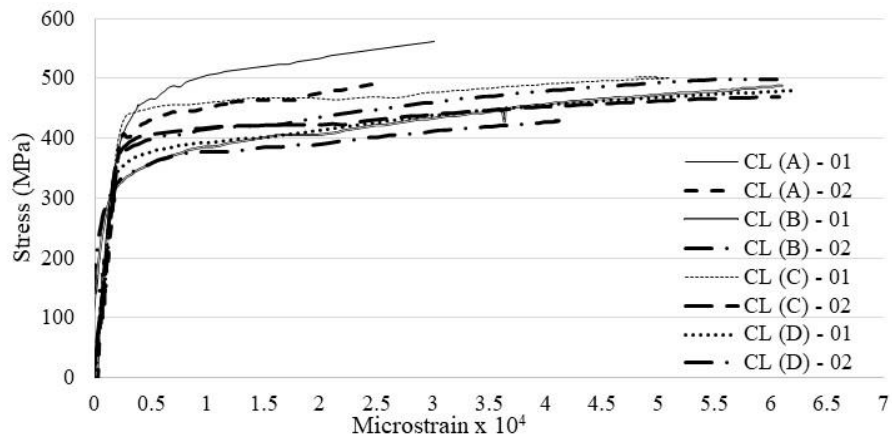


Figure 3.13: Stress – Strain curves obtained from steel samples of Corrosion level A, B, C and D

Table 3.4: Mechanical properties of steel samples

	Corrosion Level (A)	Corrosion Level (B)	Corrosion Level (C)	Corrosion Level (D)
Ultimate Load At Failure (kN)	14.68	12.18	15.88	14.43
Ultimate Tensile Strength (MPa)	583	487	508	513
Elasticity Modulus (GPa)	206.3	159.85	193.0	193.9

3.5 Summary

In this chapter, the material properties determined by performing tensile coupon tests are presented. Materials used in the process of investigation are X – Wrap C 300 - High strength carbon fibre uni-directional fabric, Araldite 420 A/B adhesive and structural steel with four different rust levels. The observed tensile test data for these materials are summarized below.

- ✓ Failure mode of CFRP test coupons was edge delamination occurred in the middle gauge area.
- ✓ The average mode of elasticity, average ultimate strength and the average ultimate strain of CFRP fabric are, 175.6 GPa, 1575 MPa and 8980.6 $\mu\epsilon$ respectively. It was observed that all the measured material property data are lesser than the manufacturer provided material property values. Hence, it highlights the importance of carrying out material property evaluation testing locally in accordance with the guidelines.
- ✓ Failure mode of adhesive test coupons was identified to be a brittle failure.
- ✓ The average tensile strength and its standard deviation of adhesive test coupons were 30.13 MPa and 16.7 MPa.
- ✓ The steel plates used in the experiments had been deteriorated under tropical environmental conditions and their initial material properties or the corrosion process are unknown. The steel specimens were identified to be in four different corrosion levels, namely, A) almost no rust, B) visible rust and flaking mill scale C) visible of pits and rusted mill scale and D) more pits with large in size. The average ultimate tensile strength of steel with corrosion levels A, B, C and D are 583 MPa, 487 MPa, 508 MPa and 513 MPa respectively.
- ✓ The stress – strain curves of steel coupons show a similar elastic region, deducing an unchanged nature of secant modulus, or the tangent modulus of steel plates.

CHAPTER 04

SEM (SCANNING ELECTRONIC MICROSCOPIC) ANALYSIS ON THE SURFACE MORPHOLOGY OF CORRODED STEEL SURFACES

4.1 Introduction

In order to ensure a better bond performance in CFRP bonded steel joints, it is essential to understand the factors affecting for the adhesion bonding. The adhesion strength of a bonded surface is dependent on its surface energy, surface chemical composition and the surface roughness & topography (Fernando, 2010). The method of surface treatment influences all these three surface characteristics and plays a major role in increasing the bonding capability of the substrate.

When the surface is prepared for bonding, initially, any contaminants present like oil, grease and water are removed by solvent cleaning or any other degreasing method which in general does not affect for the change of surface properties. However, based on the mechanical abrasion method used to roughen the surface, the surface characteristics can be changed. A proper technique is capable of increasing the surface energy so that the adhesive wets the adherend surface to create an intimate contact (Dawood, 2014; Fernando, 2010). Higher the free surface energy there is, the higher adhesion strength there will be. The chemical composition of the surface should be such that stronger primary chemical bonds can be formed. Hence, the steel surfaces are often cleaned after mechanical abrasion to remove any fine abrasive dust left in the surface and properly formulated primer is used to apply in the surface to achieve primary chemical bonding (Dawood, 2014).

Based on the roughness and the topography of the surface, force transfer through friction of the interfaces is rest. This mechanism is known as “Mechanical interlocking”. The literature has shown that in order to achieve a better interlock between the surfaces, the roughness of the surface should be maintained in such a way that the contact is secured in the roughened surface. Hence, it is essential to determine the optimum surface roughness characteristics required in adhesive bonding of CFRP/Steel joints to increase the bond durability of the strengthening system.

In practice, both profile roughness parameters and aerial field parameters are used to quantify the surface roughness characteristics. Areal field parameters are used to measure the areal surface texture while the profile parameters can be used to calculate the primary roughness and waviness profiles which only consider specific points and lines. In the present study, S_a (Arithmetical mean height of the irregular surface), S_z (Maximum peak height (S_p) + Maximum pit height (S_v)) and S_q (Root mean square height) have been used to evaluate areal parameters according to ISO 25178 while R_a (arithmetic mean roughness/mean height of the sampling length), R_z (Maximum Profile peak height (R_p)+ Maximum Profile pit height (R_v)) and R_q (root mean square roughness) were used to evaluate the profile roughness features based on ISO 4287. Mathematical expressions of these surface/profile parameters are as follows.

$$R_a = \frac{1}{l} \int_0^l |y(x)| dx$$

$$S_a = \frac{1}{A} \iint_A |Z(x, y)| dx dy$$

$$R_z = R_p + R_v$$

$$S_z = S_p + S_v$$

$$R_q = \sqrt{\frac{1}{l} \int_0^l \{y(x)\}^2 dx}$$

$$S_q = \sqrt{\frac{1}{A} \iint_A |Z^2(x, y)| dx dy}$$

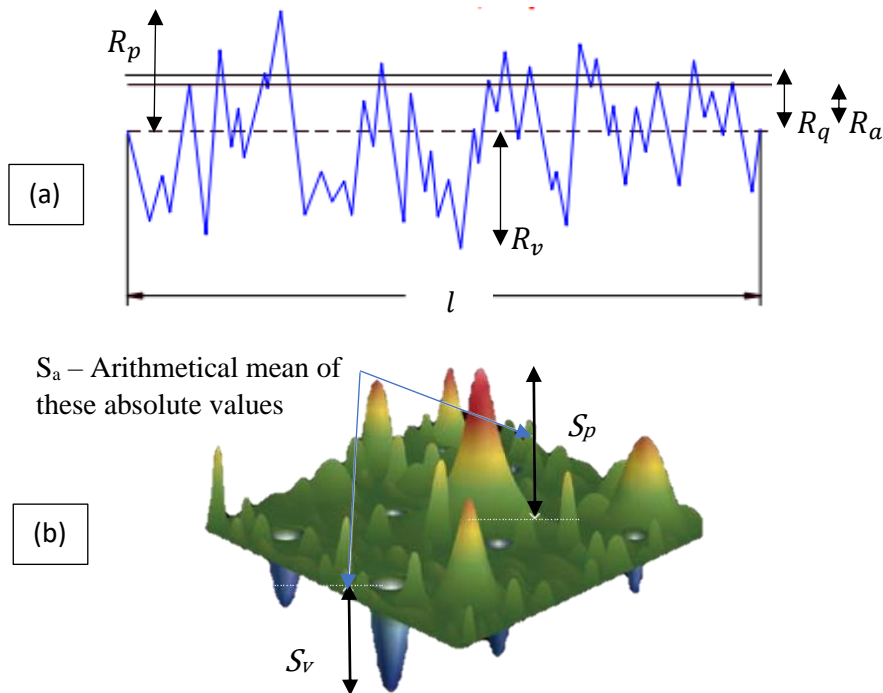


Figure 4.1: sampling wavelength (a) Profile roughness parameters (b) Area roughness parameters

In the present case of study, the influence of surface roughness characteristics of the corroded steel surfaces on the bond performance of the steel/CFRP composite joints were to be analysed. To determine the roughness properties of the steel specimens, an image analysing technique was used. SEM (Scanning Electronic Microscopic) images were taken of these metal samples and then the images had been analysed by a computer software. The procedure for the experiment is described as follows.

4.2 Surface Morphology

Analytical imaging techniques can be successfully engaged in characterization of surface topographical features. These methods can produce high resolution images using sophisticated microscopes. Scanning Electron Microscope (SEM) is one such advanced instrument which uses a beam of electrons to reveal detailed investigation on surfaces.

4.2.1 SEM Stereo - imaging

The surface morphology of the present study was performed by acquiring SEM stereoscopic pair of images for each steel surfaces with four different corrosion levels. A pair of 2D SEM images with two different tilted angles are used to evaluate the elevation of a particle/object surface. Knowing the heights/depths of the particle surface, these 2D images can be reconstructed to 3D images by applying a stereo-photogrammetric algorithm. For the effectiveness of the study, there are several commercially available computer programs developed to perform this image analysis technique. In the current study, MountainsMap® SEM : Version 7.2 by Digital Surf (Digital Surf, n.d.) has been used to gather information of corroded steel surfaces. The software also allows 3D enhancement of single SEM images by using an oblique electron beam.

Scanning electronic microscope used for the study is an instrument manufactured in Germany by the brand name of “ZEISS” and a model name of EVO 18 – Research. The maximum allowable size of an SEM analysing sample is 1 cm x 1 cm. The thickness of the sample should be limited to 1 cm and the thickness of the steel plates used in this experiment does not exceed 6 mm. Three numbers of 1 cm x 1 cm samples of each corroded steel plate with four different rust levels were cut and used for the

SEM imaging. The average surface property values were used for the evaluation of surface characteristics.

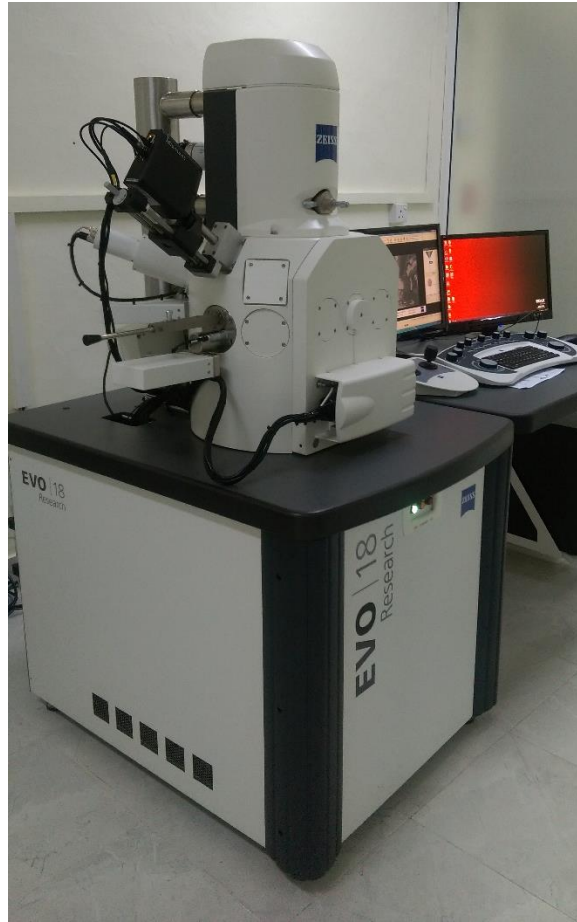


Figure 4.2: Scanning Electronic Microscope

4.2.2 Acquisition of the roughness parameters using 3D reconstruction

As mentioned in the previous section, a pair of 2D images are required to extract a 3D reconstructed image from the MountainsMap® software. The difference between the two tilted angles used for the present study varied between $3^\circ - 5^\circ$.

4.2.2.1 Evaluating the surface roughness parameters

The basic steps followed in obtaining the surface roughness (S) parameters are as follows.

Step 01: Uploading the SEM images (referred to as the studiabiles in the software).

Step 02: Scaling the uploaded images as per the scale mentioned in the SEM image by using the scale operator (Figure 4.3)

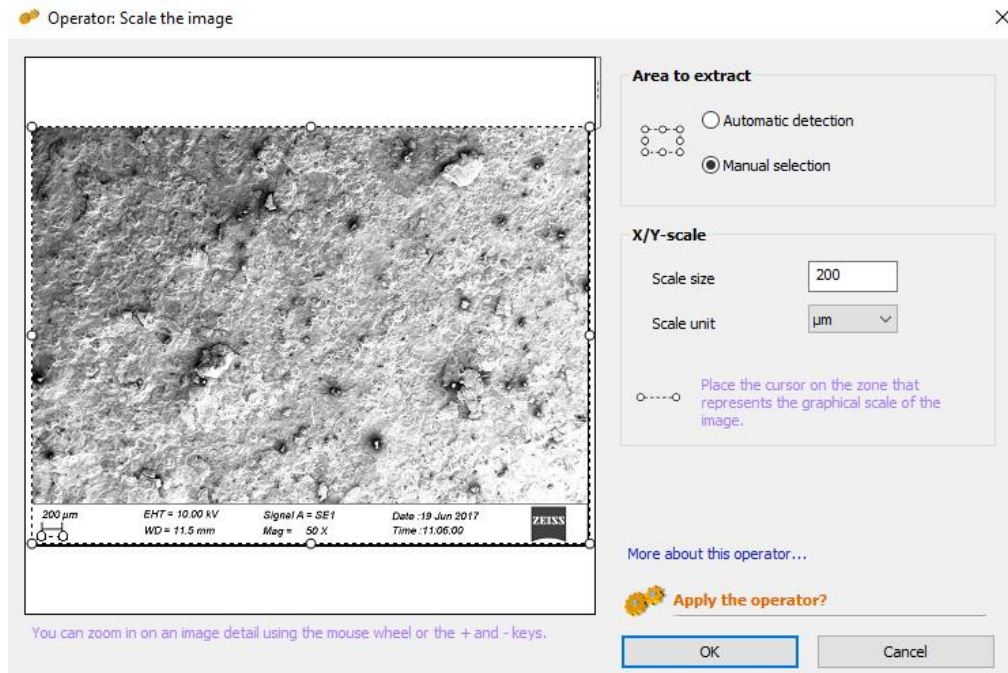


Figure 4.3: The scale operator

Step 03: Using the stereoscopic reconstruction operator and obtaining the 3D reconstructed image. Direction of the tilt, tilt angle and the end-effect adjustments are done here. The figure 4.4 shows the stereoscopic reconstruction operator when two images of the same surface with different tilted angles are loaded. A general view of a reconstructed 3D image in both pseudo-colour view and 3D view are shown in figure 4.5.

Step 04: Levelling the surface. Least square method is used (Figure 4.6).

Step 05: Removing the form which might be in the sample due to the acquisition, if it can be visually seen on the sample (Figure 4.7).

Step 06: Applying a standard filter to obtain the roughness – Gaussian filter with 0.8 mm cut-off length is used (Figure 4.8).

Step 07: Extracting the parameters table on the roughness obtained (Table 4.1).

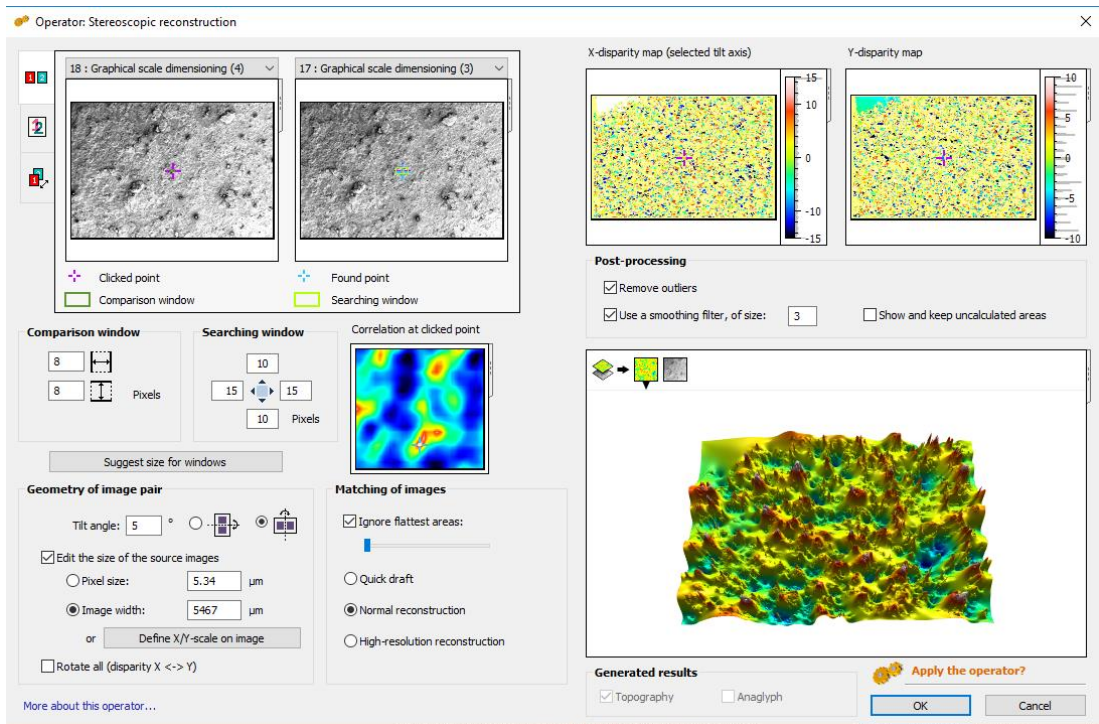


Figure 4.4: 3D stereoscopic reconstruction

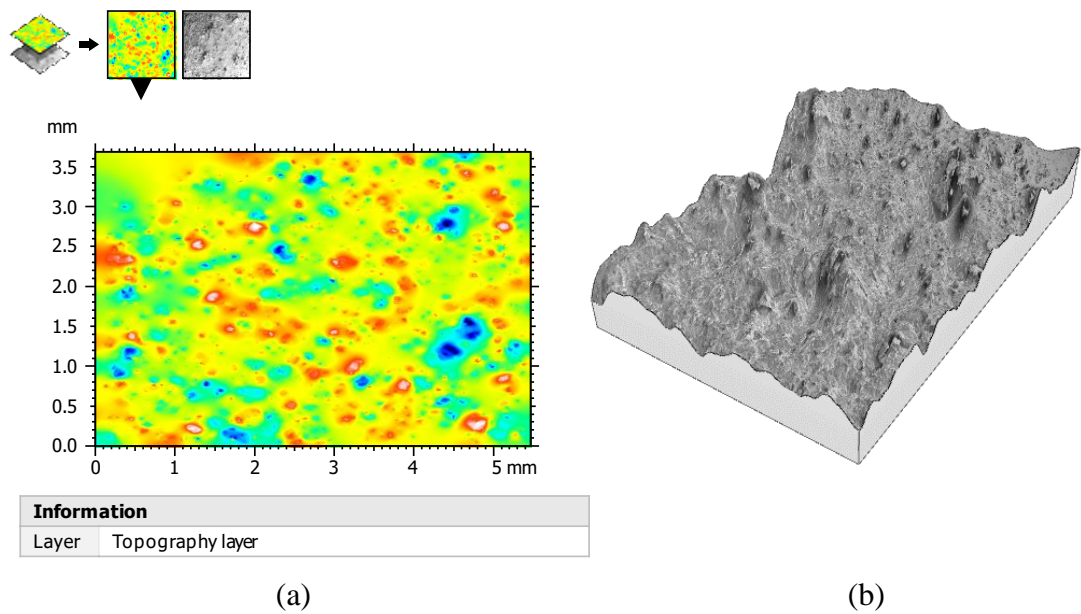


Figure 4.5: A 3D reconstructed image (a) Pseudo-colour view (b) 3D view

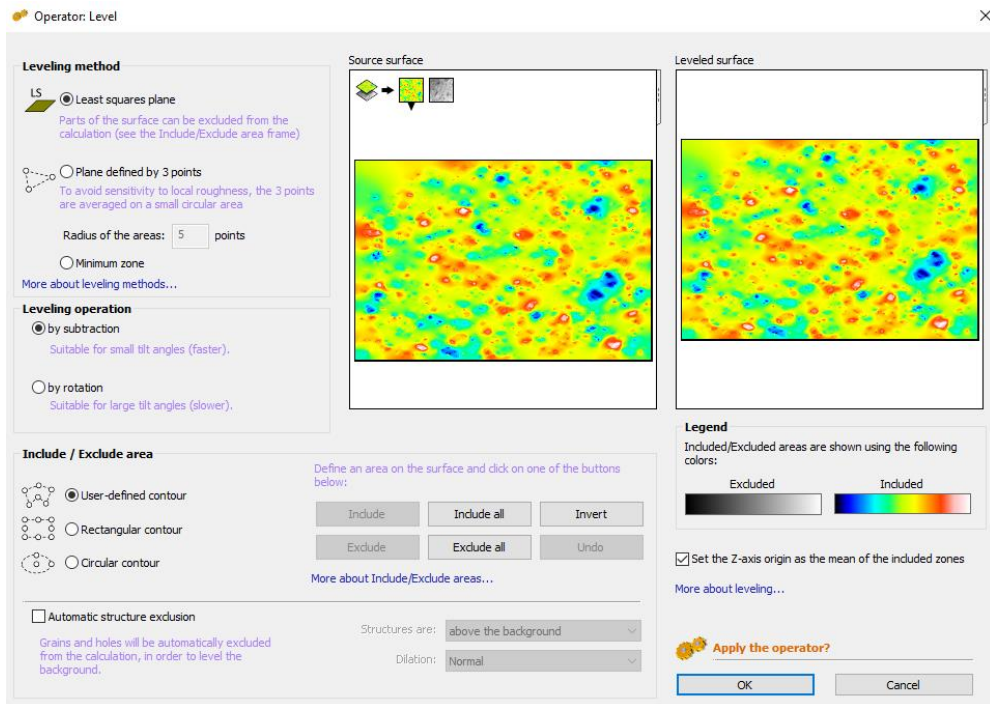


Figure 4.6: Levelling the surface using the Least Square Method

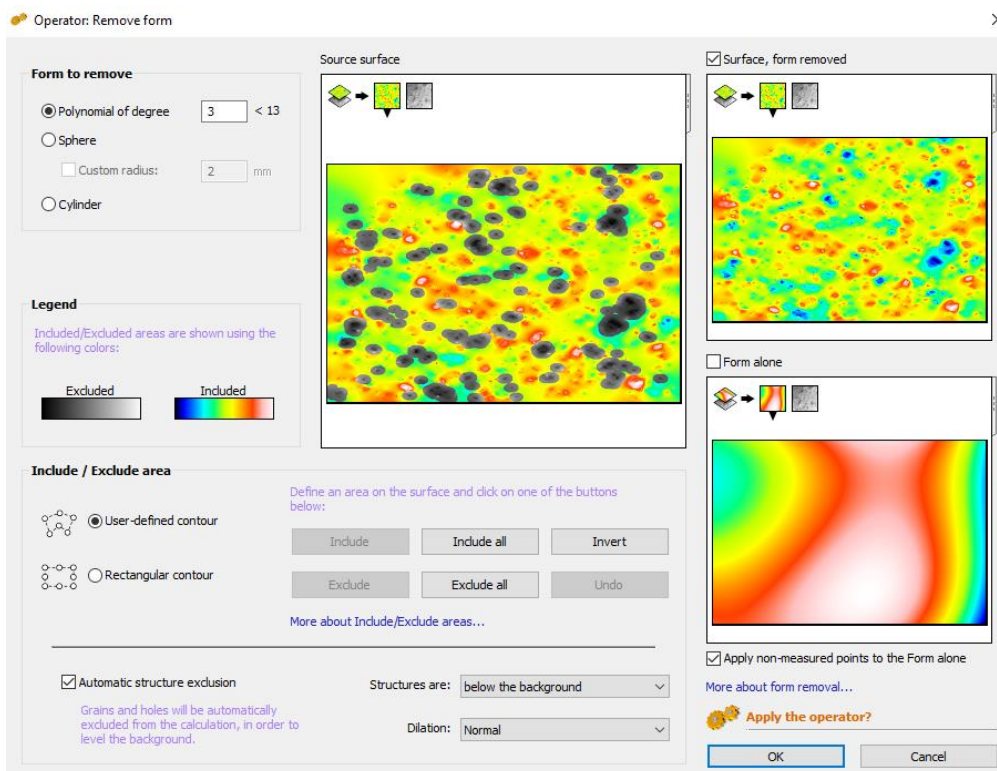


Figure 4.7: Form removal

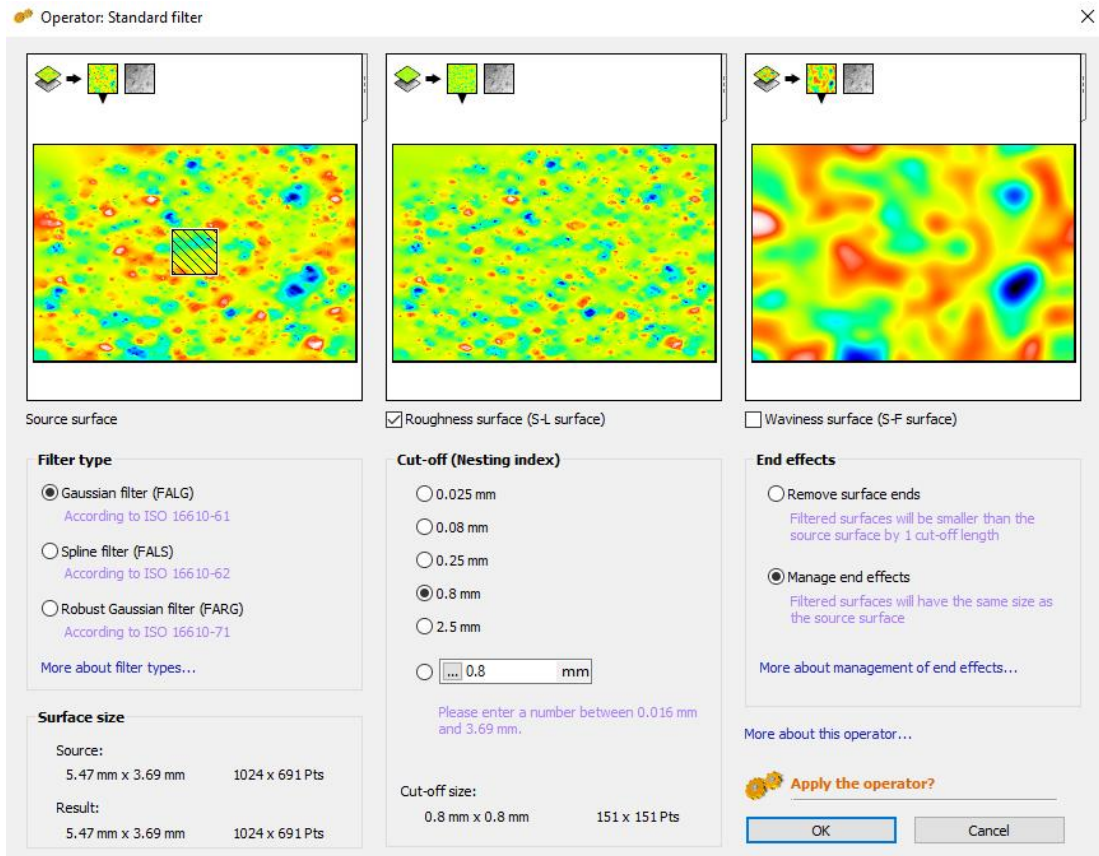


Figure 4.8: Using the standard filter (Gaussian filter, cut-off length = 0.8 mm)

Table 4.1: Parameters table obtained according to ISO 25178

Parameter		Value	Unit	Description
Functional parameters	Smr	0.000141	%	Areal material ratio
	Smc	0.277	mm	Inverse areal material ratio
	Sxp	0.561	mm	Extreme peak height
Height parameters	Sq	0.256	mm	Root-mean-square height
	Ssk	-		Skewness
	Sku	6.43		Kurtosis
	Sp	1.46	mm	Maximum peak height
	Sv	1.42	mm	Maximum pit height
	Sz	2.89	mm	Maximum height
	Sa	0.174	mm	Arithmetic mean height
Functional Parameters (Stratified surfaces)	Sk	0.00284	mm	Core roughness depth
	Spk	0.0259	mm	Reduced summit height
	Svk	0.0238	mm	Reduced valley depth
	Smr1	20.3	%	Upper bearing area
	Smr2	77.7	%	Lower bearing area

4.2.2.2 Evaluating the profile roughness parameters

Step 01- 05: Same as the steps described in the section 4.2.2.1.

Step 06: Extracting a profile on the surface where the profile roughness parameters are required (Figure 4.9).

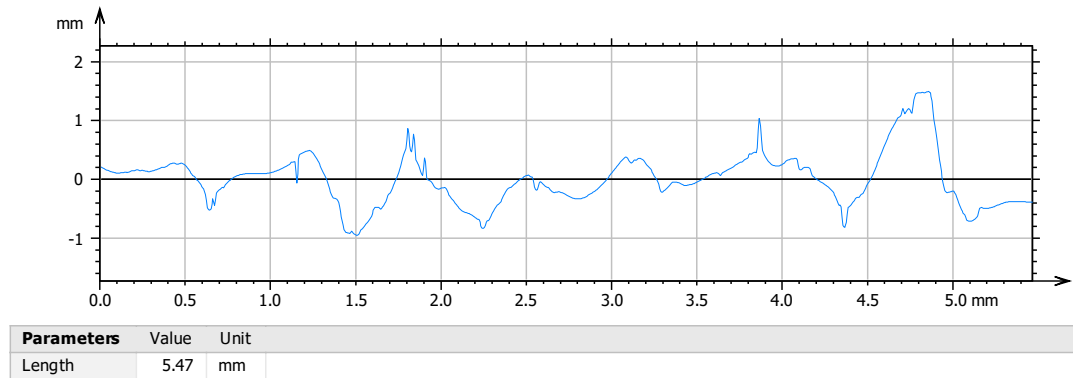


Figure 4.9: Extracted profile curve obtained for a corroded steel plate (Corrosion level (B)) before surface preparation

Step 07: Obtaining the parameters table. The filter size can be adjusted directly within the parameters table (Table 4.2).

Table 4.2: Parameters table obtained according to ISO 4287

Parameter	Value	Unit	Description	
Amplitude parameters - Roughness profile	Rp	0.482	mm	Maximum peak height of the roughness profile.
	Rv	0.477	mm	Maximum valley depth of the roughness profile.
	Rz	0.959	mm	Maximum Height of roughness profile.
	Rc	0.669	mm	Mean height of the roughness profile elements.
	Rt	1.58	mm	Total height of roughness profile.
	Ra	0.149	mm	Arithmetic mean deviation of the roughness profile.
	Rq	0.197	mm	Root-mean-square (RMS) deviation of the roughness profile.
	Rsk	-0.461		Skewness of the roughness profile.
	Rku	3.88		Kurtosis of the roughness profile.
Material ratio parameters	Rmr	0.114	%	Relative Material Ratio of the roughness profile.
	Rdc	0.331	mm	Roughness profile Section Height difference

4.3 Surface Metrology

4.3.1 General

R_a is the most commonly adopted parameter in the field to measure the surface roughness (Fontana, 1987; Kayser & Nowak, 1989; Rahgozar & Sharifi, 2011). It provides a better description of height variation of a surface along a specific sampling length. Alternatively, “ S_a ” extends this idea to a next level by measuring a mean height of the entire surface by considering the differences in heights at each point.

4.3.2 Profile and aerial field parameters

Tables 4.3 and 4.4 give the average surface texture measures obtained for each corrosion level after analysing the SEM images, before and after surface preparation.

Table 4.3: Profile Parameters (ISO 4287)

Corrosion Level	Before Surface preparation			After Surface Preparation					
				Method (1) – Fully grinded			Method (2) – Partially grinded		
	R_a (μm)	R_z (μm)	R_q (μm)	R_a (μm)	R_z (μm)	R_q (μm)	R_a (μm)	R_z (μm)	R_q (μm)
Non – Corroded/ Level (A)	1.65	7.09	1.96	53.50	407.75	80.65	3.48	20.45	4.57
Level (B)	4.30	20.58	5.30	45.24	305.74	65.75	14.62	74.20	17.95
Level (C)	12.10	60.05	14.80	26.90	156.50	35.80	14.48	96.15	19.70
Level (D)	77.88	643.50	127.73	17.78	94.43	22.63	14.77	93.18	20.07

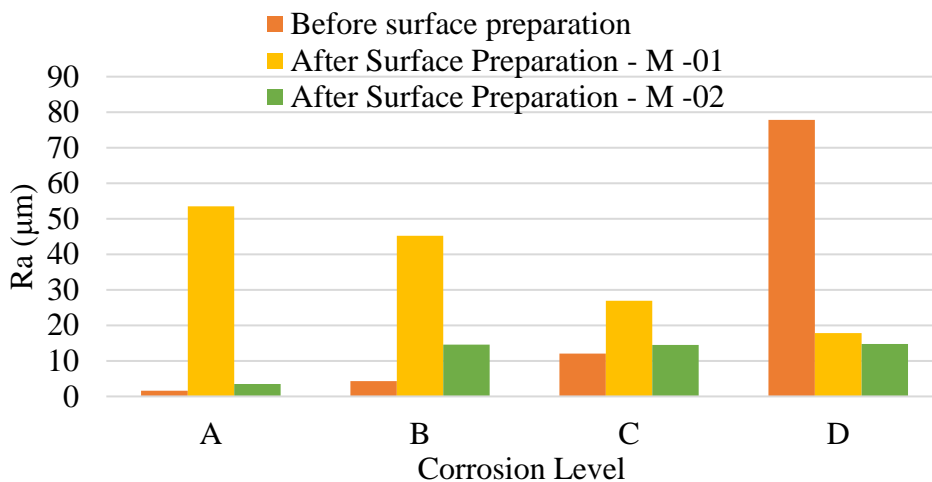


Figure 4.10: Variation of S_a with respect to the level of corrosion

Table 4.4: Areal Field Parameters (ISO 25178)

Corrosion Level	Before Surface preparation			After Surface Preparation					
				Method (1) – Fully grinded			Method (2) – Partially grinded		
	Sa (μm)	Sz (μm)	Sq (μm)	Sa (μm)	Sz (μm)	Sq (μm)	Sa (μm)	Sz (μm)	Sq (μm)
Non – Corroded/ Level (A)	4.08	51.45	5.22	72.90	2735.00	111.50	5.57	87.60	7.91
Level (B)	9.18	129.43	11.88	54.15	3555.75	95.28	16.48	362.25	21.68
Level (C)	16.45	297.00	21.30	35.40	774.50	49.30	14.85	498.00	38.15
Level (D)	40.20	5455.00	95.50	18.55	416.00	24.45	12.27	715.00	21.47

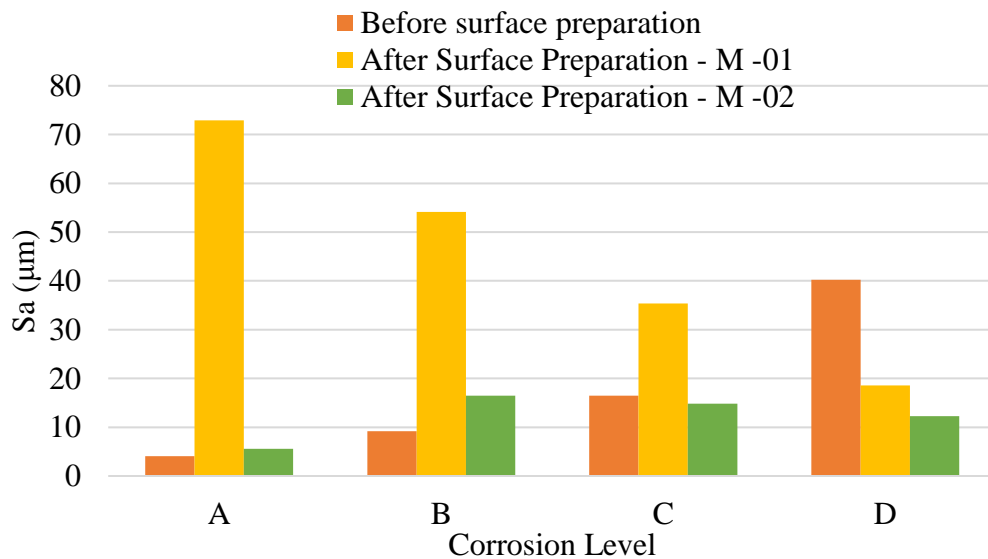


Figure 4.11: Variation of Sa with respect to the level of corrosion

The variation of roughness properties (figures 4.10 and 4.11) with respect to the level of corrosion clearly demonstrates the increment in the surface roughness with the increased degree of roughness characteristics of the surface. The M-01 method of which the surface was roughened by grinding showed increased roughness in non-corroded steel plates and a gradual declination of roughness properties with the increased dips and peaks on the surface. This can be explained as shown in the figure 4.12. In the bare steel plates, since the surface is having a uniform and regular roughness, the grinding disturbs the surface properties and increase the roughness

characteristics. In corroded steel plates, there are pits occurred due to the corrosion. When the surface is ground, the pit depths reduce, and the surface roughness properties are decreased.

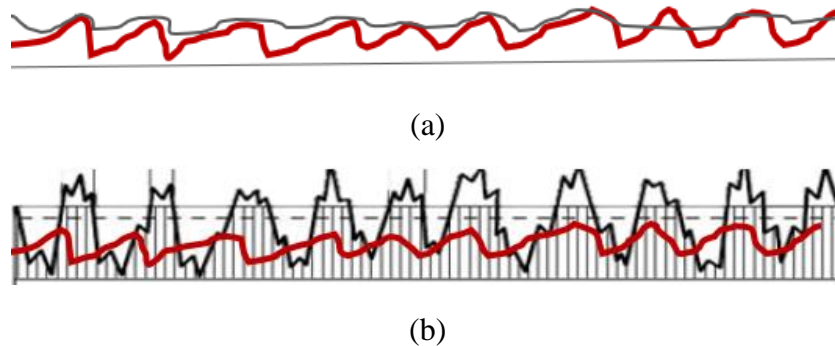


Figure 4.12: The effect of surface preparation by M-01 method (a) Non – corroded steel (b) Corroded steel

The M-02 method shows roughness characteristics varying in between a narrow range (S_a – in between 10 to 20 μm) for all M-02 treated corroded steel plates. In this surface preparation method, the corroded layer was completely ground away. Hence, almost all the pit depths of steel plates with all corrosion types were flattened. Thus, the final surface of a steel plate was relatively smoother compared to the surface made of M-01 method.

4.4 Summary

- ✓ Computer image analysing software has been used to evaluate the surface roughness characteristics of the corroded surface. Scanning electronic microscopic images have been used for this purpose.
- ✓ Both profile roughness parameters and the aerial field parameters were obtained and compared.
- ✓ An increased values of roughness measures were observed with the increased corrosion levels.
- ✓ When M-01 surface preparation method was used, the roughness characteristics increased with the increased corrosion level. The reason is the removal of the rust peaks on the corroded surface. The other method (M-02 method) resulted similar roughness properties on the steel surface due to the flattened dips and peaks on the substrate.

CHAPTER 05

EXPERIMENTAL PROGRAMME

5.1 Introduction

One of the main objectives of this research study is to investigate the effectiveness of using CFRP composite fabric in strengthening corroded steel structures. Since it has been identified that the weakest link of CFRP strengthened metallic joints is the adhesive bond between CFRP material and the steel substrate, the attention on evaluating the bond performance between these two adherents has grown interest in the field. However, most of the experimental studies present on this matter are carried out using non – corroded structural steel. Even though these steel plates are subjected to a surface preparation process to achieve a better bond, surface characteristics of the steel substrate may differ based on the initial surface roughness of the substrate. Therefore, a special interest has been paid in this study to consider the initial surface characteristics of the steel substrate to be strengthened by using naturally corroded steel plates with four different corrosion levels. The corroded steel plates used in the experiment are not gone under any artificial corrosion process and taken from naturally corroded steel elements. Double strap joints were made for the bond testing.

The experimental procedure was programmed into different stages as shown in the following flowchart (Figure 5.1). First, a preliminary investigation has been carried out to determine the effective bond length of the CFRP bonded steel joints. Then, a detailed investigation was performed to examine both short term and long-term bond performance. In this chapter, an introduction is given on how the experiments were planned and performed. The test and the analysis results are included in the forthcoming chapters under relevant category.

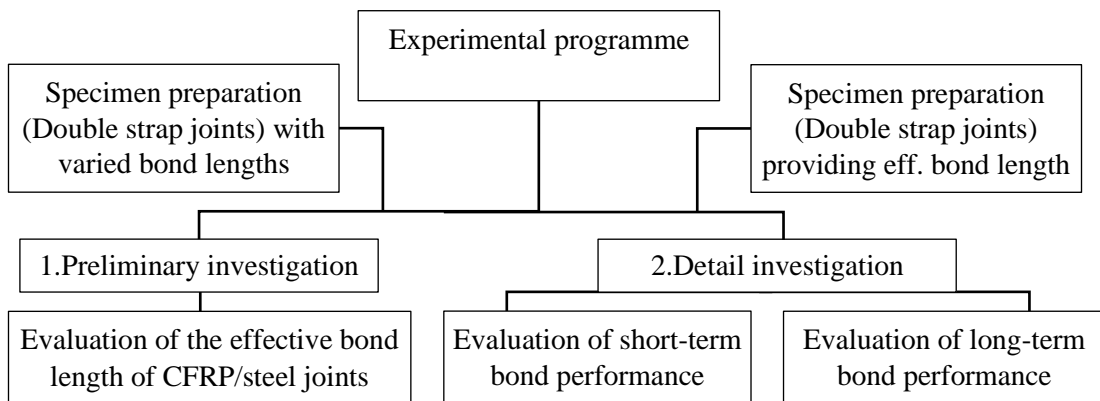


Figure 5.1: Summary of the experimental programme

5.2 Specimen Preparation and Instrumentation

5.2.1 General

The steel specimens used for the experiment are 38 mm wide and have a length of 162 mm. Rust levels of the steel plates were categorized into four levels; A) almost no rust, B) visible rust and flaking mill scale C) visible of pits and rusted mill scale and D) more pits with large in size. Figure 5.2 and Figure 5.3 show the original surface images and the SEM (Scanning Electronic Microscopic) images of the steel plates of all four rust levels, respectively. Araldite 420 A/B adhesive and normal modulus CFRP sheets were used in preparation of double strap bonded joints. The measured and manufacturer provided material properties are thoroughly described in a previous chapter, i.e. Chapter 03.

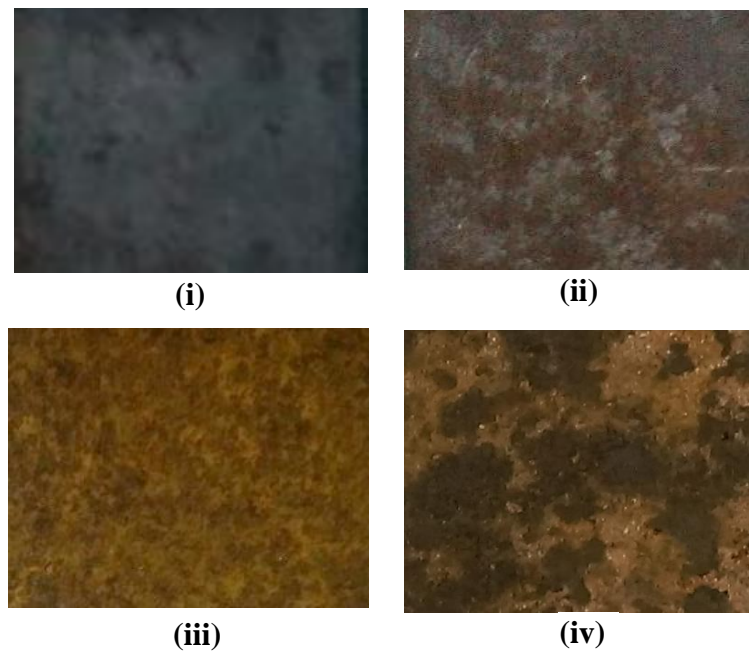


Figure 5.2: Visual images of Rust Levels (i) A (ii) B (iii) C and (iv) D

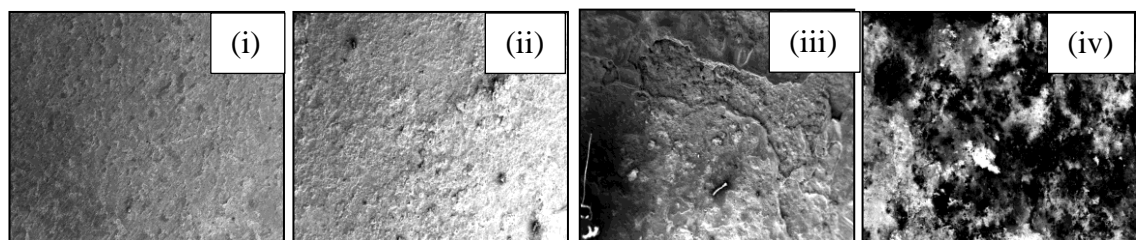


Figure 5.3: Scanning Electron Microscopic (SEM) Images of Rust Levels (i) A (ii) B (iii) C and (iv) D

5.2.2 Surface preparation

All the samples were cleaned and surface treated to remove any rust, impurities and chemically inactive oxide layers. Surface preparation of these steel plates was carried out by grinding the surfaces by an angle grinder in two different methods; removing the surface rust such that a roughened surface is achieved (M – 01) (Figure 5.4 (a)) and removing a thin layer of rust to achieve a smoother surface (M – 02) (Figure 5.4 (b)). Steel specimens of all corrosion levels were prepared using these surface preparation methods. The SEM images were taken after the grinding process in order to analyse the surface texture parameters of the cleaned specimens.

Generally, after a process of mechanical abrasion is carried out, the surface can remain with fine abrasive dust. Hence, prior to the application of adhesive material, the surfaces were thoroughly dry - wiped.

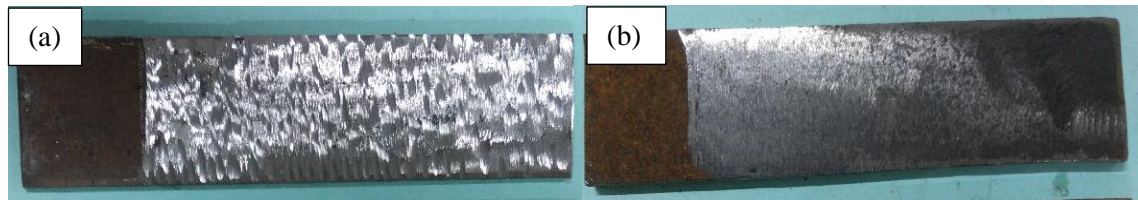


Figure 5.4: Corrosion level (C) samples after the surface preparation
(a) M – 01 (b) M - 02

5.2.3 Preparation of double strap joints

After the surface preparation, a thin layer of two-part epoxy primer (Figure 5.5) was applied using a brush and kept curing as the manufacturer had specified (6 – 24 hours). Then, CFRP sheets were bonded to the steel substrate using wet-lay-up method. An evenly distributed adhesive layer without air being entrapped in between was achieved by ribbed rolling into the fibre direction. All the specimens were kept for curing more than 7 days. Schematic diagram of a double strap joint and a prepared test specimen are shown in figures 5.6 and 5.7, respectively.

In the Figure 5.6, the locations of the strain gauges are denoted by X, Y and Z which are 35mm, 55mm and 60 mm away from the joint location. Strain readings were recorded using a data logger.

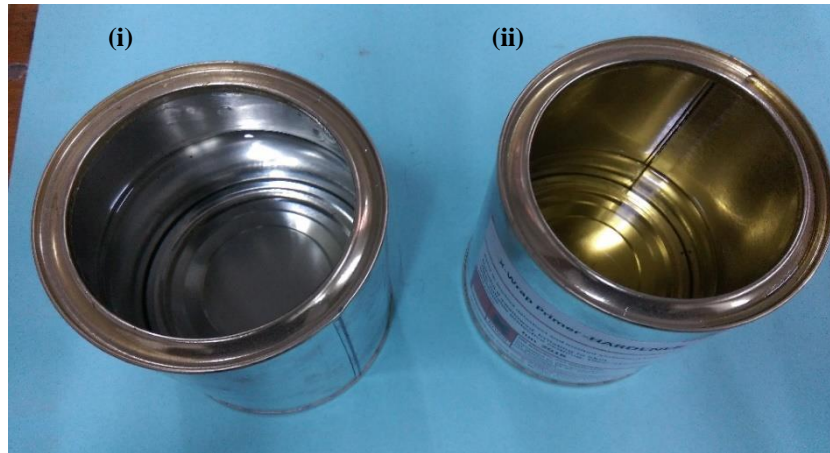


Figure 5.5: X – Wrap Primer (X – Calibur Structural Systems) (i) Base (ii) Hardener

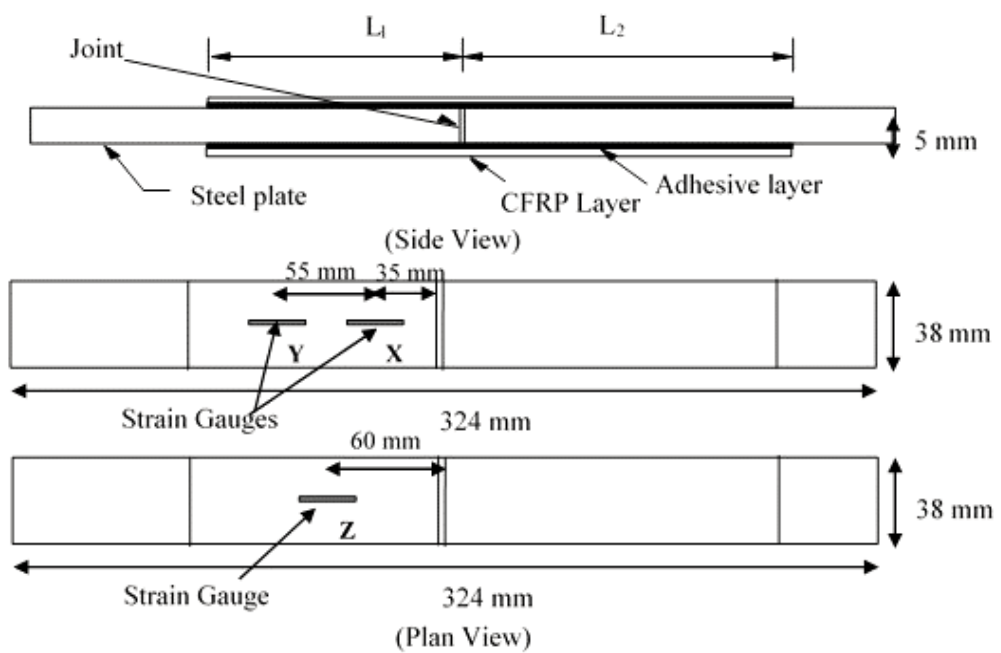


Figure 5.6: Schematic diagram of a double strap joint



Figure 5.7: Prepared test specimen of a double strap joint

When the sample preparation is finished, the double strap joints were tested in tension using a 1000 kN Universal Testing Machine at a displacement rate of 2mm/min. The Testing machine is shown in figure 5.8.



Figure 5.8: Universal Testing Machine

5.3 Preliminary Investigation

5.3.1 Effective bond length

The initial step of the test series was to determine the effective bond length of the CFRP/Steel double strap joint. In this regard, fully surface prepared pure steel plates were used. Unequal CFRP bond lengths, varying from 40 mm to 120 mm, were selected to prepare the double strap joints. A total of 14 specimens (Figure 5.9) were tested in tension using the testing machine. Table 5.1 summarizes the test results

obtained and the average load at failure against the bond length is plotted in Figure 5.10. As shown in the figure, the ultimate bond strength increases up to the 110 mm bond length. Beyond this length, the joint strength does not change significantly with the increased CFRP bond length. Hence, the effective bond length is determined as 110 mm and specimens with 120 mm bond length were chosen for the detailed investigation so that a full transfer of stresses can be ensured.

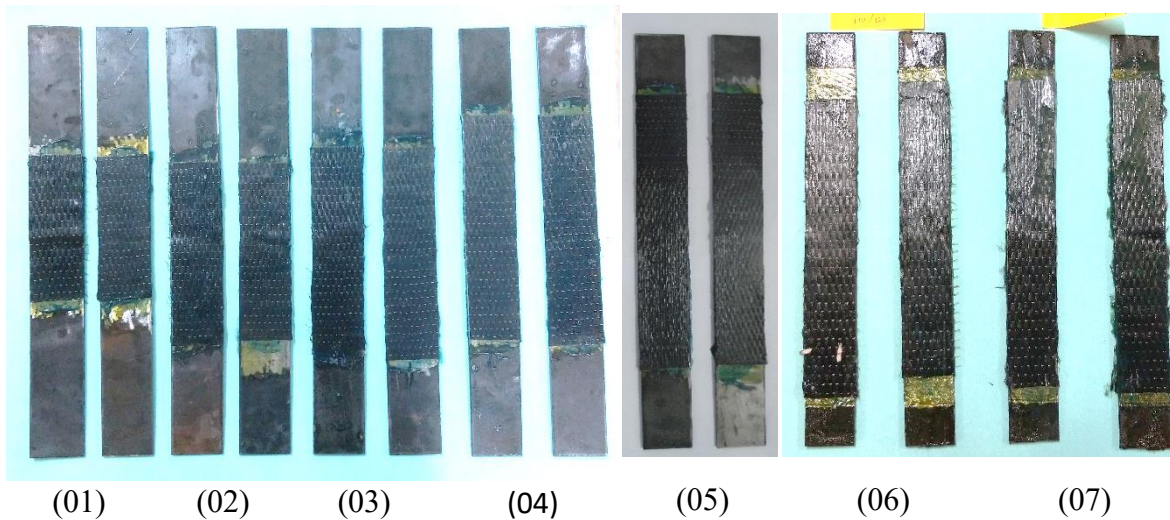


Figure 5.9: Double strap joints with unequal bond lengths

Table 5.1: Test results obtained for effective bond length investigation

Specimen No.	CFRP Bond Length (mm)		Average Load at Failure (kN)	Failure Mode
	L1	L2		
01	40	60	4.63	Steel – Adhesive interface debonding
02	60	75	5.95	Steel – Adhesive interface debonding
03	75	100	6.80	Steel – Adhesive interface debonding
04	90	100	8.53	Steel – Adhesive interface debonding
05	100	120	9.35	Steel – Adhesive interface debonding
06	110	120	15.15	Steel – Adhesive interface debonding
07	120	125	15.43	Steel – Adhesive interface debonding

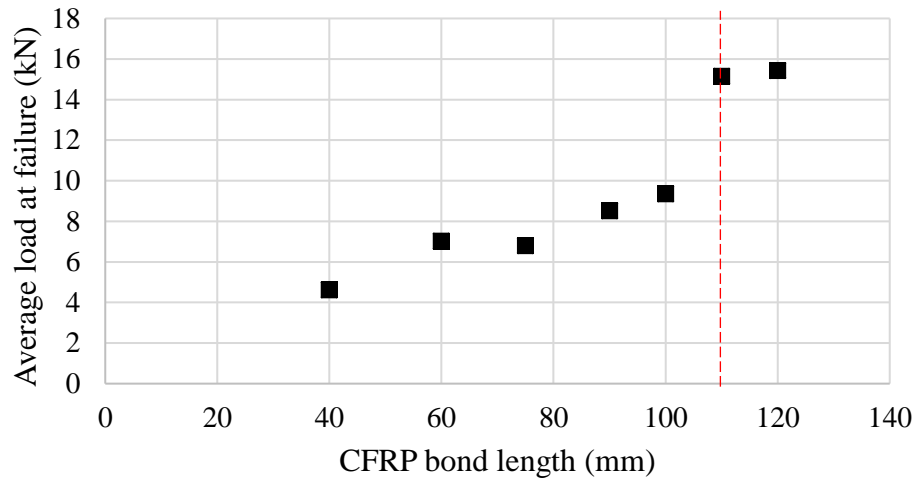


Figure 5.10: Average load at failure Vs. CFRP bond length

5.4 Detailed Investigation

A total of seventy-four specimens were tested. Twenty - eight samples were used to determine the short-term bond performance of corroded steel members with different surface textures, strengthened with CFRP. The remaining forty-six specimens were subjected to environmental conditioning for a period of 6 months. A full report on the detailed investigations carried out are well – described in the prospective chapters; i.e. Chapters 6, 7 and 8 as follows (Figure 5.11).

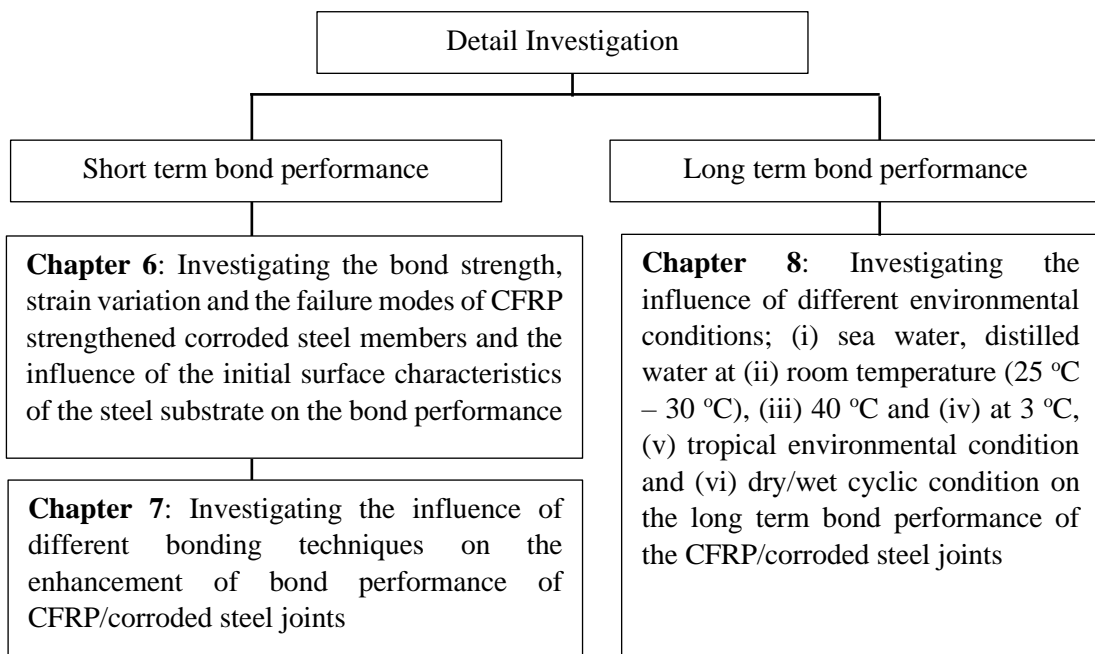


Figure 5.11: Flowchart of the programme for the detail investigation

5.5 Summary

This chapter is about the experimental programme designed to evaluate the effectiveness of using CFRP/steel composite systems in corroded steel surfaces. Thus, the content is sub categorized into 3 sections to describe the bond testing specimen preparation, preliminary investigation, and detailed investigation.

1. Specimen preparation

- ✓ Double strap joint specimens were made to test in tension using a 1000 kN Universal Testing Machine. Steel plates with all four rust levels have been used along with CFRP sheets, the adhesive and the epoxy primer.
- ✓ Surface preparation of the steel substrate has been done in two different methods; removing the surface rust such that a roughened surface is achieved (M – 01) and removing a thin layer of rust to achieve a smoother surface (M – 02).
- ✓ The surface texture parameters of steel surfaces have been achieved by analysing SEM images both before and after the surface preparation.

2. Preliminary investigation

- ✓ The effective bond length of the CFRP/steel double strap joint was determined as 110 mm.
- ✓ 120 mm bond length was used for the specimen preparation in the detailed investigation so that a fully transfer of stresses is ensured.

3. Detailed investigation

- ✓ Short term bond performance of CFRP composites in corroded steel surfaces is evaluated by investigating the bond strength, strain variation, the failure modes and by adopting different bonding techniques.
- ✓ Long term bond performance of CFRP/steel joints was evaluated by considering 6 different environmental conditions; (i) sea water, distilled water at (ii) room temperature (25 °C – 30 °C), (iii) 40 °C and (iv) at 3 °C, (v) tropical environmental condition and (vi) dry/wet cyclic condition.

4. A full description of both short term and long-term bond testing is provided in the successive chapters for clarity.

CHAPTER 06

SHORT TERM BOND PERFORMANCE OF CFRP STRENGTHENED CORRODED STEEL PLATES

6.1 Introduction

Most of the research studies present, which focused on strengthening corroded steel members, are performed using deteriorated steel bridge girders (Ahn, Kainuma, Yasuo, & Takehiro, 2013; Photiou, Hollaway, & Chryssanthopoulos, 2004) or circular hollow sections/pipes (Elchalakani, 2016; Shamsuddoha, Islam, Aravinthan, Manalo, & Lau, 2013). Hence, these studies highly concerned either on the flexural, axial performance or internal pressure capacities. Also, these steel members used are either artificially degraded by accelerated corrosion methods or subjected to simulate corrosion by thinning the member or inducing a notch. No amount of studies could be found which performed bond testing methods (described in Chapter 02) using corroded steel plates. The present experimental study was performed to suppress this research gap by considering both corroded and non-corroded steel plates in bond strength evaluation. Apart from assessing the joint strength of CFRP/steel joints, the study also focused on the effect of surface characteristics on the bonded joints, strain variation along the CFRP bonded length and the failure modes of the CFRP strengthened corroded steel plates.

6.2 Materials, experimental programme and test setup

6.2.1 Materials

Naturally corroded steel plates with four different rust levels have been used. Those rust levels were categorized as; A) almost no rust, B) visible rust and flaking mill scale C) visible of pits and rusted mill scale and D) more pits with large in size. The ultimate tensile strength of the steel plates of corrosion level A, B, C and D were identified as 583MPa, 487 MPa, 508 MPa and 513 MPa, respectively. Normal modulus CFRP sheets with a modulus of 175.6 GPa and an ultimate tensile strength of 1575 MPa were bonded to the steel substrate using the adhesive, Araldite 420 A/B. The measured average tensile strength of the adhesive is 30.13 MPa. Further, a layer of X – Wrap primer material was used in between the adhesive and steel substrate in order

to increase the durability of the bond. Chapter 03 provides all the necessary information of the material properties used in the experimental process.

6.2.2 Specimen preparation, instrumentation and testing

A total of twenty-eight double strap joint specimens were prepared in order to assess the short-term bond performance of CFRP/naturally corroded steel. Specimen preparation procedure is sequentially described in the previous chapter on the Experimental Program (Chapter 05). The effective bond length has been identified, which is 110 mm, from the preliminary investigation as described also in Chapter 05. A total of sixteen samples which are made with all four corrosion levels (Corrosion levels A, B, C and D) had been tested for their bond strength and strain distribution along the bonded length. The rest of the samples, i.e. twelve samples, were made only with rust levels B, C, and D and tested only for bond strength evaluation. Both surface preparation methods explained in Chapter 05; M – 01 (roughened surface) and M – 02 (smoother surface), have been adopted in the test series.

6.2.3 Profile roughness parameters

In order to obtain the surface characteristics of the steel specimens, SEM (Scanning Electronic Microscopic) images were used. Steel plates with all four rust levels have been used to take SEM images in their natural condition, i.e. before surface preparation. After the steel exteriors are surface treated with both M – 01 and M – 02 methods, SEM images were taken for each corrosion level and the surface preparation method. A detail description is provided on the SEM image analysis in the Chapter 04. Table 6.1 shows the test configuration of the experimental programme with the surface roughness characteristics of the steel plates.

Table 6.1: Test configuration of the experimental programme

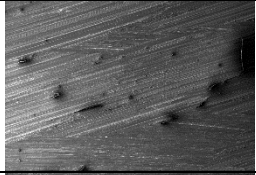
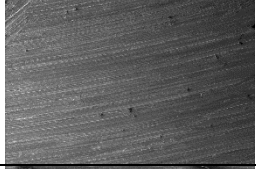
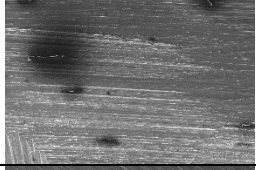
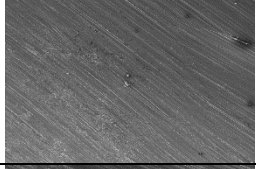
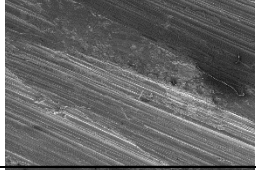
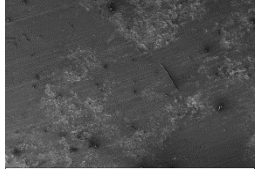
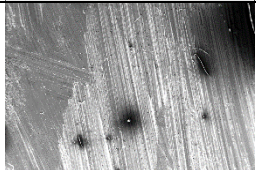

Specimen Name		Before surface preparation		After surface preparation	
Corrosion Level	Surface Preparation Method	R _a (μm)	S _a (μm)	R _a (μm)	S _a (μm)
		CL (A)	M – 01	1.65	4.08
M - 02	3.48		5.57		
CL (B)	M – 01	4.30	9.18	45.24	54.15
	M - 02			14.62	16.48
CL (C)	M – 01	12.10	16.45	26.90	35.40
	M - 02			14.48	14.85
CL (D)	M – 01	77.88	40.20	17.78	18.55
	M - 02			14.77	12.27

6.3 Test results

6.3.1 Ultimate bond strength

Table 6.2 summarizes the experimental results obtained from the short-term bond testing series along with the joint strength capacities and the failure modes. Bond strength evaluation of the double strap joint specimens was done by comparing the joint capacities with respect to the level of corrosion and the method of surface preparation. Fig. 6.1 shows the variation of average joint strength, with respect to the level of corrosion and the surface preparation technique. The double strap joints prepared under M-02 type showed higher short-term strength over M-01 samples for all corrosion types. The results show the highest increased joint strength of M-02 samples over M-01 samples for the corrosion level B (30% increment) and for the rest of the samples, it is around 15% increment. The range is observed to be in between 10% to 25% for the M-02 type corroded samples with respect to the joints prepared under similar conditions using pure steel plates. This is attributed to the fact that the removal of larger pits and thicker layer of corrosion products on the surface may result in average uniform surface profile and bond line which cause for uniform load transfer between the CFRP sheet and the substrate.

Table 6.2: Short term bond testing results

Sample No.	SEM (Scanning Electron Microscopic) Image	Failure Load (kN)	Ave. Ultimate Failure Load (kN)	Failure Mode
CL(A) M01-a		18.20	19.3	Steel/Adhesive interface debonding
CL(A) M01-b		20.40		
CL(A) M02-a		25.10	21.98	Steel/Adhesive interface debonding
CL(A) M02-b		18.85		
CL(B) M01-a		17.70, 16.10	18.63	Steel/Adhesive interface debonding and CFRP delamination
CL(B) M01-b		19.9, 20.8		
CL(B) M02-a		25.30, 21.55	24.27	Steel/Adhesive interface debonding and CFRP delamination
CL(B) M02-b		27.7, 22.45		
CL(C) M01-a		21.90, 21.60	22.87	Steel/Adhesive interface debonding and CFRP delamination
CL(C) M01-b		20.5, 27.45		
CL(C) M02-a		24.75, 27.15	26.94	Steel/Adhesive interface debonding and CFRP delamination
CL(C) M02-b		28.8, 27.05		
CL(D) M01-a		29.95, 27.00	23.58	Steel/Adhesive interface debonding and CFRP delamination
CL(D) M01-b		18.95, 18.4		
CL(D) M02-a		21.60, 28.50	27.45	Steel/Adhesive interface debonding and CFRP delamination
CL(D) M02-b		33.75, 25.95		

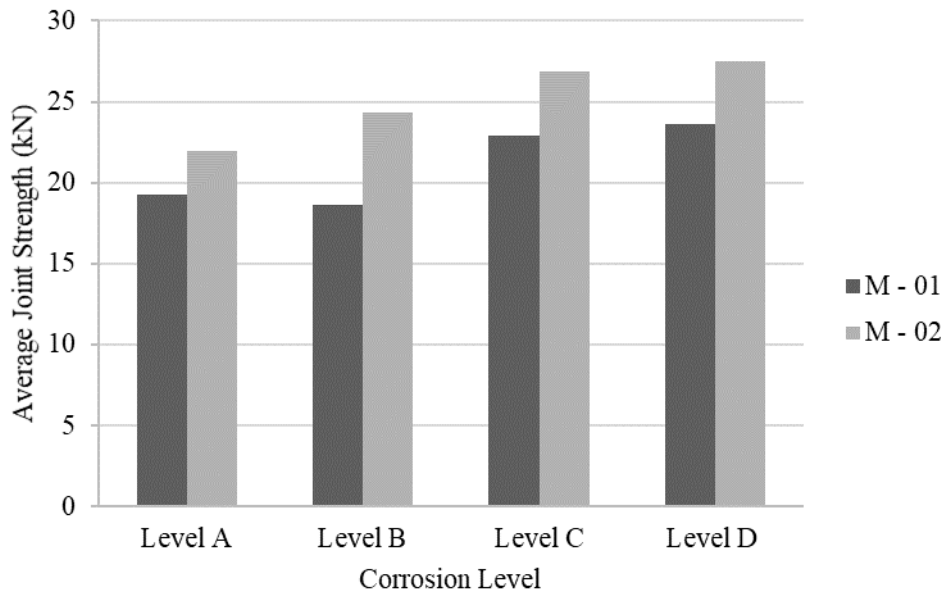


Figure 6.1: Variation of joint strength with the level of corrosion

An increased trend of bond strength values with the increased levels of corrosion was observed in the test results. This observation was detected in the samples prepared by both surface preparation methods. The results provide evidence for achieving higher strength gains (short-term) even though the steel plates are exposed to heavy corrosions, irrespective of the degree of surface treatment. This gives an indication that the bond performance of CFRP/Steel double strap joints is influenced by the initial surface roughness properties of the steel substrate.

Most importantly, the fact that attaining a higher joint capacity with the increased corrosion levels suggests the importance of pre-surface preparation of substrates to a standard/known roughness level so that the bond performance can be increased. With a known level of roughness and its required distribution, it will enable to adopt any of the available surface preparation methods in the field such as grit blasting, sand blasting or grinding with proper instrumentation and measurement.

6.3.2 The effect of surface roughness properties

Surface texture parameters obtained from the SEM images as explained in the Chapter 04 are used to analyse the roughness characteristics of steel specimens in both before and after the surface preparation. Among the various profile parameters

obtained, R_a which is the arithmetic mean roughness / mean height of a sampling length, and S_a which is the arithmetic mean roughness / mean height of a sampling area are used for the interpretation of results. Other useful profile parameters are R_z and R_q which symbolize the maximum height of the profile and root mean square deviation of the assessed profile respectively.

Information summarized in Figure 6.2 clearly depicts the increment in surface roughness of untreated corroded steel elements with the increased rust levels. After the surface preparation, a more or less same R_a value was observed in all corroded steel samples treated with M – 02 method (Partial surface preparation). This may be due to the flattening of the surface with the removed pits and peaks. Samples treated with M – 01 have shown a higher level of roughness than they had prior to the surface modification in non – corroded and lightly and medium corroded specimens (Corrosion levels A, B & C). The reason for this observation can be interpreted, as these corroded steel specimens do not consist of thick rust layers, grinding process must have disturbed its initial level of surface characteristics. For highest corrosion level (Corrosion level D) it is the other way around. This is mainly due to heavy dips and peaks in rust level D. This observation is visible with the areal roughness parameters as well. This aspect is graphically explained in the Chapter 04.

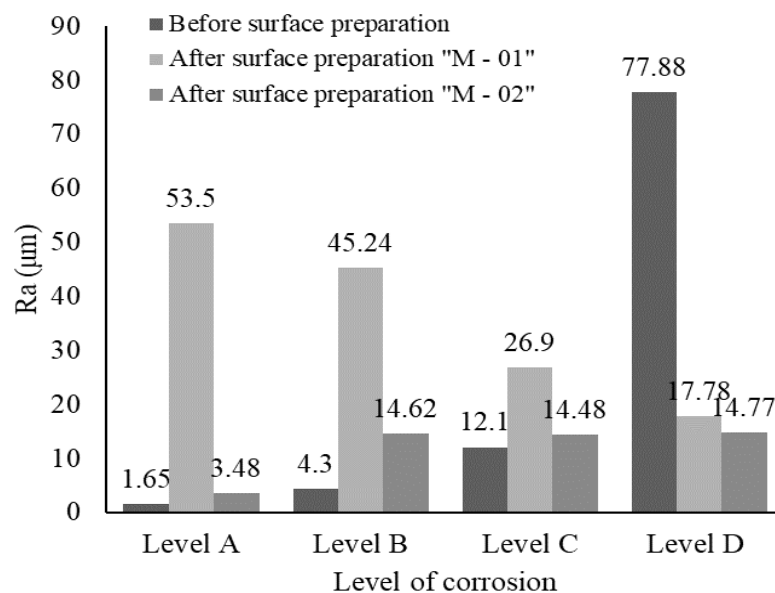


Figure 6.2: Variation of surface roughness measures with respect to the corrosion level

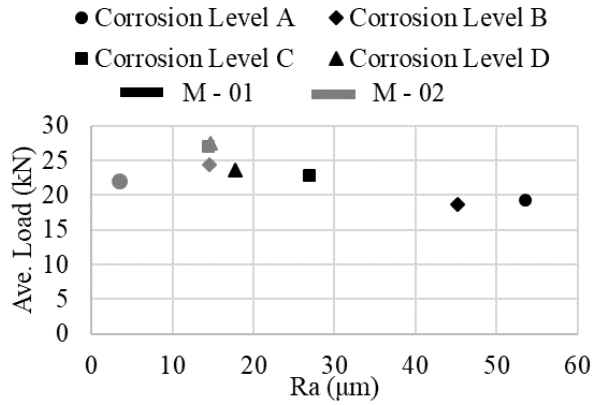


Fig 6.3: Variation of Joint strength with the R_a

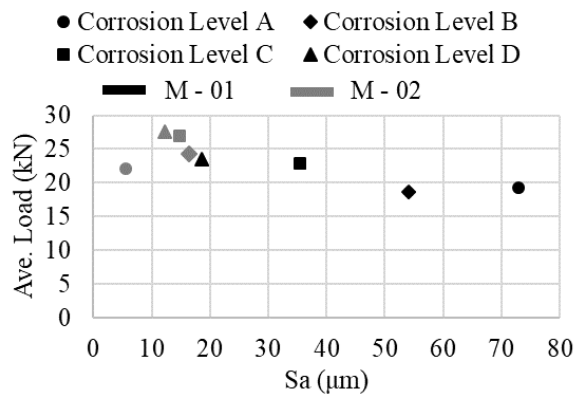


Fig 6.4: Variation of Joint strength with the S_a

According to the graph (Figure 6.3) plotted to explore the relationship between the average ultimate load and the profile surface roughness parameter (R_a), the highest ultimate loads were achieved for corrosion levels C and D when R_a is in the range of $10 \mu\text{m} - 20 \mu\text{m}$. Apparently, these results indicate a need for maintaining a lower surface roughness level for the corrosion levels A and B when the M-01 surface preparation is used. The reason for obtaining different bond performances and roughness parameters for the same method of preparation is due to the inherent roughness characteristics of corroded steel surfaces. Even though the mechanical abrasive methods are used to roughen the surface, this inherent surface roughness of the corroded steel plates contributes for the final roughness characteristics of the steel surface. The important thing noticed from these test results is the importance of having a uniform roughness distribution along with a high frequency to obtain maximum bond strengths as in the case of corrosion level D.

According to the comments made by Phan et al (Phan, Holloway, & Jiao, 2015), the profile surface roughness values are required to be between $0.73 \mu\text{m}$ and $7.75 \mu\text{m}$ in order to minimize the effect on bonding behaviour as well as the tensile capacity of the joints. Moreover, the profile roughness parameter obtained for the highest bond strength by Fernando et al., 2013 is about $2.95\mu\text{m}$. Yet, they have used steel plates with minimum initial roughness conditions (non – corroded steel) and did not consider the contribution of the inherent roughness properties induced by corroded steel surfaces. However, from the results illustrating in the Figures 6.1, 6.2, 6.3 and 6.4 it can be commented that the method of surface treatment must be changed for different corrosion levels depended on the initial roughness characteristics of the surface/substrate.

6.3.3 Strain variation along the CFRP bonded length

In order to attain the ultimate strains at failure and the variation of strains with respect to the considered parameters, strain gauges were attached to the shortest length (L_1) of the double strap joint specimens at 3 different locations. X,Y,Z denote these strain gauge locations which were 35 mm, 90 mm and 60 mm away from the joint, respectively (Figure 6.5).

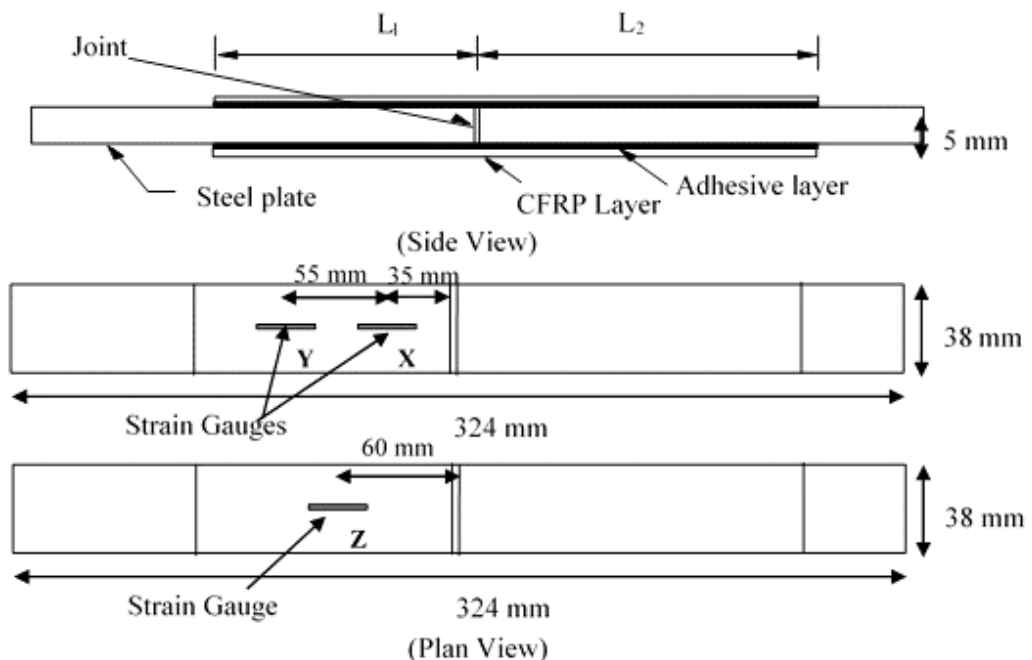


Figure 6.5: Schematic view of a double strap joint and the locations of the strain gauges

Figure 6.6 shows the variation in strain readings with respect to the increased tensile loading at X and Y locations. An important fact that we can extract from this graph is that the strain values getting decreased from location X to Y which is attributed to the fact of higher bond stresses closer to the joint and decreased shear stress distribution away from the joint that had observed by several previous studies (Fawzia et al, 2005). Unusual strain behaviour of CL (A) – M 02 – X had occurred due to the delamination of strain gauge in the process of loading. A sudden increase in the strain variation denotes the initiation of debonding of the CFRP/Steel joint. This occurs when the “X” strain reading is about 1100 microstrains for the M – 02 specimens with $R_a = 14.5 - 14.8 \mu\text{m}$ and 900 microstrains for the M – 02 specimens with $R_a = 3.5 \mu\text{m}$. But the strain reading at the same location for the M – 01 specimen with $R_a = 53.5 \mu\text{m}$ is only 280 microstrains. This indicates the load transfer between two elements depends on the roughness of the substrate.

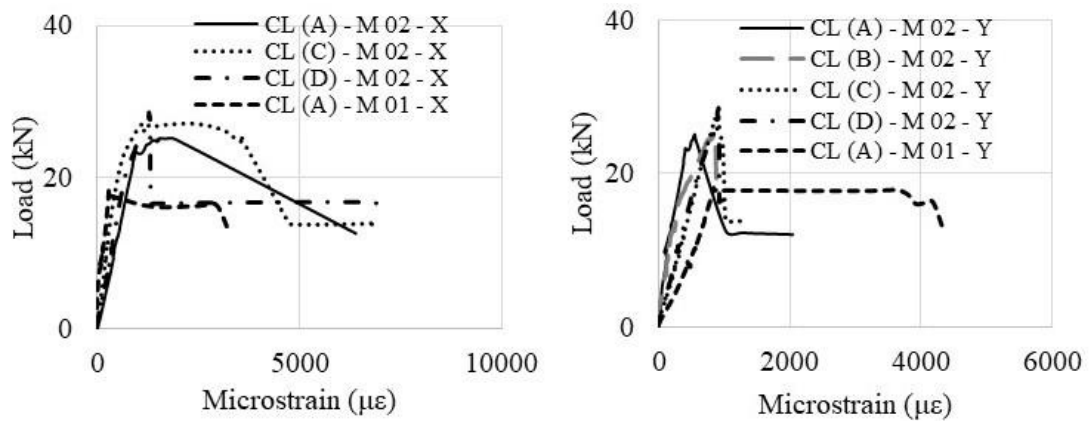


Figure 6.6: Strain variation in CFRP/Steel joint (a) 35 mm (b) 90 mm away from the joint

6.3.4 Failure Modes

It has been identified that an FRP – steel adhesive bonded joint can be failed basically in six different failure modes. They are a) Steel/adhesive interface debonding, b) Adhesive layer failure (Cohesion failure), c) FRP/adhesive interface debonding, d) FRP delamination and e) FRP rupture (Chapter 2, Section 2.4.2). The typical failure mode of the CFRP/ Steel double strap joints was steel/adhesive interface debonding for the corrosion level A while it was a combination of

steel/adhesive interface debonding and CFRP delamination for all other corrosion levels (Figure 6.7). This shows that the failure mode has transferred to become more of a cohesive failure for the higher corrosion levels. Non – uniform surface profile with the presence of corrosion pits might be the reason for this observed failure modes which caused non-regularity in the adhesive thickness. However, in the literature it confirms that the failure modes for a normal modulus CFRP sheet are steel/adhesive debonding and FRP delamination (Zhao & Zhang, 2007). Steel samples which are already corroded are having a certain roughness itself because of the pits formed and hence this observation implies that an increased surface roughness is required for a better bonding of the CFRP sheets to the steel substrate.



Figure 6.7: Failure modes observed for the specimens

6.4 Summary

The purpose of this test series is to evaluate the short-term performance of CFRP/steel joints considering the surface roughness characteristics of the rusted steel surface. Thus, the bond strength, strain variation and the failure modes are considered. Twenty-eight number of double strap joint specimens have been prepared as described in the Chapter 05. Steel plates with all corrosion levels were used in sample preparation and two methods of surface preparation were adopted as mentioned. Observations and the conclusions obtained from the testing are summarized below.

- ✓ Average joint strength was observed to be higher when CFRP/steel joints were prepared with M – 02 method for all corrosion types. The M – 02 samples prepared with corrosion level (B) showed the highest increment in joint strength over M – 01 samples which was about 30 % and it was about 15 % for all other corrosion types.
- ✓ According to the test results obtained, increased joint capacities were observed with the increased rust levels. This remarks the importance of

considering the surface roughness level of steel substrate in CFRP/ steel metallic joints. Also, the M – 02 treated CFRP/Steel joints showed the higher bond capacity over the M – 01 treated joints in all corrosion levels.

- ✓ Surface roughness parameters obtained for untreated steel plates confirm the increment in rust level with the increased surface roughness values.
- ✓ Similar roughness characteristics were observed for all corroded samples prepared with M – 02 method ($R_a = 14.5 - 14.8 \mu\text{m}$). However, decrement in roughness parametric value was observed after the surface treatment for corrosion level D when prepared with M – 02.
- ✓ Roughness properties increased in non-corroded steel plates when treated with M – 01 method and decrement in these properties was observed with the increased corrosion levels.
- ✓ Strain variation along the bonded length confirms the decreased shear stress distribution away from the joint as observed by previous research.
- ✓ The failure mode was steel/adhesive interface debonding for the corrosion level A while it was a combination of steel/adhesive interface debonding and CFRP delamination for all other corrosion levels.

CHAPTER 07

EFFECTS OF BONDING TECHNIQUES OF CFRP STRENGTHENED CORRODED STEEL PLATES ON SHORT TERM PERFORMANCE

7.1 Introduction

When the already corroded members are to be strengthened with CFRP materials, the durability of the strengthening scheme should be assured by taking necessary actions to prevent further progression of corrosion. When the strengthened units are exposed to different environmental conditions, it can negatively influence for the structural and the durability performance of the structure. CFRP/Steel joints in aggressive environments are in risk not only due to the general forms of corrosion such as uniform and pitting corrosion, but also due to the possibility of occurring galvanic corrosion. The literature (Tavakkolizadeh & Saadatmanesh, 2001) has identified that CFRP strengthened steel members can be subjected to galvanic corrosion when there is a direct contact between the Carbon fibres and the steel plate in the presence of an electrolyte with a sufficient conductivity. The literature suggests preventing the contact in between a CFRP/Steel joint by introducing a non – conductive barrier (Tavakkolizadeh & Saadatmanesh, 2001). Providing a GFRP (Glass Fibre Reinforced Polymer) is recommended by many a research studies as it provides an additional benefit of strength enhancement as well (Mertz, Gillespie, Chajes, & Sabol, 2002; Miller, Chajes, Mertz, Hastings, & Member, 2001; Tavakkolizadeh & Saadatmanesh, 2001)

The current research study is carried out to determine the bond strength enhancements of CFRP/Steel joints with a presence of an interfacial barrier layer in between CFRP and steel by considering surface roughness of corroded steel plates. In this regard, a layer of GFRP and a commercially available polymer mesh had been utilized to avoid direct contact between CFRP and steel. Six number of bonding techniques were considered for the make of double strap joints and total of 12 steel/CFRP joints were tested in direct tension for the bond strength evaluation.

7.2 Materials, experimental programme and test setup

A total 12 number of double strap joints were prepared with 6 different bonding configurations. All the samples were tested in tension by 1000 kN Universal Testing Machine for the bond strength evaluation.

7.2.1 Materials

Naturally corroded steel plates chosen for the experiments were having slight pits and mill scale has rusted away (Corrosion level C as defined in Chapter 05). Surface roughness parameters of a steel plate were found to be as follows; 12.10 $\mu\epsilon$ and 16.45 $\mu\epsilon$ of arithmetic mean heights of the sampling length (R_a) and the irregular surface (S_a) respectively, 60.05 $\mu\epsilon$ and 297.00 $\mu\epsilon$ of maximum height difference of the profile length (R_z) and the surface (S_z) respectively, 14.80 $\mu\epsilon$ and 21.30 $\mu\epsilon$ of root mean square heights of the profile length (R_q) and the surface (S_q) respectively. These corroded steel plates used for the double strap joint specimens were having a thickness of about 5 mm average. Araldite 420 A/B was the adhesive used for the bonding of strengthening sheets. Apart from the materials described in the Chapter 03, GFRP and a commercially available polymer mesh were used as an insulation material in between the steel surface and the CFRP sheet. Mechanical properties of the materials used in the investigation were tested according to the relevant ASTM standards (Chapter 03) and the obtained results are summarized in Table 7.1.

Table 7.1: Material Properties

Mechanical Property	Elasticity Modulus (GPa)	Ultimate Tensile Strength (MPa)	Thickness (mm)
Steel	193	508	5
Adhesive	1.495	30.13	< 1
CFRP	175.6	1575	0.166
GFRP (manufacturer provided)	76	2300	0.36

7.2.2 Specimen preparation

A schematic diagram of a double strap joint with the relevant dimensions and the strain gauge locations is shown in figure 7.1. Effective bond length of the

test specimens was determined by carrying out a series of experiments with varying bond lengths and it was found out to be 110 mm (Chapter 05, Section 5.3.1). Hence, L_1 and L_2 were taken as 115 mm and 120 mm separately.

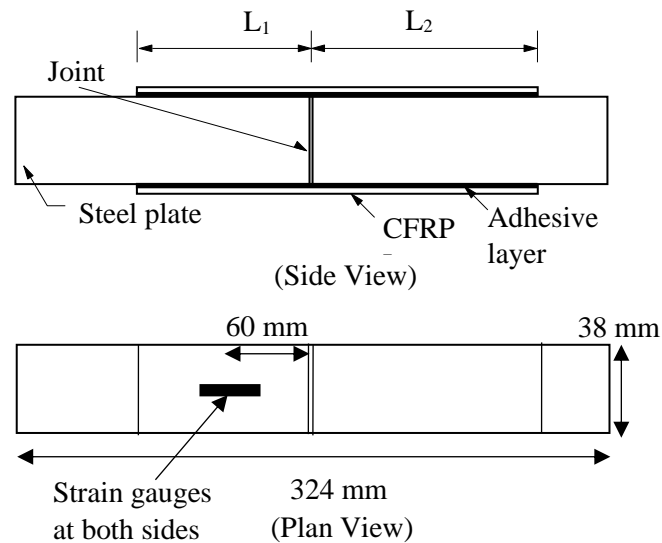


Figure 7.1: Schematic diagram of a double strap joint and the location of strain gauges

Surface preparation of the steel plates was achieved by grinding away the rust and other contaminants on the steel substrate. This method of surface treatment is defined as “M – 01” in the Chapter 05, Section 5.2.2 which was achieved by removing a thin layer of rust to achieve a smoother surface.

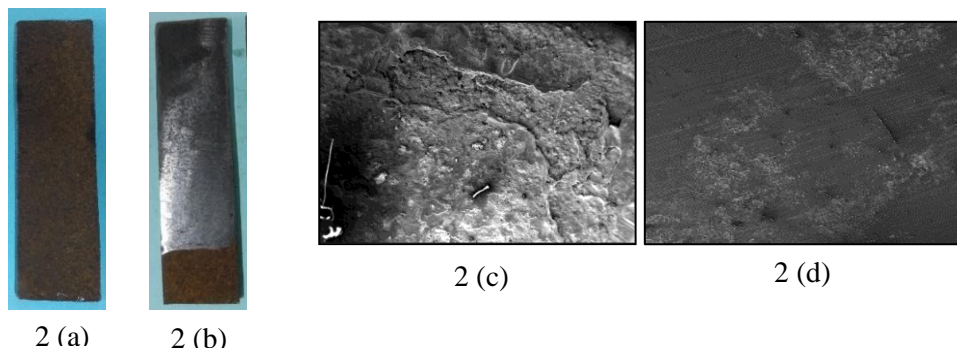


Figure 7.2: (a & b) corroded plate before and after surface preparation, (c & d) relevant SEM images, respectively

Figure 7.2 shows a prepared and a non – prepared steel surface and their relative SEM (Scanning Electron Microscopic) images. Soon after the surface preparation, a primer layer was applied in order to protect the surface before the CFRP bonding and improve the bond strength as well as the durability. After minimum of 6 hour curing time, yet

not more than 24 hours, double strap joints were made as described in the Chapter 5, Section 5.2.3.

7.2.3 Bonding configurations

The double strap joints were made in six different bonding arrangements as described in figure 7.3: (a) CFRP only, (b) GFRP only, (c) Polymer mesh only (d) GFRP layer embedded in between steel and CFRP (e) Polymer mesh embedded in between steel and CFRP and (f) CFRP layer sandwiched in between GFRP layers. All the FRP and polymer layers are saturated with an adhesive layer and it is not shown in figure 7.3 for clarity.

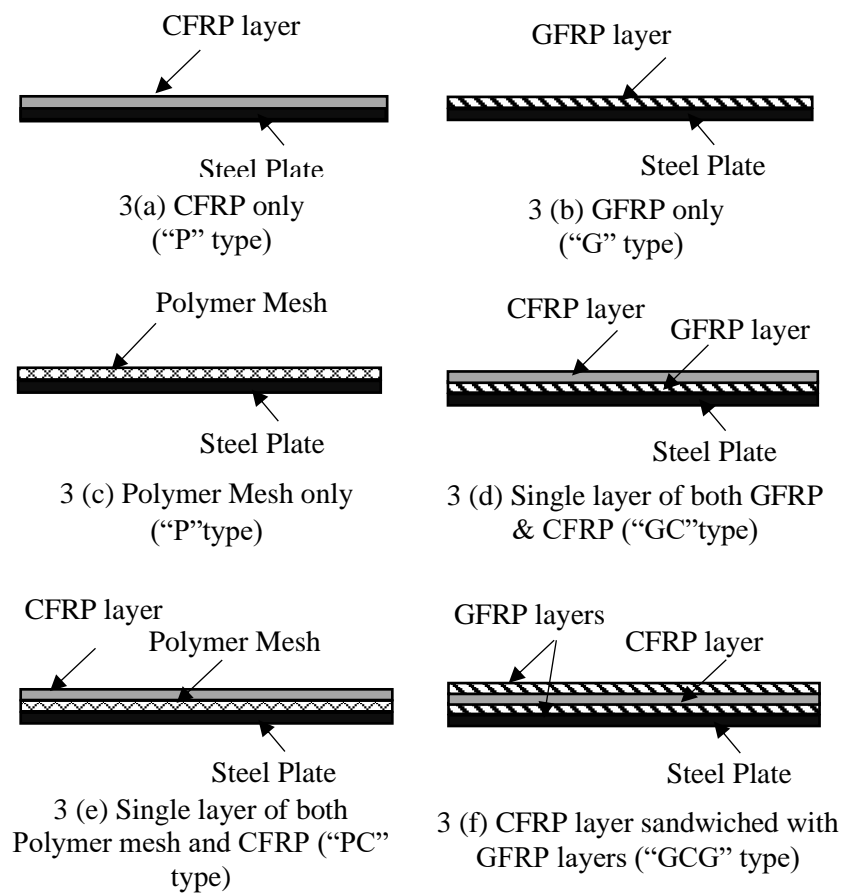


Figure 7.3: Bonding Configurations

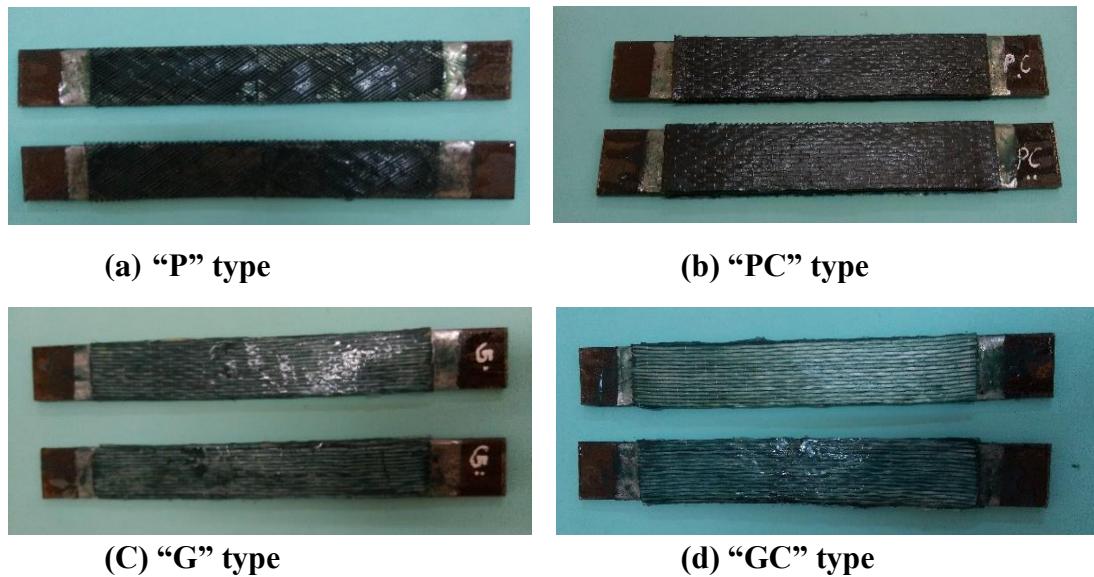


Figure 7.4: Samples prepared with (a) “P” type, (b) “PC” type, (c) “G” type and (d) “GC” type bonding configurations

7.3 Test Results

7.3.1 Ultimate bond strength

Table 7.2 shows the summary of the results obtained for the CFRP/steel joints which were tested in direct tension. The double strap joints made only out of a single layer of CFRP (C – 01 & 02) and GFRP (G – 01 & 02) are showing a similar test result of about 24.75 kN.

The joints bonded with only a polymer mesh (P – 01 & 02) failed at a very low load due to the ruptured polymer sheet at the location of the joint. When the Polymer sheet was used as the interface barrier between the steel and the CFRP sheet (PC 01 & 02), a strength increment of about 24.6% was observed over the joints with only CFRP (C 01 & 02). However, a mixed mode failure was determined as mentioned in Table 7.2 which concludes a complex nature of the failure. CFRP bonded steel plates with a GFRP barrier interface (GC 01 & 02) gained a strength increment of about 83.2% over “C” type joints and somewhat similar percentage of increment was obtained for “GCG” type joints as well. Moreover, negligible strength enhancement of GCG type joints over GC type joints can be attributed to the fact of increased chance of bond failure with the increased FRP thickness (Sbaat et al., 2003), On the other hand, the highest

standard deviation within the similar type of joints was seen in GCG type joints deducing an uncertainty of the failure prediction when the number of strengthened layers is increased.

The main objective of using a polymer mesh in between two substrates was only to incorporate a barrier layer to prevent the direct contact of Carbon fibres with the steel. Therefore, a commercially available polymer mesh of about 1 mm thickness had been used. Yet, using GFRP layers fulfils this requirement with an additional strength gain to the strengthened system. Therefore, it can be further concluded the use of GFRP is preferred, as recommended by several research studies (Tavakkolizadeh & Saadatmanesh, 2001), considering the short term bond performance results obtained from the current research.

Table 7.2: Bond strength results

Bonding Technique	Ultimate Load (kN)	Average Ultimate Load (kN)	Failure Mode
01. C – 01	24.75	25.95	Steel/Adhesive interface debonding and CFRP delamination
02. C – 02	27.15		
03. G – 01	22.05	23.55	Steel/Adhesive interface debonding
04. G – 02	25.05		
05. P – 01	5.75	5.55	Fibre breakage
06. P – 02	5.35		
07. GC – 01	43.85	47.53	Steel/Adhesive interface debonding
08. GC – 02	51.20		
09. PC – 01	34.70	32.33	Mixed modes of Steel/Adhesive interface debonding, FRP rupture, interface delamination between CFRP and Polymer mesh, Cohesive failure between steel and Polymer mesh, CFRP and Polymer mesh
10. PC – 02	29.95		
11. GCG – 01	53.60	47.05	Steel/Adhesive interface debonding
12. GCG – 02	40.50		

7.3.2 Strain variation along the CFRP bonded length

Strain measurements were obtained by the strain gauges attached at the locations of 60 mm away from the joint. Figure 7.5 shows the strain variations of all types of CFRP/Steel joints except for “P” type since the obscuring occurring due to the comparatively lower ultimate strength. An extreme nature of ductile failure was observed for both “P” type specimens at the joint location. Strain variation pattern is similar for both “C” type and “G” type specimens while higher average strain values were prominent for “GC” and “GCG” type of joints. The strain values obtained for “GC” and “GCG” type joints are $2610.89\mu\epsilon$ and $1749.59\mu\epsilon$ respectively. One of the noticeable observations is the increased chances of occurring a sudden brittle failure with the increased FRP layers which is true for all “GCG” type of joints.

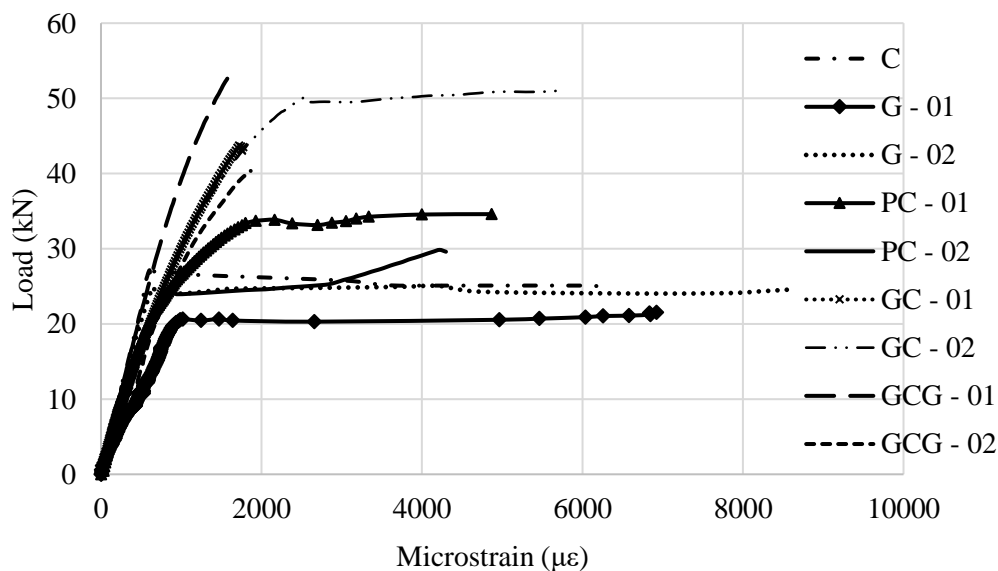


Figure 7.5: Strain variation of double strap joints

7.3.3 The effect of surface roughness parameters

The corroded steel plates used in this test series were having a profile roughness parametric (R_a) value of about 12.10 and it has been increased to 14.48 after the surface preparation was done. Short term bond performance analysis carried out for “C” type bonding configuration for different corrosion levels, in the Chapter 06, showed the highest joint capacity for samples prepared with M – 02 method. Hence, the same

observation can be expected for all type of adopted bonding configurations in this experimental program. Also, increased joint strengths can be anticipated for a greater degree of corrosion level (Corrosion level D) as observed for “C” type bonded joints for the reason of increased surface roughness properties. Yet, these are to be proven by conducting a similar series of testing.

7.3.4 Failure modes

Figure 7.6 illustrates the modes of bond failure observed in the present test series. According to these figures and the results summarized in the table 7.2, “C” and “G” type bonded joints have shown similar failure mode. Both of these joints were failed due to steel/ adhesive interface debonding and hence the maximum capacity of the FRP sheets had not been profited. As the corroded surface was only partially cleaned to remove the rust layers, remained contaminants and the fairly smooth surface may have been the cause for this failure mode. However, as per the adhesive thickness provided of about 0.5 mm, the achieved observation can be likely.

For the “P” type steel/CFRP joints, the braking of fibres was observed at a very low bond strength. However, several modes of failure could be observed when a CFRP layer is occupied along with the polymer sheet with approximately five times increased joint strength.



(a₁)



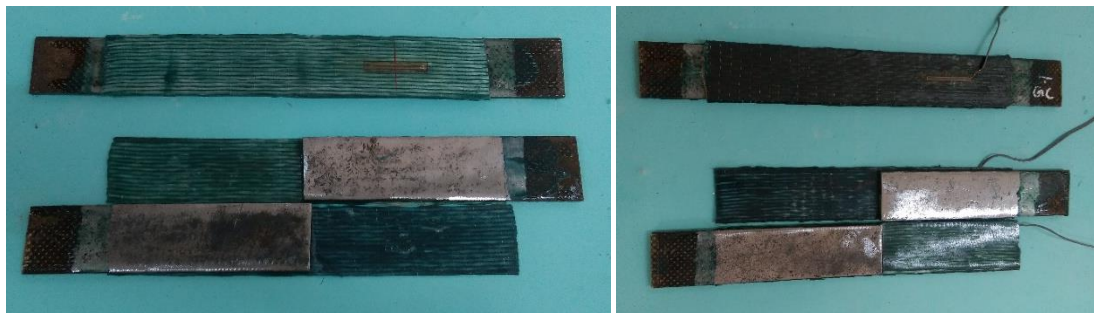
(a₂)



(b)



(c)



(d)

(e)



(f)

Figure 7.6: Failure modes observed for bonding configurations; (a_{1,2}) “P” type, (b) “C” type, (c) “PC” type, (d) “G” type, (e) “GC” type and (f) “GCG” type

The failure mode of the all GC and GCG type joints were limited to steel/ adhesive interface debonding. No delamination between intermediate FRP sheets was seen as some of the observations of past researchers who used more than a single layer of FRP layers (Borrie, Zhao, Raman, & Bai, 2016).

7.4 Summary

Naturally corroded steel plates with the surface characteristic value, $R_a = 12.10$ (Corrosion Level (C)) were used to investigate the short-term bond performance of CFRP strengthened double strap joints. Six different bonding configurations were considered to prevent possible galvanic corrosion effects by providing an intermediate barrier layer.

- ✓ Bonding configurations used are; (a) CFRP only (“C” type), (b) GFRP only, (“G” type) (c) Polymer mesh only (“P” type) (d) GFRP layer embedded in between steel and CFRP (“GC” type) (e) Polymer mesh embedded in between steel and CFRP (“PC” type) and (f) CFRP layer sandwiched in between GFRP layers (“GCG” type).
- ✓ Both “G” type and “C” type joints were seen to be having a similar joint strength and both of these specimens failed due to steel/adhesive interface de-bonding which does not occupy the fullest capacity of the FRP sheets. Strain variation pattern for both of these specimens was also similar within the range of 550 – 775 $\mu\epsilon$.
- ✓ Use of a Polymer mesh in between the two substrates (CFRP and Steel) could enhance the joint capacity for about 25%. However, a vast range of failure modes was observed during the testing.
- ✓ Bond strength attained from the bonding arrangement which sandwiched a CFRP layer in between GFRP layers (GCG Type) showed more or less same as that of “GC” type specimens and it was about 83% of strength enhancement over “C” type joints. “GCG” type of specimens were made with the intention of providing an insulation for the CFRP layer. However, there was no benefit with respect to the joint strength and moreover, it increases the chances of a brittle failure.
- ✓ Higher average strain values were prominent for “GC” and “GCG” type of joints with strain values of 2610.89 $\mu\epsilon$ and 1749.59 $\mu\epsilon$ respectively.
- ✓ Long-term performance analysis should be carried out in order to study the capacity of these intermediate layers to prevent galvanic corrosion in an adverse environmental condition.
- ✓ The current research considered merely a minimum surface preparation level considering such cases where fully cleaned surface preparation could not be achieved. Further studies should be performed using a sizing agent and silane application as recommended by some past research studies.

CHAPTER 08

LONG TERM BOND PERFORMANCE OF CFRP STRENGTHENED CORRODED STEEL PLATES

8.1 Introduction

Steel structures like bridges, offshore platforms and marine infrastructures are often exposed to different environmental conditions during their life span. Some of these environments lead these structures to corrode. The main objective of this research study is to evaluate the efficiency of the CFRP strengthening technique in restoring the strength and stiffness deficiencies of steel structures caused due to corrosion. Hence, the adopted strengthening technique should have excellent weathering/corrosion resistance qualities and be subjected to minimum deterioration in adverse conditions. This is one of the reasons why the CFRP materials are recommended to be used in such conditions for satisfying the required mechanical/physical properties. However, durability characteristics and the bond performance are important aspects to be assessed in the development of this strengthening scheme.

The present research study used non – corroded and corroded steel plates to prepare the double strap joints. Specimens are subjected to six different environmental conditions; (i) sea water, distilled water at (ii) room temperature (25 °C – 30 °C), (iii) 40 °C and (iv) at 3 °C, (v) tropical environmental condition and (vi) dry/wet cyclic condition. Joint strength and the failure modes of the steel/CFRP joints were examined and analysed based on the surface characteristics of the steel substrates.

8.2 Materials

Steel plates were chosen with two different corrosion levels. One set of specimens were non-corroded, and the other half was corroded. Non-corroded steel plates are in corrosion level “A” while the corroded steel plates are in corrosion level “C” where pits and rusted mill scale are visible (Chapter 3, Section 3.4.1). The reason for selecting corroded steel plates with only one degree of deterioration is the non – availability of naturally corroded steel at a enough in other rust levels. The ultimate tensile strength of the non – corroded and the corroded steel plates are 583 MPa and 508 MPa, respectively. Double strap joint

specimens were prepared by adhesively bonding the normal modulus CFRP sheets to the steel surface using the adhesive, Araldite 420 A/B. The material properties of these constituents are well – described in the Chapter 03. Most importantly, a primer layer is coated before the application of adhesive to ensure a better bond between the adhesive and the steel substrate.

8.3 Experimental Programme and test set up

8.3.1 Specimen preparation

The long-term bond strength evaluation was performed by testing seventy – six number of double strap joints. Out of these test specimens, forty-four were made with corroded steel plates and the rest of the specimens, i.e. thirty - two specimens, were prepared with non – corroded steel plates. The chapter 05 which is on the “Experimental programme”, describes the procedure for specimen preparation. Both surface preparation techniques; M – 01 (roughened surface) and M – 02 (smoother surface) defined in Chapter 05, Section 5.2.2 have been adopted in the testing process.

8.3.2 Environmental conditioning

Six different environmental exposures were considered. They are; (i) sea water, distilled water at room temperature (ii) (25 °C – 30 °C), (iii) 40 °C and (iv) at 3 °C. In addition to these, some of the specimens were exposed to (v) the tropical open environmental condition and others were under (vi) dry/wet cyclic condition. Even though two surface preparation techniques were used, the achieved roughness level of the substrate varies due to the difference in exposed corrosion level.

For all exposure conditions other than the tropical environmental condition, distilled water has been used. Water quality properties such as water chemistry and temperature were attained prior to the immersion testing. Table 8.1 tabularises the water quality properties of distilled water used in different exposure condition.

Table 8.1: Water quality properties of distilled water

Exposure condition	pH	Conductivity (mS)	Turbidity (ntu)	Temperature (°C)
Sea water (distilled water + 5% NaCl)	5	92.9	1.02	27.1
distilled water at (25°C – 30°C), 40°C and at 3°C	5	94.7	0.95	26.9
cyclic condition at 5% NaCl solution when subjected to wet condition	5.3	90.7	1.24	25

Sea water condition

The effects of (Test Series 01) sea water (SW) were simulated by adding 5% NaCl by weight to the distilled water as proposed by previous studies (Kabir, Fawzia, Chan, & Badawi, 2016; Nguyen, Bai, Zhao, & Al-Mahaidi, 2012). The samples were immersed in sea water for 6, 12 months at room temperature (Figure 8.1). At the end of each exposure period, the ultimate bond strength was measured at ambient conditions.

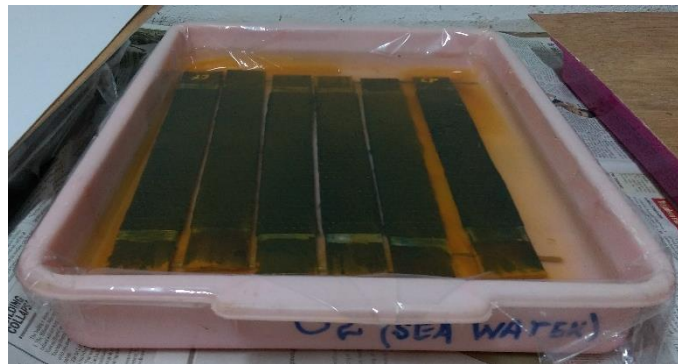


Figure 8.1: Specimens immersed in simulated sea water condition

Distilled water condition at different temperatures

The specimens under test series 02, 03 and 04 were immersed in distilled water, yet at different temperatures; room temperature (average 27°C), 40°C and 3°C. The main purpose of these test conditions was to identify the effect of moisture ingress at different temperatures.

Figure 8.2 shows the samples which were immersed in distilled water and kept at room temperature. In order to sustain an elevated temperature (40°C), the samples were immersed in a hot water bath as shown in Figure 8.3. A cold condition was attained by keeping the samples in a freezer at 3°C (Figure 8.4).



Figure 8.2: Samples immersed in distilled water at room temperature (25°C-30°C)



Figure 8.3: Samples immersed in distilled water at 40°C

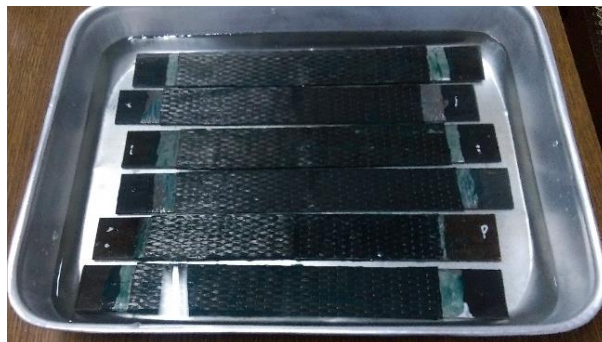


Figure 8.4: Samples immersed in distilled water at 3°C

Tropical environmental condition

The specimens tested under test series 05 were exposed to the local tropical environment (Figure 8.5) so that they were subjected to rainy/monsoon and dry periods time to time; Northeast monsoon season (Dec – Feb), first and second inter monsoon seasons (March - April/ October - November). The exposed temperature range was 21°C to 36°C and the relative humidity (RH) varied from 33% to 100%. High and low weather summary taken from web data are summarized in table 8.2.



Figure 8.5: Samples exposed to tropical environmental condition

Dry/Wet Cyclic condition

The last series was intended to undergo dry/wet cyclic moisture conditions. It simulates an accelerated corrosion behaviour. Specimens were kept in the cycles of 2 months in the indoor environment and 2 months immersed in a 5% NaCl solution (Figure 8.6). The same cycle was repeated twice.

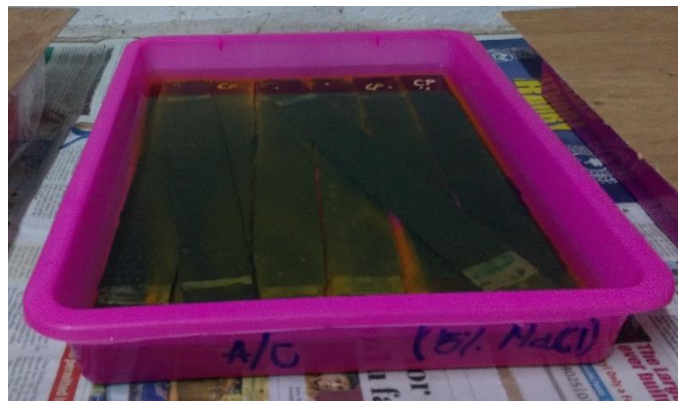


Figure 8.6: Samples subjected to dry/wet condition – in a 5% NaCl solution (Wet condition)

Table 8.2: Weather summary in Colombo (data taken from *timeanddate.com*)

Month	Temperature (°C)			Humidity (%)			Pressure (mbar)		
	High	Low	Ave.	High	Low	Ave.	High	Low	Ave.
01	31	24	27	98	58	83	1013	1002	1009
02	36	23	27	100	42	77	1015	1007	1011
03	32	21	27	95	33	73	1015	1006	1010
04	34	22	27	98	39	74	1016	1007	1011
05	32	24	28	96	55	78	1013	1007	1010
06	32	24	28	97	58	79	1012	1002	1009
07	33	24	28	98	60	84	1012	1004	1008
08	31	25	28	95	59	82	1012	1006	1009
09	31	24	28	94	69	80	1013	1005	1009
10	31	24	28	96	63	81	1013	1007	1010
11	31	24	28	96	61	78	1013	1007	1011
12	32	24	27	97	64	85	1014	1007	1010

8.4 Test results

Table 8.3 shows the test results obtained as the joint failure loads of the test specimens subjected to each exposure condition. Figure 8.7 illustrates these results along with the short-term bond test results obtained for both corrosion levels and surface preparation techniques. Significant outcomes achieved are discussed in following sub sections.

8.4.1 Behaviour in sea water

The specimens submersed in 5% NaCl solution for a duration of 6 months have shown a reduction of almost half of its bond strength. This strength reduction was observed only for M2 type samples which was almost same for both non – corroded (CL (A) – M2; 46%) and corroded (CL (C) – M2; 49%) steel/CFRP composites. The residual strength of M1 type samples showed a higher value of about 90% in both 6 months and 12 months. (Figure 8.7). Thus, a negligible amount of strength reduction was observed between 06 months and 12 months of exposure for CFRP/Steel joints made with corroded steel plates (CL (C)). This observation supports the findings by Nguyen et al [5] who concluded that the remained strength of the CFRP/Steel joints immersed

in sea water is about 86% in 20°C, after 04 months of exposure. They have also witnessed that after 4 months of exposure, the strength reduction rate is only 3%. Yet, the residual strength of M2 type non – corroded samples (CL (A)) increased up to 71% of its initial strength after 12 months of exposure which is a 21% of increment after 6 months of exposure. Likewise, an increased joint strength of about 30% was observed for DW samples as well. The reason might be due to the fact that prolonged exposure to the moisture has led to reduce the stress concentration in the CFRP/Steel joint interface. However, the surface conditions of type M1 seems to be ideal for the surface treated corroded steel plates in marine conditions.

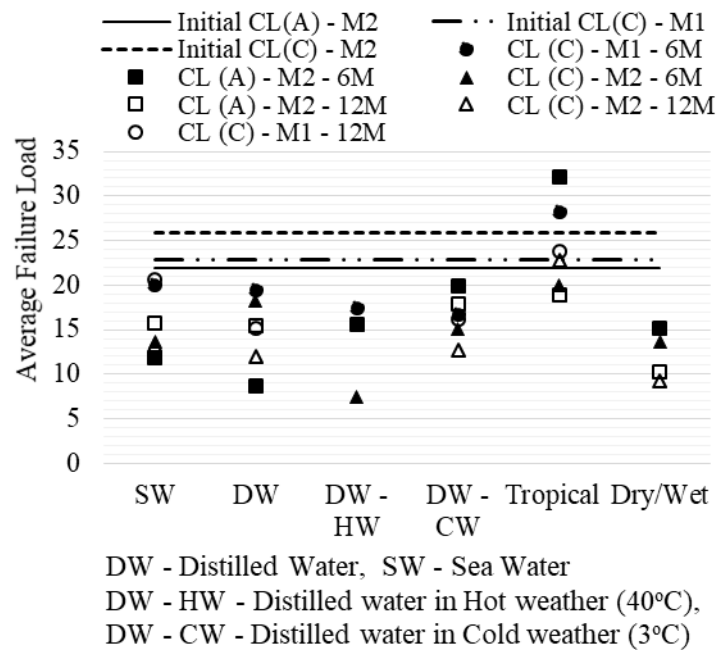


Figure 8.7: Variation of average joint strength with the exposure condition

The steel/adhesive interface debonding was the common failure mode of all the samples. In addition, CL (A) samples showed a rupture in the CFRP material in the joint location while CL (C) samples were witnessed with CFRP delamination. These failure modes were same for both exposure durations. This implies that the non – corroded samples are having an adhesive interface failure while the corroded CFRP/Steel joints are experiencing a cohesive failure. Moreover, discoloration of CFRP bonded joints due to corrosion particles were seen in the CFRP surface as well as in the bonded area. Thus, the moisture has partaken in interface degradation by contributing to degrade both adhesive and the interface. The reason for the CFRP

Table 8.3: Long term test results

Specimen Designation	Test sample no.	Sea water (5% NaCl)		Distilled water (Room Temperature)		Distilled water (Hot condition – 40°C)	Distilled water (Cold condition 3°C)		Tropical condition		Accelerated corrosion condition	
		6M	12M	6M	12M	6M	6M	12M	6M	12M	6M	12M
CL(A)-M1	1	_a	_a	_a	_a	13.4	30.1	11.9	_a	_a	_a	_a
	2	-	-	-	-	13.9	15.9	24.1	-	-	-	-
	3	-	-	-	-	14.1	-	-	-	-	-	-
	4	-	-	-	-	24.0	-	-	-	-	-	-
Average		-	-	-	-	16.3	23.0	18.0	-	-	-	-
Std. Dev		-	-	-	-	5.1	10.0	8.6	-	-	-	-
Co. of Var.		-	-	-	-	31.2	43.5	47.9	-	-	-	-
CL(A)-M2	1	10.9	14.4	10.1	17.5	12.3	26.4	21.2	36.3	18.4	14.5	10.0
	2	12.7	17.0	7.4	13.6	17.0	13.5	14.7	28.1	19.6	15.8	10.4
	3	_b	_b	_b	_b	17.1	_b	_b	_b	_b	_b	_b
	4	-	-	-	-	16.0	-	-	-	-	-	-
Average		11.8	15.7	8.7	15.5	15.6	19.9	18.0	32.2	19.0	15.2	10.2
Std. Dev		1.2	1.9	1.9	2.8	2.2	9.2	4.6	5.8	0.8	0.9	0.2
Co. of Var.		10.5	12.0	22.3	17.8	14.4	46.0	25.6	18.1	4.5	6.1	2.4
CL(C)-M1	1	21.2	18.6	22.1	15.2	18.6	10.9	18.1	26.2	26.5	_a	_a
	2	20.1	22.7	16.9	15.2	18.1	22.7	14.2	30.3	21.2	-	-
	3	_b	_b	_b	_b	18.2	_b	_b	_b	_b	-	-
	4	_b	_b	_b	_b	15.2	_b	_b	_b	_b	-	-
Average		20.6	20.7	19.5	15.2	17.5	16.8	16.1	28.3	23.9	-	-
Std. Dev		0.8	2.9	3.7	0.0	1.6	8.3	2.7	2.9	3.7	-	-
Co. of Var.		3.8	14.0	19.1	0.2	8.9	49.7	16.9	10.3	15.7	-	-
CL(C)-M2	1	16.8	9.2	19.3	16.0	*23.8	12.9	14.8	20.5	28.8	15.4	9.1
	2	10.6	17.5	17.2	8.1	7.1	17.4	10.8	19.5	16.9	12.0	9.37
	3	_b	_b	_b	_b	6.8	_b	_b	_b	_b	_b	_b
	4	_b	_b	_b	_b	8.4	_b	_b	_b	_b	_b	_b
Average		13.7	13.4	18.2	12.0	7.4	15.1	12.8	20.0	22.9	13.7	9.3
Std. Dev		4.4	5.9	1.5	5.6	0.9	3.2	2.8	0.7	8.4	2.4	0.2
Co. of Var.		32.3	44.0	8.3	46.2	11.9	21.3	21.9	3.5	36.8	17.3	1.8
Number of specimens		12		12		16	16		12		8	

“*” the specimens disregarded for the consideration

“a” specimens with this corrosion type were not tested

“b” only two samples were tested

rupture is due to the degraded CFRP material over the marine exposure. Gravimetric studies performed by Nguyen et al (2012) has shown that the strength degradation of

the CFRP material due to saltwater conditions over a one year of time duration is negligible. However, as the result obtained by the current study, Heshmati et al (2017) have concluded that the long-term saltwater immersed condition can be more influential to the inter-laminar strength reduction of the CFRP material.

8.4.2 Behaviour in distilled water under different temperatures

Figure 8.8 shows the normalized joint strength of the corroded and non – corroded steel/CFRP joints. DW type CL (A) – M02 samples showed a higher joint strength reduction (60%) over the SW samples after 6 months. This statement corroborates the fact that the elastic modulus and the tensile strength of the adhesive decrease at a slower rate and to a lesser degree for salt water than for distilled water (Heshmati, Haghani, & Al-Emrani, 2016). Thus, the residual strength of SW samples is 14% higher than that of the DW samples in 6 months (Figure 8.7). Also, this has been the highest strength reduction obtained for the CL (A) – M02 specimens among all other exposure conditions. However, 30% of increment in joint strength has been observed after 12 months as mentioned in the previous sub-section. There are some research studies which observed an increase in the joint strength when exposed to low moisture contents (Bowditch, 1996; Heshmati et al., 2016). Moreover, the joint strength reduction of DW samples after 6 months is in the lower range for the strengthened corroded substrate; 15% for CL (C) M1 samples and 32% for CL (C) M2 samples. The reason may be due to the optimum surface roughness achieved before strengthening using CFRP. The bond between the two materials is strong so that the effect of moisture ingress into the steel/adhesive interface is least. Yet, a similar rate of degradation was observed to be continuing further up to 12 months for CL (C) – M1 samples and the degradation rate had reduced by 10% for the CL (C) – M2 samples. Thus, long term exposure to moisture seems to be one of the critical environmental condition that CFRP strengthening system should be taken necessary durability precautions, especially when there is pre-installed corrosion on the surface.

Non – corroded CFRP/Steel joints immersed at 40°C for 6 months showed a higher joint strength than DW samples and a lower value than the joint strength of samples immersed at 3°C, both by a percentage of 24. The double strap joints subjected to cold

weather indicated a 19% increment in residual joint strength for non – corroded samples prepared with the M1 method. These specimens open to cold weather showed an increased joint strength over DW samples even after 12 months of exposure. According to the data illustrated in Figure 8.9, surface roughness characteristics induced by M1 method seem to be suitable over M2 method for steel which are exposed to cold weather irrespective of its level of corrosion.

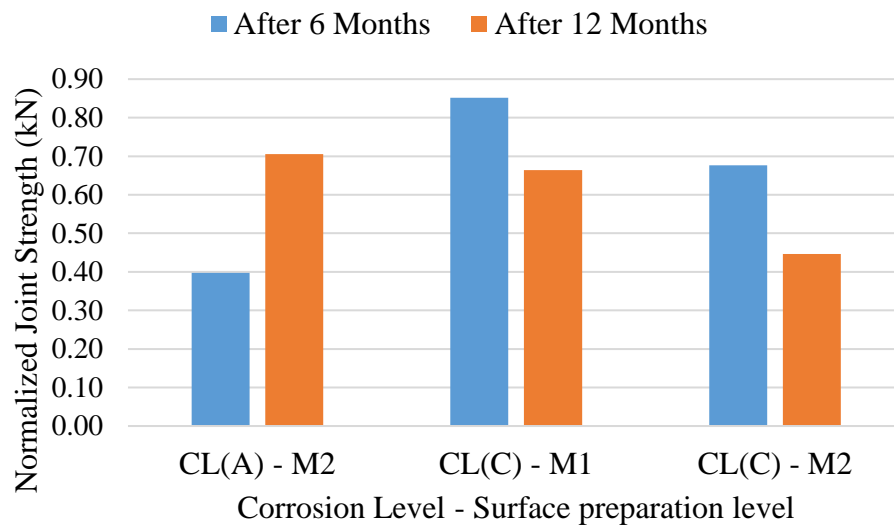


Figure 8.8: Normalized joint strength of DW samples

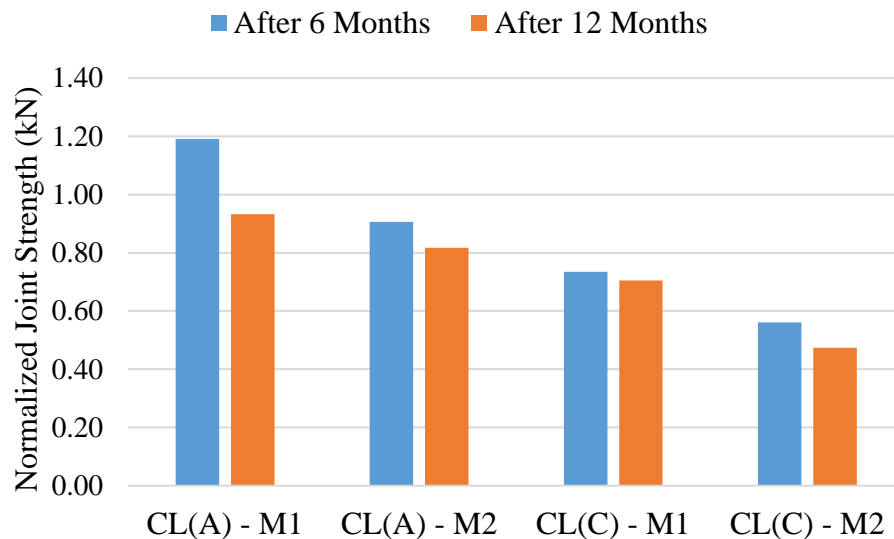
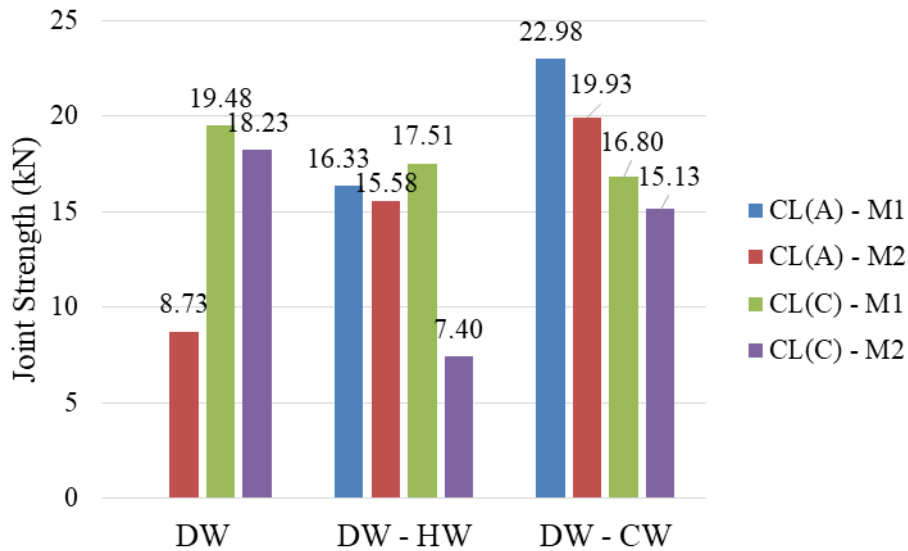


Figure 8.9: Normalized joint strength of DW - CW samples

However, the corroded samples tend to lose their joint strength in a comparatively high amount when exposed to moisture in hot temperatures (24% and 73%) and near sub-

zero temperatures (27% and 44%) at 6 months duration. Apparently, the corroded samples prepared with the M2 method indicated lesser joint strengths over the M1 method in all 3 cases and in all durations (Figure 8.10).



DW - Distilled Water, DW - HW - Distilled water in Hot weather (40°C),
DW - CW - Distilled water in Cold weather (3°C)

Figure 8.10: Joint strength variation of conditioned samples immersed in distilled water after 6 months

The failure modes of the DW samples were similar as the SW samples. In cold weather, irrespective of the level of corrosion of steel, the only failure mode observed after 6 months of exposure was the Steel/adhesive interface debonding. This adhesive interface failure mode transferred to cohesive failure by the 12 months of time. The non - corroded samples exposed to high temperatures in distilled water also failed due to the same nature of failure (steel/adhesive interface debonding), while the corroded samples showed some delamination in the CFRP material (Figure 8.11).

8.4.3 Behaviour in tropical environmental exposure

The CFRP/Steel joints subjected to tropical climatic changes showed the highest residual strength gains for both strengthened corroded and non – corroded steel substrates when compared to all other exposure conditions (Figure 8.7). On average, 47% and 24% of increment in residual strength for CL (A) – M2 and CL (C) – M1 samples, respectively, were achieved at 6 months. Interestingly, 12 months of long

exposure had caused an increment of 11% for corroded Steel/CFRP joints, surface treated with M2 method, which was never the case for any other. In this environmental condition, rainfall exposure duration was a variant, mostly few hours. Temperature variation lied in between 36°C to min 21°C and relative humidity (RH) varied from 100% to 33%. Thus, the thermal variation is insignificant, and variation of RH is somewhat noteworthy. This reflects the behaviour of CFRP strengthened outdoor steel structures in the real tropical environmental exposure. The reason for increased strength gain should be due to the swelling/shrinkage of the adhesive in shorter time periods which allows the bond between steel and adhesive to become stronger by reducing the fracture energy of the surface.

The failure mode also shows a rupture in the CFRP material, implying a lower rate of degradation of the bond between CFRP and steel over the rate of degradation of CFRP sheet. The bonded edges were observed to be slightly corroded.

8.4.4 Behaviour in dry/wet conditions

Corroded samples showed a bond strength reduction of 49% and 31% in non – corroded, CL (A) samples when they were surface prepared with the M2 method. These joint strength reductions were achieved after 6 months of exposure duration and these values were not the highest at that time duration. However, after 12 months of exposure, highest strength reductions for both corroded and non-corroded DLS joints were attained by 54% and 65% respectively. Dawood and Rizkalla (2010) performed residual strength tests for CFRP strengthened steel specimens which were subjected to accelerated exposure consisted with wet/dry cycling, 5% NaCl at 38°C and suspended load of 35% of the ultimate bond strength of non-exposed specimens. The findings exposed that the bond strength degradation was due to the degraded interfacial properties and the addition of silane coupling agent and glass fiber layer in between the adherends can improve the bond durability. Batuwitige et al (Batuwitige, Fawzia, Thambiratnam, & Al-Mahaidi, 2017) used 5% NaCl with a DC power supply to accelerate the environmental condition and observed strength reductions of 24 %, 51% and 66% for 5%, 10% and 15% mass losses, which were similar to the results of the present study. The observed failure mode implies the level of impact of cyclic conditions on the steel/adhesive interface which is greater than the CFRP degradation

effect. Severe corrosion was observed in the bonded area as well as in the surface of the discoloured CFRP/Steel joint.

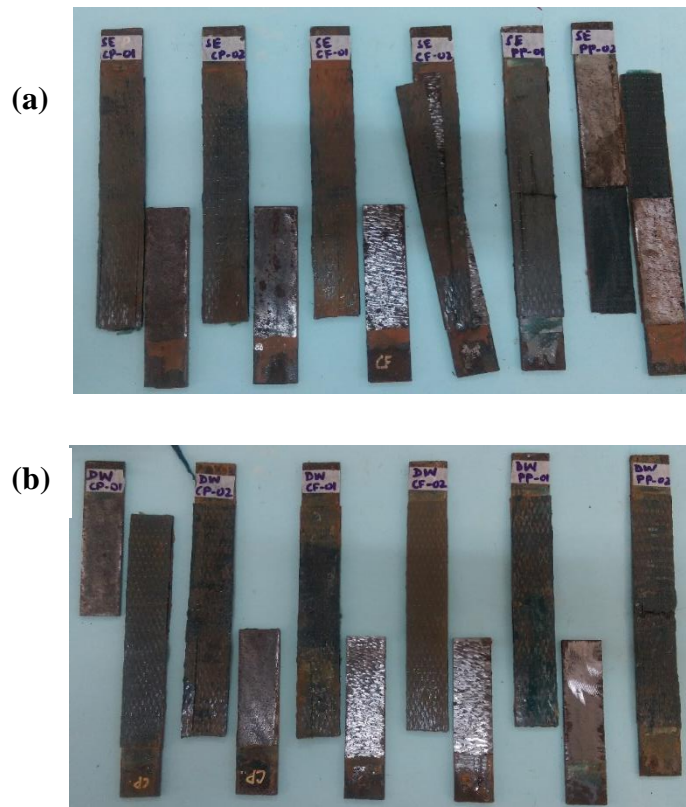
8.4.5 Failure modes

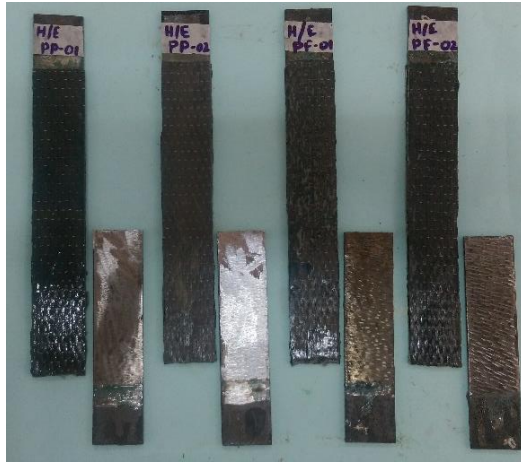
Table 8.4: Failure modes of samples exposed for 6 months duration

Exposure Condition	Exposure Duration	Failure Mode	
		Non – corroded samples CL (A)	Corroded samples CL (C)
SW	6 months	Steel/adhesive interface debonding CFRP rupture	Steel/adhesive interface debonding CFRP delamination
	12 months	Steel/adhesive interface debonding	Steel/adhesive interface debonding CFRP delamination
DW	6 months	Steel/adhesive interface debonding CFRP rupture	Steel/adhesive interface debonding CFRP delamination
	12 months	Steel/adhesive interface debonding	Steel/adhesive interface debonding CFRP rupture
DW - HW	6 months	Steel/adhesive interface debonding	Steel/adhesive interface debonding FRP delamination
DW - CW	6 months	Steel/adhesive interface debonding	Steel/adhesive interface debonding
	12 months	Steel/adhesive interface debonding CFRP delamination	Steel/adhesive interface debonding FRP fiber rupture and delamination
Tropical	6 months	Steel/adhesive interface debonding FRP fiber rupture and delamination	Steel/adhesive interface debonding FRP rupture
	12 months	Steel/adhesive interface debonding	Steel/adhesive interface debonding FRP fiber rupture and delamination
Dry / Wet	6 months	Steel/adhesive interface debonding	Steel/adhesive interface debonding FRP delamination
	12 months	Steel/adhesive interface debonding	Steel/adhesive interface debonding

According to the literature presented by Zhao and Zhang, 2007, failure modes for a normal modulus CFRP sheet are steel/adhesive debonding and FRP delamination. This

conclusion is made consistent with the short-term bond test results. When the CFRP bonded steel joints are exposed to different exposure conditions, the failure mode is noticeably shifting from steel adhesive interface debonding to a combined failure mode. This outcome is attributed to the fact of degradation of CFRP material in adverse environmental conditions with time. Both failure modes, FRP delamination and Fiber rupture, are more brittle than the interface debonding and indicates the maximum joint strength which can be taken by the CFRP/Steel joint. Also, slightly corroded steel edges were observed in the failed specimens which had been exposed to DW – CW, Tropical and Dry/Wet conditions. However, failure mode remained as steel/adhesive debonding in DW – CW samples in which we can assume the degradation of the resin of the CFRP material is lesser than that of the adhesive. Hence for a proper clarification, an investigation should be carried out to identify the rate of CFRP degradation in different conditions. Figure 8.11 (a - j) shows failure modes of all the specimens tested evaluate the long-term bond performance.

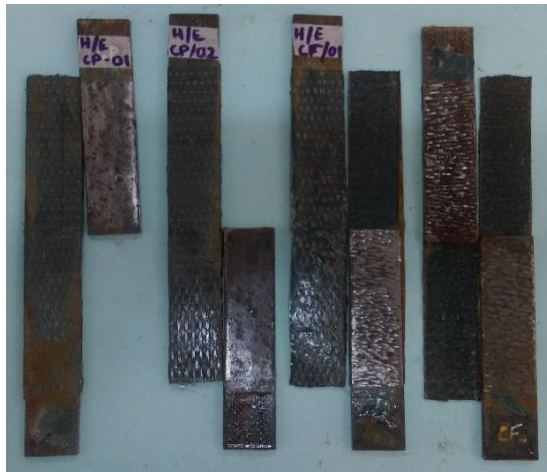




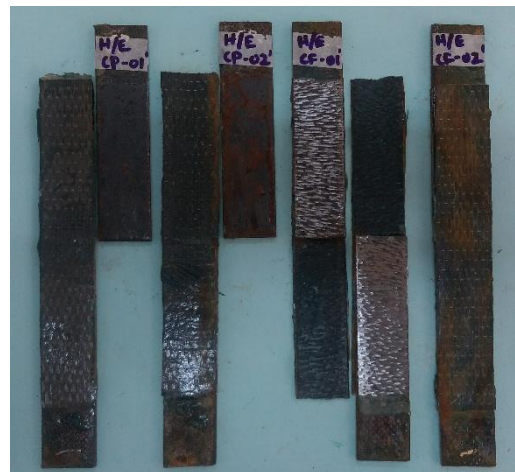
(c)



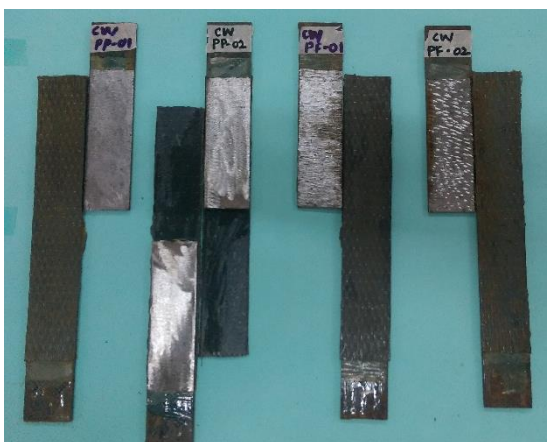
(d)



(e)



(f)



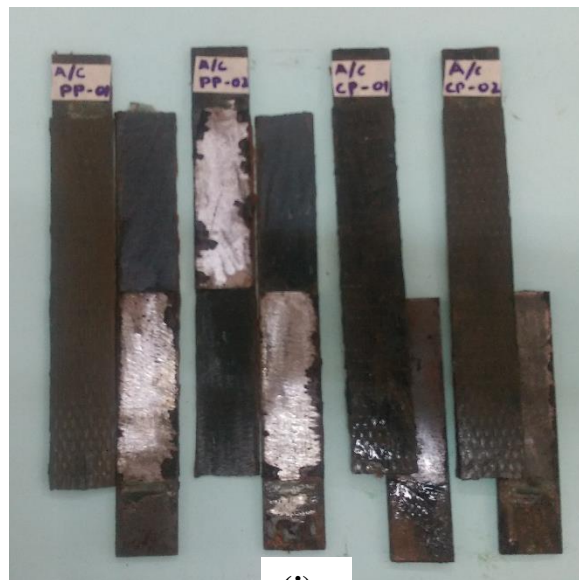
(g)



(h)



(i)



(j)

Figure 8.11 Failed specimens of all exposure conditions after 6 months(a) SW samples, (b) DW samples, (c) & (d) DW – HW non-corroded samples, (e) & (f) DW – HW corroded samples, (g) DW – CW non-corroded samples, (h) DW – CW corroded samples (i) Tropical exposure and (j) dry/wet cyclic conditioned samples

8.4.6 The effect of surface properties of the steel substrate

In the current series of test program, only two levels of corrosion were examined; Corrosion Level (A) and Corrosion Level (C). Surface profile characteristic (R_a) of the former before the surface preparation is 1.65 while the latter is 12.10. These values are

changed based on the method of surface preparation adopted. Non corroded steel plates treated with M – 01 method have a R_a value of 53.50 and it is 3.48 when the M – 02 method is used. For corroded steel plates, the R_a value after adopting M – 01 and M – 02 surface preparation techniques are 26.90 and 14.48, respectively.

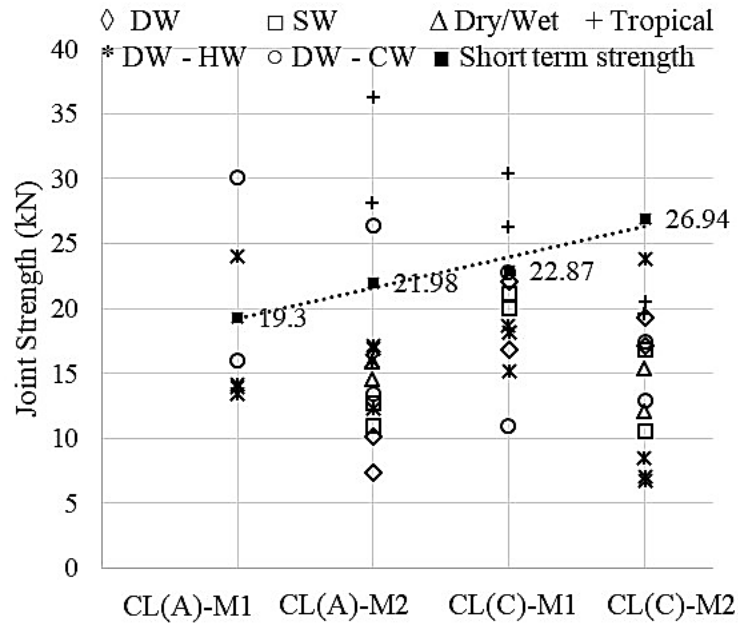


Figure 8.12: Joint strength variation with the quality of substrate (6 months)

According to the short-term bond strength evaluation results, the highest joint strength (26.94 kN) for the CL (C) specimens were achieved when $R_a = 14.48 \mu\text{m}$ while it was (21.98 kN) when $R_a = 3.5 \mu\text{m}$ for non – corroded (CL (A)) steel specimens. Otherwise stated, the CFRP/Steel joint strength was maximum for both corroded and non – corroded steel specimens when the surface preparation was done as to M – 02 technique. However, observations reflected from the long-term joint specimens with 6 months and 12 months exposure duration were noticeably different. When the joint strength variation is plotted against the quality of the steel substrate as shown in Figure 8.12, it shows some interesting details. These outcomes are changed based on the surface roughness as well as the exposure condition.

The long-term bond performance of the CFRP/steel double strap joint specimens were also influenced by the degree of deterioration and the surface preparation method of the steel substrates. Even though the control CL (C) - M2 specimens showed the highest bond strength, the conditioned CL (C) - M2 specimens subjected to all ageing mechanisms showed a significant declination in the ultimate failure load. This can be

mainly attributed to the presence of surface impurities and rust particles available in corroded steel which could not have been completely removed by the M-02 surface preparation technique. These surface rust particles promote further corrosion of the steel substrate and thereby expedite the bond degradation. Most importantly, hot weather conditions accelerate the steel corrosion process causing substantial reductions in bond strength. Accordingly, CL (C) - M2 specimens exposed to HW-06 ageing condition indicated the least ultimate failure load amongst all CFRP/steel specimens. Therefore, special care should be taken in removal of the top corroded layer of the steel elements in existing structures prior to CFRP bonding application.

Apart from the CL (C) - M2 steel specimens, long-term bond strength of CFRP/steel double strap joints subjected to hygrothermal aging conditions mostly did not vary on the type of steel used. Especially, the specimens exposed to hot weather condition (HW-06) indicated almost similar strength reductions of 29%, 29%, and 23% corresponding to the steel types of CL (A) – M1, CL (A) - M2, and CL (C) – M1, respectively. Moreover, CL (A) - M2 - DW-12 and CL (C) – M1-DW-12 specimens showed relatively similar residual bond strengths of about 70%. These results illustrate that in both ambient and hot moist conditions, the rate of CFRP/Steel bond degradation is independent of the pre-deterioration level of steel if an appropriate surface preparation technique had been adopted. However, in cold moist weather conditions (CW-06 and CW-12), the type of surface preparation as well as the degree of the pre-deterioration clearly influenced the bond performance of CFRP/steel joints. Particularly, in non-deteriorated steel specimens, substrates prepared with M1 technique performed better than with M2 method. In fact, NDM1-CW-06 indicated 19% strength increment compared to the control CFRP/steel specimen. The bond performance of CFRP/steel specimens exposed to CW condition can be ranked as CL (A) – M1 > CL (A) - M2 > CL (C) – M1. Reduced bond strength in CFRP/steel joints with corroded steel plates exposed to CW condition could have probably occurred due to the physio-chemical absorption by the rust particles present in steel.

8.5 Comparison to existing guidelines and literature

Table 8.5 compares the durability design factors obtained for conditioned specimens and their surface roughness parameters. These values depict the ratios between the

short-term strength and the strength of a relevant conditioned specimen. Higher values of strength remained factors have been obtained for the specimens with $R_a = 1.67 \mu\text{m}$. It shows the importance of maintaining proper surface characteristics for the long-term behaviour of the CFRP/steel joints. Ariyachandra et al (Ariyachandra, Gamage, Al-Mahaidi, & Kalfat, 2017) also noted the similar behaviour from CFRP/concrete composites.

There are few standards and guidelines which have been published concerning the strengthening of steel structures using FRP materials. The partial safety factors attained from the present study are compared with the factors recommended in those publications. According to the “ICE design and practice guide FRP composites” (Gholami, Sam, Yatim, & Tahir, 2013), the multiplication parameter value is 0.5 when outdoor service conditions are concerned under adverse environmental exposure. The same parameter is observed in the CIRIA design guidelines (Cadei, Stratford, Hollaway, & Duckett, 2004). This value is considered as overly conservative (Kabir, Fawzia, Chan, & Gamage, 2013) other than the situations where required surface characteristics cannot be achieved by surface preparation. In the Italian guidelines (CNR – DT 200 – 202) [26], the reduction factor is 0.85 for both external and aggressive environmental exposure conditions. However, this value matches only with the SW and DW conditions of the present study. When the moisture is present in hot/cold weather conditions, 0.7 is recommended as per the experimental results of the current study. This is the chosen value by Kabir et al (Kabir et al., 2016) as well. According to the results obtained, tropical environmental conditions can be considered as the best suitable exposure condition for the CFRP/Steel joints which showed no reduction in bond performance. However, experiments should be carried out for more than 12 months and those results should be considered in verifying these factors for the long-term bond behaviour of the CFRP/ Steel joints.

Table 8.5: Proposed Environmental durability design factors (based on the strength results obtained after 12 months exposure duration)

Environmental condition	Surface Preparation Method			
	M1 Method		M2 Method	
	Ave. Ult. Load (kN)	Strength reduction factor	Ave. Ult. Load (kN)	Strength reduction factor
SW	20.65	0.90	13.35	0.50
DW	15.18	0.66	12.03	0.45
DW – HW*	17.5	0.77	7.40	0.27
DW - CW	16.13	0.71	12.78	0.47
Tropical	23.85	1.04	22.85	0.85
Dry/Wet	-	-	9.30	0.35

* based on the strength results obtained after 06 months exposure duration

8.6 Summary

Following conclusions were made from the detail investigation which was focused on the short term and long-term performance of corroded and non – corroded steel substrates strengthened with CFRP:

- ✓ CFRP strengthening technology can be used to strengthen any steel structure exposed to any degree of corrosion. The surface preparation technique should be selected based on the nature/rust level of the structure to be strengthened to achieve a uniform surface profile for better bond performance.
- ✓ The composites with heavily corroded and partially treated substrates indicated a low level of strain in the CFRP sheet at 35 mm from the joint, which is less than 25% of strain in other specimens near failure.
- ✓ Saltwater (SW) immersed corroded samples, prepared to have a $R_a - 26.90 \mu\text{m}$ (M1 method), showed 88% of the strength retention after 6 months of conditioning. When the M2 type was used for the surface preparation, both corroded and non-corroded specimens lost half of its bond strength. Non – corroded SW specimens indicated a higher joint strength (14%) over distilled water (DW) immersed specimens.

- ✓ The cold-water conditioned samples (DW – CW) showed a 20% increment in bond strength for non – corroded steel substrates and the highest strength reduction (27%) for corroded steel substrates. However, when the specimens prepared with corroded steel substrates are concerned, both DW – CW and hot water conditioned (DW – HW) specimens displayed a higher degradation of bond strength (23% - 27%) over DW samples.
- ✓ A 24% increment in residual joint strength was observed in the samples with a corroded substrate which were exposed to the tropical environmental condition. However, for this exposure condition, non – corroded samples showed a 50% increment in the residual strength in 6 months.
- ✓ The effects of cyclic (Dry/Wet) condition increase the bond strength degradation of CFRP strengthened corroded steel plates.
- ✓ The study suggests a strength reduction factor of 0.7 for long-term performance with the maintenance of proper substrate properties. If the exposure condition is a tropical environment, the study suggests the value of strength reduction factor as 1.0.

CHAPTER 09

THEORETICAL/NUMERICAL MODELLING

9.1 Introduction

Since conducting experimental studies to evaluate the bond performance is time-consuming and resource-intensive, the development of analytical/numerical models may help designers to identify the bond strength performance and detail the composite to maximize the service performance of composite members. Theoretical models which have been developed for this purpose are summarized in a recent study by da Silva et al. (Lucas, Paulo, Adams, & Spelt, 2009a). These analyses are developed for single and double lap joints and capable of considering the linear and non-linear behaviour of adhesives and adherends in two-dimensional (2D) and Three-dimensional (3D) scenarios (Lucas, Paulo, Adams, & Spelt, 2009a). Among these, the Hart-smith model (1973) is often used and known to predict accurate results in the CFRP/steel joints made of ductile adhesives and elastic adherends (Lucas, Paulo, Adams, Wang, & Spelt, 2009b). Finite Element Analysis (FEA) tools have been also designed based on these analytical tools and used by many researchers in the recent studies.

In this chapter, bond strength results achieved by using Hart-Smith model are presented and compared with the experimental results. A numerical model was also developed using a commercially available FEA modelling software and bond-slip curves were predicted for the exposed samples.

9.2 Theoretical modelling

9.2.1 Short term bond performance - Joint strength degradation

The Hart-Smith model which was published in 1973 and derived for adhesive-bonded joints is still used in the field with necessary modifications. This publication derives numerical solutions required in the designing of composite bonded joints. Previous models only addressed the elastic behaviour of the adhesive material and this model extends its validity by considering the elastic-plastic behaviour of adhesives.

The Hart – Smith model was used to calculate the joint strength degradation. Ultimate joint strength (P_{ult}) of a double lap joint is specified as the lesser of the values of P_i and P_o and defined by the following equations.

$$P_i = \sqrt{\left[2 \tau_f t_a \left(\frac{1}{2} \gamma_e + \gamma_p\right) 2 E_i t_i \left(1 + \frac{E_i t_i}{2 E_o t_o}\right)\right]} \dots\dots\dots \text{where, } 2 E_o t_o > E_i t_i \quad \text{Eqn 01}$$

$$P_o = \sqrt{\left[2 \tau_f t_a \left(\frac{1}{2} \gamma_e + \gamma_p\right) 4 E_o t_o \left(1 + \frac{2 E_o t_o}{E_i t_i}\right)\right]} \dots\dots\dots \text{where, } 2 E_o t_o < E_i t_i \quad \text{Eqn 02}$$

Where,

- E_i and t_i - Elastic modulus and the thickness of inside adherend (Steel)
- E_o and t_o - Elastic modulus and the thickness of outside adherend (CFRP)
- P_i - Ultimate joint strength per unit width for $2 E_o t_o > E_i t_i$
- P_o - Ultimate joint strength per unit width for $2 E_o t_o < E_i t_i$
- τ_f and t_a - The shear strength and the thickness of the adhesive
- γ_e and γ_p - The elastic and the plastic shear strains of the adhesive

Table 9.1: Table of Data

Parameter	Method of data acquisition	Value
$E_o = E_{cfRP}$	Measured	175.6 GPa
$t_o = t_{cfRP}$	Measured / manufacturer provided	0.17 mm
$E_i = E_{steel}$	Measured	CL (A) – 195.25 GPa CL (B) – 159.85 GPa CL (C) – 193.00 GPa CL (D) – 193.90 GPa
$t_i = t_{steel}$	Measured	3.5 mm - 5.5 mm
t_{total}	Measured (total thickness of the double strap joint specimen)	Refer Table 9.2
t_a	$t_a = 0.5 \{t_{total} - 2 t_{cfRP} - t_{steel \text{ plate}}\}$	
τ_f	$\tau_f = 0.8 f_{t,a}$ (ultimate strain of the adhesive, width of the FRP plate) (Xia & Teng, 2005) where, $f_{t,a}$ – tensile strength of the adhesive = 30.13 MPa (Measured)	24.104 MPa

γ_e	$\gamma_e = \tau_f / G_a$ where, G_a – Shear Modulus of the adhesive = 730 MPa (manufacturer provided)	0.033
γ_p	$\gamma_p = 3 \gamma_e$ (Fawzia, 2007)	0.099

Table 9.2: Layer thicknesses in the CFRP / Steel joint

Corrosion Level	Surface preparation method	t_{total} (mm)	t_{steel} (mm)	t_{cfrp} (mm)	t_a
CL (A)	M - 01	5.03	3.86	0.17	0.415
	M - 02	5.02			0.41
CL (B)	M - 01	5.28	3.85	0.17	0.545
	M - 02	5.33			0.57
CL (C)	M - 01	6.35	5.16	0.17	0.425
	M - 02	6.18			0.34
CL (D)	M - 01	5.01	4.47	0.17	0.1
	M - 02	5.04			0.115

❖ $E_o t_o = 175.6 \text{ GPa} * 0.17 * 10^{-3} = 29.85 * 10^6 \text{ N/m}$

❖ $E_i t_i (\text{average}) = 185.5 \text{ GPa} * 4.5 * 10^{-3} = 834.75 * 10^6 \text{ N/m}$

Thus, $2 E_o t_o < E_i t_i$

Therefore, P_o is considered as relevant equation for the present study.

❖ Ultimate joint strength (Failure Load) = joint width * P_o

❖ Joint width = 38 mm

In general, the experimental results and the theoretical model results are in good agreement (Figure 9.1). The reason for the great discrepancy between the experimental and the theoretical model results in the steel samples with the higher corrosion levels is the inability to measure the adhesive occupied in the pits spread across the surface.

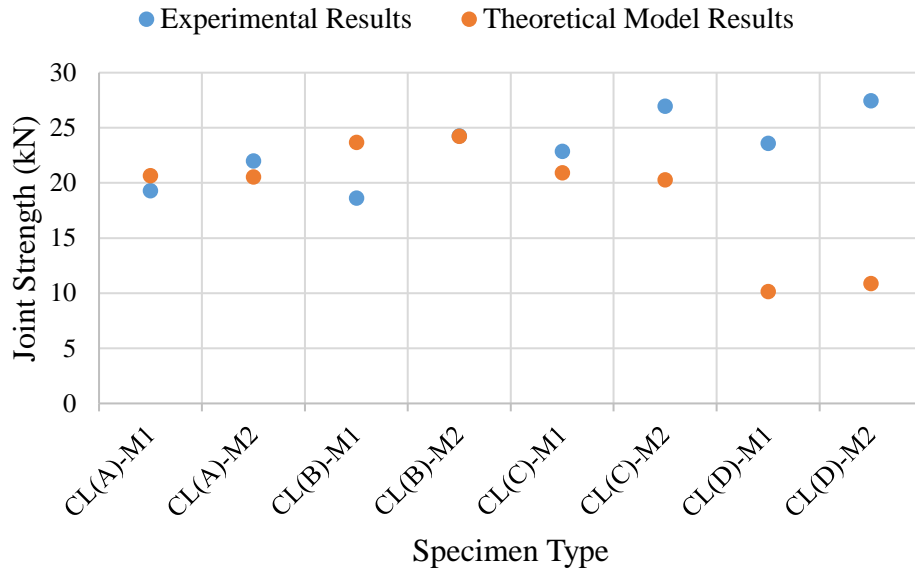


Figure 9.1: Comparison of the experimental and the theoretical model results

9.2.2 Long-term bond performance – sea water and distilled water immersed conditions at ambient temperature

9.2.2.1. Material degradation

The moisture intrusion affects the strength depletion of bonded joints as well as the individual joint components. The adhesive material and the CFRP resin tend to degrade at a higher rate, compared to the Carbon fibres or the steel substrates. Since no signs of fibre rupturing were seen in the failed specimens, a lower rate of CFRP material degradation can be assumed at all exposure conditions in the current study. This assumption had been validated by previous studies for the exposure duration of 360 days (Heshmati, Haghani, & Al-emrani, 2017; Nguyen, Bai, Zhao, & Al-Mahaidi, 2012). Hence, the adhesive strength degradation was considered as the key issue.

Adhesive strength degradation

Figure 9.2 (a) & (b) show the degradation of tensile strength and E-modulus of the adhesive material subjected to prolonged exposure to seawater and distilled water for 12 months. Experimental results obtained by Nguyen et al. (Nguyen et al., 2012) under seawater immersion were considered. Since the results by Nguyen et al. were obtained

for a different temperature level (i.e. 20 °C), a theoretical model was used to calculate the adhesive strength degradation rate (k) at the temperature level considered in the present study (i.e. 28 °C). Assuming two adhesive strength degradation rates at 28 °C and 20 °C; k_1 and k_2 respectively, the following form of the Arrhenius equation was used to find k_1 :

$$k_1 = k_2 * \exp(E_d / R) * (T_2^{-1} - T_1^{-1}) = - 0.0035126 \dots\dots\dots \text{Eqn. 03}$$

where k_2 is -0.0021 per day (Nguyen et al., 2012), E_d is the activation energy or the minimum energy required for moisture diffusion (47.15 kJ/mol K), R is the universal gas constant (8.3143 J/mol K), T_2 is the exposure temperature of the study by Nguyen et al. in Kelvin (293 K) and T_1 is the exposure temperature of the present study in Kelvin (301 K). A similar E_d value had obtained from a past study (Abanilla, Li, & Karbhari, 2006) and it can be experimentally determined using Arrhenius type equation and moisture diffusion data (Abanilla et al., 2006).

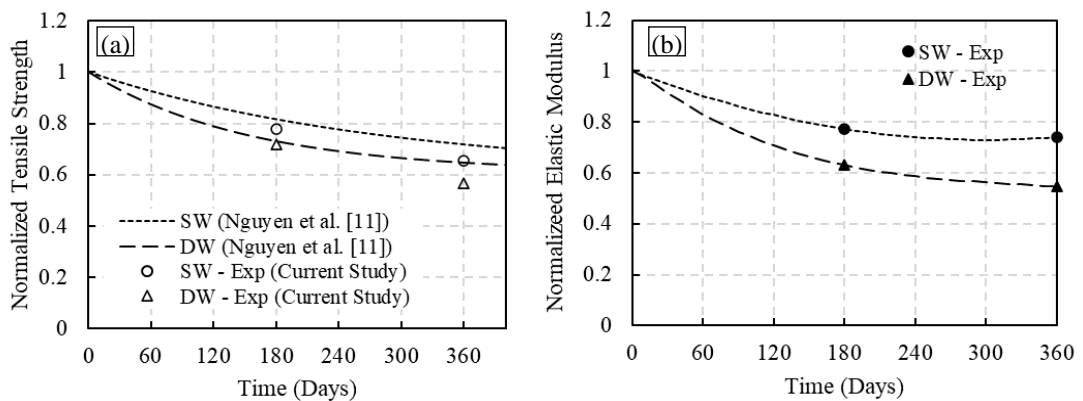


Figure 9.2 Normalized degradation behaviour of mechanical properties of adhesive in sea water and distilled water at ambient temperature (a) Tensile Strength ($f_{t,a}$) (b) Elastic modulus (E_a)

Then, the adhesive strength degradation behaviour over time was obtained using the following Phani and Bose model equation (Phani & Bose, 1987):

$$\sigma_{t,a}(t) = (\sigma_{(0)} - \sigma_{(\infty)}) \exp(k*t) + \sigma_{(\infty)} \dots\dots\dots \text{Eqn. 04}$$

where $\sigma_{t,a}(t)$ is the adhesive tensile strength after the exposure duration (t), $\sigma_{(0)}$ is the adhesive strength at ambient conditions (100%) and $\sigma_{(\infty)}$ is the ultimate asymptotic adhesive strength in moisture (62%) (Nguyen et al., 2012). It is noted that the rate of

degradation of the adhesive mechanical properties is higher in DW condition compared to the SW condition (Heshmati et al., 2017). Even though the adhesive tensile strength degradation is somewhat similar, Elastic moduli have a comparative difference between both conditions. This may be due to the different moisture absorption rates in seawater and distilled water exposures.

9.2.2.2 The time-dependent effective bond length

The maximum joint strength could be achieved only if the minimum bond length is provided in the double lap joint. Hart-Smith (1973) suggested the following equation (Eqn. 05) to predict the minimum lap length which can develop the maximum joint strength.

$$L_{min} = P / (2 * \tau_f(t)) \dots \dots \dots \text{Eqn 05}$$

Where, P is the ultimate failure load per unit width of the joint and $\tau_f(t)$ is the adhesive shear strength. However, on account of long-term exposure conditions and possible imperfections in fabrication Hart-Smith introduced Eqn. 06 to calculate the practical design lap length (L_{eff}) of a double lap joint.

$$L_{eff} = \frac{\sigma_{ult} \cdot t_i}{\tau_f(t)} + \frac{2}{\lambda} \text{ where } \lambda = \sqrt{\frac{G_a(t)}{t_a} \left(\frac{1}{E_o t_o} + \frac{2}{E_i t_i} \right)} \dots \dots \dots \text{Eqn 06}$$

Where, σ_{ult} is the ultimate tensile strength of steel, $G_a(t)$ is the shear modulus of the adhesive, E and t denote the elastic modulus and the thickness of the respective inside (i) and outside (o) adherends and t_a is the adhesive thickness. The adhesive shear strength parameters involved in this equation are the time-dependent variables. The following Eqn.07 & Eqn. 08 (Xia & Teng, 2005) were used to determine these parameters with the available results of $\sigma_{t,a}(t)$ and $E_a(t)$ in Section 3.1.

$$G_a(t) = \frac{E_a(t)}{2(1+\nu)} \dots \dots \dots \text{Eqn 07}$$

$$\tau_f(t) = 0.8 \sigma_{t,a}(t) \dots \dots \dots \text{Eqn 08}$$

Figure 9.3 shows the variation in the required bond length with the exposure duration. The curves for $L_{\text{eff}}(\text{SW})$ and $L_{\text{eff}}(\text{DW})$ denote the theoretical bond lengths obtained from Eqn.06. As per these plots, the minimum effective bond length required at ambient conditions is 136 mm ($L_{\text{eff}}(t=0)$) whereas it was found as 110 mm experimentally ($L_{\text{min,Exp}}(t=0)$). The difference in the values of about 23% must be taking into account the tolerance provided in theory for fabrication considerations in the early age of exposures. The required time-dependent variation of the required bond length in the present study ($L_{\text{min,exp}}$) was then generated observing the trend of the model predicted curve (Figure 9.3).

According to this plot, the bond length requirement increases with the variation of adhesive shear parameters over time as depicted by Eqn. 06. Thus, the lap length of the specimen should be initially designed with the maximum bond length requirement based on the exposure duration. In fact, the experimental determination of effective bond lengths for different exposure durations requires a huge resource allocation. Thus, based on the current study, the following relationships were derived for the

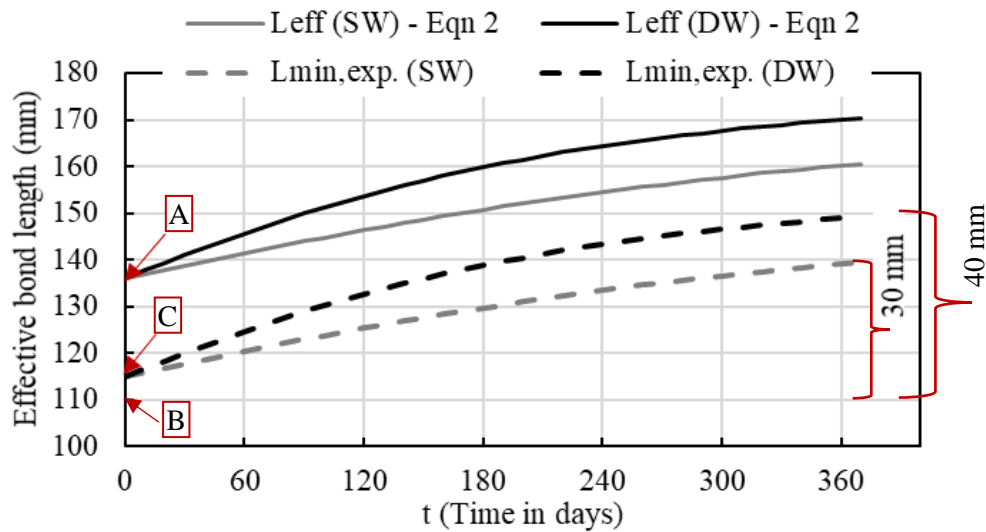


Figure 9.3 Variation of effective bond length over time in DW and SW conditions (Points A, B and C refer to $L_{\text{eff}}(t=0) = 136$ mm, $L_{\text{min,Exp}}(t=0) = 110$ mm and $L_{\text{provided}} = 115$ mm)

practical design bond length required ($L_{\text{eff,d}}$) in double strap joints with CFRP sheets and manually ground steel surfaces when exposed to DW and SW conditions

$$L_{\text{eff,d (SW)}} = L_{\text{min,Exp}} + \Delta L_{\text{dur (SW)}} + \Delta L_{\text{dev}}$$

$$L_{\text{eff,d (DW)}} = L_{\text{min,Exp}} + \Delta L_{\text{dur (DW)}} + \Delta L_{\text{dev}}$$

Where, ΔL_{dur} is the additional bond length required due to the long-term exposure and ΔL_{dev} is taking into account the possible issues in joint fabrication. Since the adhesive mechanical properties are almost in an asymptotic state after the exposure to 12 months of duration, as shown in Figure 9.3, a barrier of 10 mm would be sufficient for the future variation of material properties. Thus, the bond length required due to the long-term exposure more than 360 days (ΔL_{dur}) to both SW and DW conditions was obtained as 40 mm (30 + 10 mm) and 50 mm (40 + 10 mm), respectively (i.e. $\Delta L_{\text{dur (SW)}} = 40$ mm, $\Delta L_{\text{dur (DW)}} = 50$ mm). A minimum of 10 mm allowance can be accommodated for ΔL_{dev} .

9.2.2.3 The joint strength degradation

The experimental results showed the adhesion failure modes as the dominant failure mode which implied the impact of both interface and adhesive degradation. The residual joint strengths in the adhesive failure mode (cohesive) were theoretically estimated using the available variation of material properties of the adhesive throughout the exposure period. The Hart-Smith (1973) model (Hart-Smith, 1973) was used for this purpose. This model had been successfully used in previous studies to predict the residual CFRP/steel joint capacities in both moisture environments and elevated temperatures (Nguyen, Bai, Zhao, & Al-Mahaidi, 2011; Nguyen et al., 2012). Since it was developed considering the non-linearity of the adhesive, the model predicts the ultimate load of the joints which failed due to the depletion of the adhesive rather than the interfacial properties.

The Hart-Smith model equations (Eqns. 01 & 02) were considered to calculate the joint strength per unit width of the double-lap joints with a single layer of CFRP adherend.

The unknown adhesive strain properties over time were calculated using the relationships as in (Hart-Smith, 1973; Nguyen et al., 2012).

$$\gamma_e(t) = \frac{\tau_f(t)}{G_a(t)} \dots\dots\dots \text{Eqn 09}$$

$$\gamma_p(t) = 3 \gamma_e(t) \dots\dots\dots \text{Eqn 10}$$

In the current study, $2E_o t_o < E_i t_i$ and hence the Eqn. 02 was used. The joint failure load P_{fail} was then achieved as recommended in the Hart-Smith model (Eqns. 11 & 12). The width of the joint (b) is 38 mm.

$$\text{If the bond length } (L_{provided}) < L_{eff}(t); P_{fail} = b \cdot P_o(t) \cdot (L_{Provided}/L_{eff}) \dots \text{Eqn 11}$$

$$\text{Otherwise; } P_{fail} = b \cdot P_o(t) \dots\dots\dots \text{Eqn 12}$$

Theoretically predicted bond strength capacities from the above equations were then compared with the experimental results for both SW and DW conditions (Figure 9.4). These plots prove that a greater strength could be expected when the failure was merely due to the adhesive degradation being provided with better interfacial properties and adequate lap lengths. According to Figure 9.4 (b), the theoretical and experimental curves seem to be similar for the provided lap length, $L_{Provided}$. This implies the bond strength of CFRP/steel joints in a seawater condition was mainly dominated by the degradation properties of the adhesive. Thus, the designers should focus more on this matter at the preliminary design stage. However, extra-precaution against the galvanic corrosion might be needed for the durability of the bond.

In DW condition (Figure 9.4(a)), the model predicted bond strength curve when provided with L_{eff} predicts no bond degradation throughout the exposure period. The reason is the decrement in the stress concentrations in the joint induced due to the plasticization effect of the adhesive with the absorption of water. On the contrary to SW immersion, a gap was observed in the curves related to $L_{Provided} < L_{eff}$ (Figure 9.4(b)) which indicates an additional bond strength reduction due to steel-adhesive interface degradation. By analysing these plots, a primitive theoretical relationship between adhesive failure and interface degradation could be derived as follows.

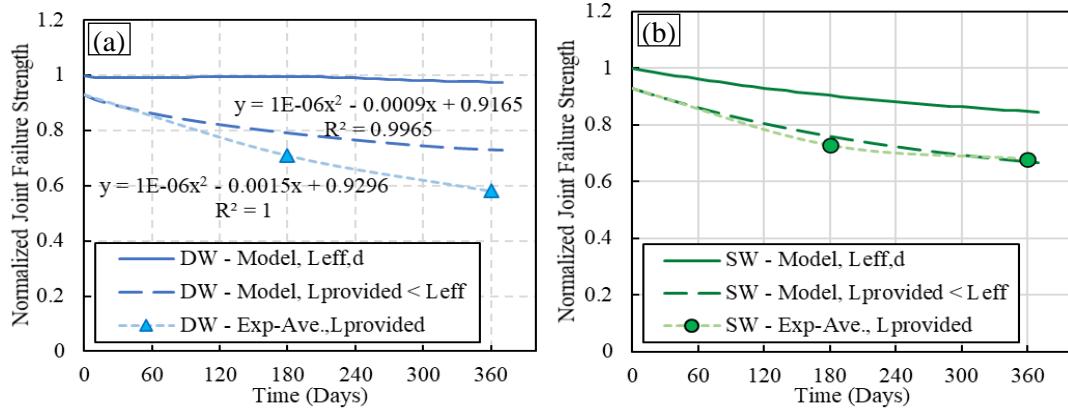


Figure 9.4 Comparison of experimental and model predicted joint strength degradation over time (a) DW condition (b) SW condition

At a time (t) where $0 < t \leq 365$ days and $2E_{ot_0} < E_{it_i}$;

$$F_{ult} = F_{adh} + F_{int}$$

Where, F_{ult} is the ultimate bond capacity, F_{adh} is the bond capacity of the degraded adhesive and F_{int} is the adhesion bond capacity of the degraded interface.

If F_{adh} was expressed as a percentage of F_{ult} ; $F_{adh} = n * F_{ult}$

The factor “ n ” depends on the surface energy on the substrates and its value was determined from the trendlines of the bond strength degradation curves in Figure 9.4(a).

$$n = \frac{1E-06 t^2 - 0.0009.t + 0.9165}{1E-06 t^2 - 0.0015.t + 0.9296} = 0.0012.t + 0.9491$$

$$F_{int} = F_{ult} - F_{adh} = F_{ult} - n * F_{ult} = (1-n) F_{ult} = (0.0509 - 0.0012.t) F_{ult}$$

$$\text{Thus, } F_{int} / F_{adh} = \frac{(0.0509 - 0.0012.t)F_{ult}}{(0.0012.t + 0.9491)F_{ult}} = -0.009.t + 0.0395 \approx -0.009 * t = -0.9\% * t$$

According to the above-mentioned derivation, the effect of long-term joint strength degradation due to interface degradation is approximately 1% of the contribution from the adhesive degradation, at a time (t). In the present study, since the surface roughening was achieved by grinding this relationship may valid only for such manually ground steel surface conditions. Thus, to minimize the interface failure in a DW condition, bonded joints should be provided with an adequate bond length as suggested in Section 9.2.2.2 along with a better surface treatment process.

9.3 Numerical analysis – Hygro-thermal aging condition

A numerical model was also developed to estimate the stress-strain behaviour of CFRP/steel specimens along the bond line using a commercially available Finite Element Modelling software (“ANSYS mechanical user’s guide,” 2013). A 3-D model of one-eighth of the double strap joint was used for the numerical simulation considering the geometrical and the material symmetry. Two types of elements were used. The adhesive layer and the CFRP adherend were modelled using SOLID 186 element type, defined with 20 nodes. The steel adherend was simulated by SOLID 185 element, defined with 8 nodes (“ANSYS mechanical user’s guide,” 2013). The contact between the materials was introduced using node to node connection.

The symmetric boundary conditions were assigned to the faces concerned with symmetry as shown in Figure 9.5(a). The load was applied as a transient displacement of 2 mm/min, as same as in the test program, with 60 steps. Faces (B) and (C) show the sides of which the symmetric boundary conditions have been assigned in Y and Z directions, respectively. These faces were restrained with translational displacements and rotations in all X, Y and Z directions. Mesh sensitivity analysis was also conducted to ensure higher accuracy of the model predicted results. The developed finite element mesh is shown in Figure 9.5(b).

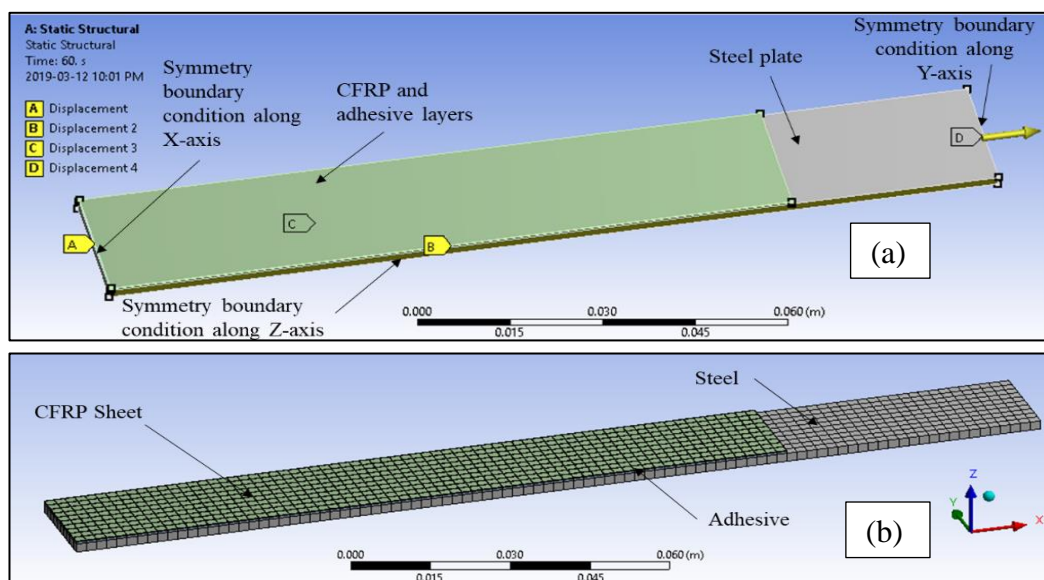


Figure 9.5: (a) Boundary conditions and (b) FE mesh used in the numerical analysis

Degradation behaviour of the materials with respect to time and the exposure condition should be evaluated prior to the numerical simulation of a durability analysis. Amongst, studying the variation in the adhesive behaviour is of utter importance for its vulnerability to the critical environments. This has been obtained by considering the bond behaviour of double strap joints (Figure 9.6). CFRP materials are highly resistant to environmental conditions. Hence, the change in materialistic behaviour of CFRP sheets and steel plates over time were assumed to be negligible.

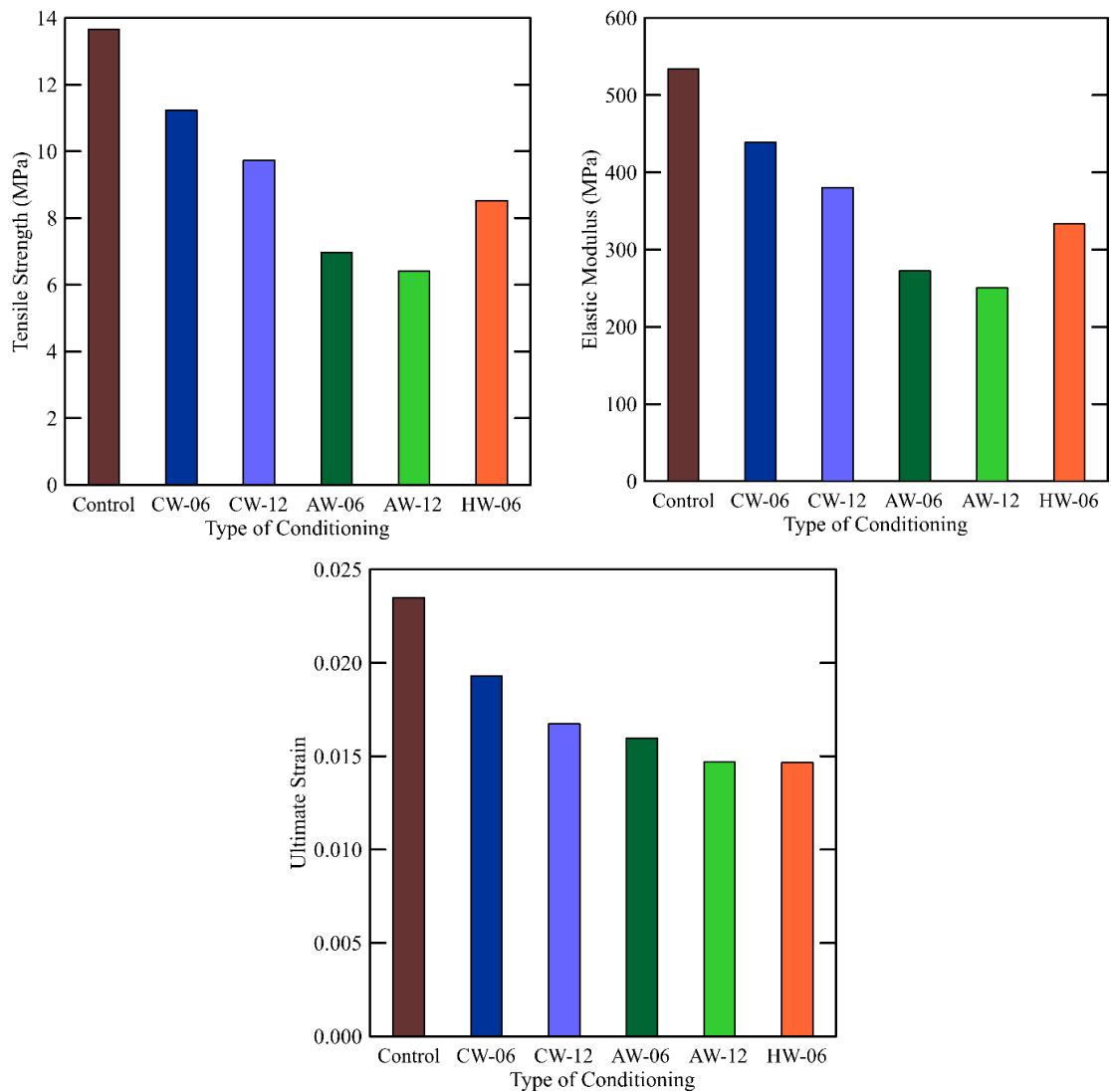


Figure 9.6: The behavioural variation in adhesive properties with respect to the type of conditioning and the exposure duration

9.3.1 Validation of the numerical model

Figure 9.7 compares the numerical and experimental failure loads of the CFRP/steel double strap joint specimens. It can be clearly identified that the numerical results are highly correlated with the experimental results with an average coefficient of correlation of 97.5%. Hence, the developed numerical model can predict the joint strength capacities at an acceptable level with less than 3% average deviation. The stress/strain variations of CFRP/steel specimens along the bond line were evaluated using the numerical model and the results are discussed in the following sections.

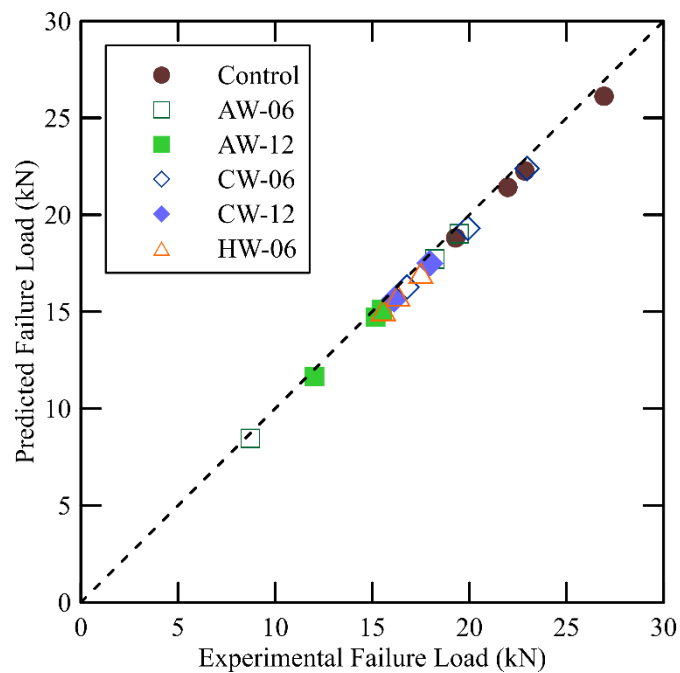


Figure 9.7 Comparison of numerical and experimental failure loads

9.3.2 Bond-slip relationships

The bond-slip relationship is one of the effective methods of bond strength evaluation since the ultimate bond strengths can be predicted for all sizes of CFRP/Steel joints and effective lengths. These models are dependent on the materialistic characteristics of the adhesive (Elastic modulus, Tensile strength, Strain capacity) and the interfacial fracture energy (Xia & Teng, 2005). Several researchers have presented bond-slip curves based on experimental or theoretical data to evaluate the short term bond

performance (Dehghani, Daneshjoo, Aghakouchak, & Khaji, 2012; Fawzia, Zhao, & Al-Mahaidi, 2010).

Yu et al. (Yu, Fernando, Teng, & Zhao, 2012) observed bond-slip curves with triangular and trapezoidal shapes depending on whether the adhesive material is linear or nonlinear, respectively. This was also observed by He and Xian (He & Xian, 2016) and further stated the shape of the bond-slip curve is independent of its failure mode. A bi-linear triangular-shaped bond-slip curve is consisted of an elastic range, softening range and a debonding stage as shown in Figure 9.8. Most of these existing bond-slip curves based on the experimental or theoretical data evaluate the short-term bond performance (Dehghani et al., 2012; Fawzia et al., 2010). However, the influence of hygro-thermal ageing on bond stress-slip behaviour is still unexplained.

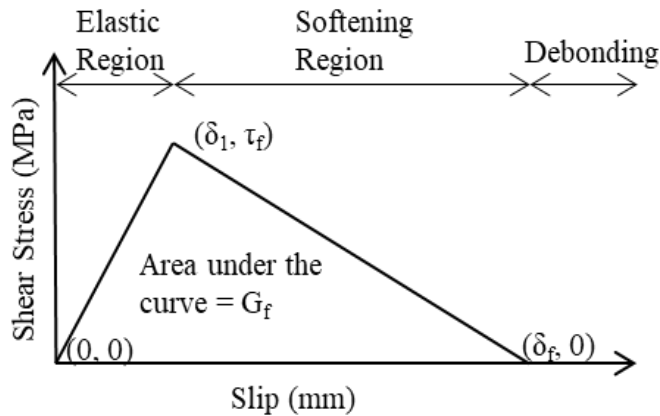


Figure 9.8. Bi-linear bond-slip curve (δ_1 , δ_f and τ_f refers to initial slip, maximum slip, and the maximum bond shear stress respectively)

Finite element analysis is one of the best approaches to develop bond shear stress - slip curves as strain measurements can be directly measured and the local slip can be easily calculated. In the experimental conditions, it is not possible to measure the displacement in the CFRP/adhesive interface as the strain gauges are attached to the external surface of the CFRP materials. Therefore, erroneous calculations and misinterpretations are possible with the increased CFRP material thickness. To get more accurate results the conventional strain gauges must be placed at closer spacings and that is limited depending on the length of the gauge and not cost-effective. Even though modern technologies such as photogrammetry techniques and linear variable

differential transformers (LVDTs) can be used, these are not available due to the limits in affordability. Hence, properly validated FEA models can prevent such drawbacks.

In the present study, bond shear stress vs slip models were developed using the model predicted stress-strain results. The slip was calculated by measuring the relative displacement between the CFRP and steel adherends at 10 mm away from the joint. Bond stress at the same location was calculated and bond-slip curves were obtained. This location was chosen since it is closer to the joint location. The joint location itself is not suitable due to possible stress concentrations and much far away from the joint location, the consistency of the stress-slip relationship will not be continuing. Finally, the effects of hygro-thermal ageing condition on the bond durability were discussed.

In 6 months, all the distilled water immersed samples under ambient conditions showed an average 0.148 mm initial slip, 0.36 mm maximum slip and 11.32 MPa maximum bond shear stress (Fig. 9.9). The respective values of the control (unconditioned) samples were, 0.154 mm, 0.397 mm and 14.90 MPa respectively. Thus, the ambient condition shows an average reduction of 3.8% in the initial slip, 9.3% in maximum slip and 24% in maximum bond stress. The hot water immersed samples showed an average 0.138 mm initial slip, 0.338 mm maximum slip and 10.47 MPa maximum bond shear stress. This shows an average reduction in the respective values by 10.3%, 14.86% and 29.7%. This also shows an average 6.5%, 5.6% and 5.7% reductions of initial slip, maximum slip, and the maximum bond stress at 40 °C condition compared to 28 °C. Thus, the degradation of the bond had further increased in the specimens exposed to a hot environment compared to the ambient conditions. The reason is the increment of the mobility of polymer particles at a temperature closer to the glass transition temperature value of the adhesive which is around 50 °C in the adhesive material used (Chandratilaka, Gamage, & Fawzia, 2019). This permits increased moisture ingress into the polymer structure to crack the Vander-Waal's forces with the cross-linked structure. Hence, the prolonged exposure to hot-humid weather condition resulted in a weaker bond between CFRP and steel. However, results obtained for extended exposure conditions should be considered for more accurate predictions.

The apparent initial slip of the all generated curves lies within 0.135 mm to 0.174 mm. These values were 0.160 mm for control specimens and 0.150 mm for hot and cold weather-controlled specimens. The initial slip varied between 0.135 and 0.174 for distilled water immersed samples in ambient temperature. This may due to the plasticization of the adhesive material with prolonged exposure to moisture. The maximum slip of all the conditioned specimens was in the range between 0.3 mm – 0.4 mm.

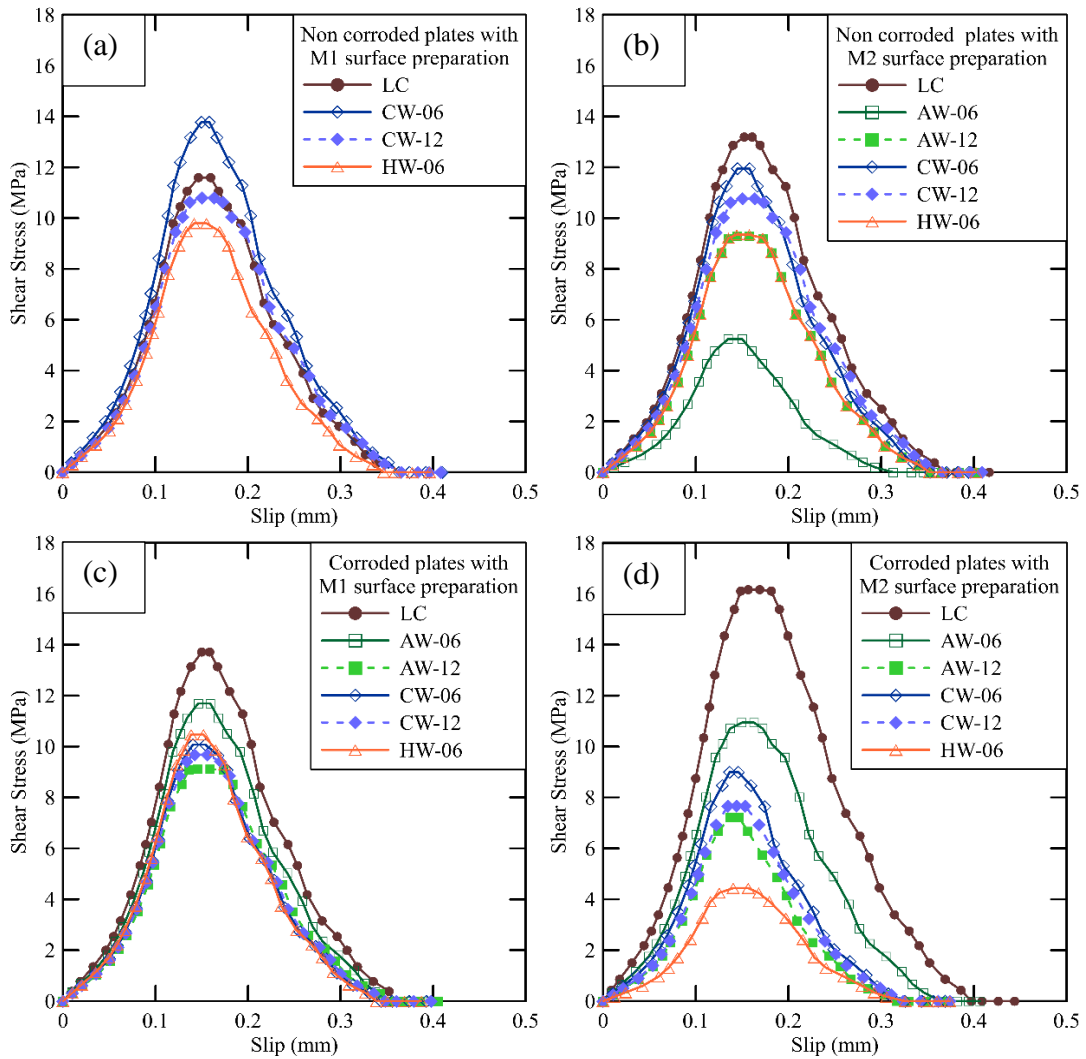


Fig. 9.9 Bond-slip curves of specimens with steel (a) NDM1 (b) NDM2 (c) DM1 (d) DM2

The maximum shear stresses in the bonded joints are significantly affected by the surface roughness characteristics. In the immersed conditions at hot and ambient

temperatures, a higher value of shear stresses was observed in DM1 specimens. In the cold water immersed condition, maximum shear stresses were visible in NDM1 specimens. It has been also noted that the range of maximum shear stresses was greater in NDM2 and DM2 specimens (4 MPa – 16 MPa) over the specimens of NDM1 and DM1. This region is between 9 MPa – 14 MPa for latter specimens. A narrow range of shear stresses in various hygrothermal conditioning situations can be considered as a desirable characteristic in the design of CFRP/Steel composites.

9.3.3 Interfacial fracture energy

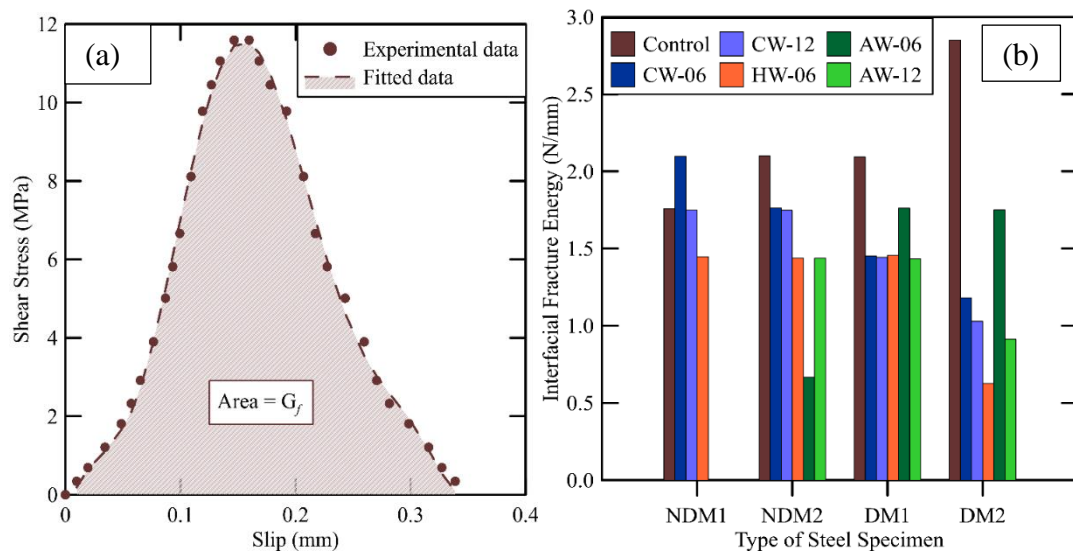


Fig. 9.10. (a) Determination of fracture energy using bond-slip curves (b) Estimated fracture energies of the test specimens

Determination of bonds-slip curves enables to estimate the interfacial fracture energy of CFRP sheet bonded to the steel substrate. In the present study, the interfacial fracture energy was calculated as the area under the best-fit curve (Fig. 9.10 (a)) fitted to the bond-slip data presented in the section 4.3.4. Estimated values of the fracture energy ranged from 0.63 to 2.85 N/mm as depicted in Fig. 9.10 (b). It can be clearly identified that the trend in fracture energy is relatively similar to that of in bond strength of the test specimens. However, CFRP/steel double strap joints with DM1 type steel exposed to CW and HW conditions indicated almost equivalent fracture energy values unlike the corresponding bond strength. Moreover, conditioned test specimens with DM2 steel substrates exhibited much lower reductions in fracture

energies compared to that of in failure loads, indicating a maximum percent reduction of 78% corresponding to HW ageing mechanism. Thus, it can be concluded that the interfacial fracture energy of CFRP/steel composites is more sensitive to the hot humid environments in comparison with other ageing mechanisms used in this study.

9.4 Summary

- ✓ The experimental results and analytical results obtained from Hart-Smith model are in good agreement, specially in the specimens with lower corrosion levels. A slight discrepancy was observed in higher corrosion levels which may be due to the inability to measure the adhesive thickness accurately.
- ✓ Special attention should be given on providing adequate bond length in the specimens exposed to long term environmental conditions since the required bond length increases with the exposure duration and environmental condition. In the current study, required bond lengths at one side of the joint in SW condition and DW condition were found to be 160 mm and 170 mm, respectively.
- ✓ The theoretical analysis results confirmed that the cohesive failure mode could be ensured for both DW and SW moisture conditions if the effective bond lengths were provided along with a proper surface treatment method.
- ✓ Specimens immersed in SW were mostly dependent on the adhesive properties while the DW conditioned specimens affected by both adhesive and adhesion degradation.
- ✓ It is identified that the effect of long-term joint strength degradation due to interface degradation is approximately 1% of the contribution from adhesive degradation, at a time (t) for DW specimens.
- ✓ Initial slip of the bond slip curves varied between 0.135 and 0.174. The range was greater in distilled water immersed specimens due to plasticization effect of the adhesive and it was only about 1.60 for hot and cold water immersed specimens.
- ✓ The least interfacial fracture energies were determined in hot humid environments.

CHAPTER 10

CONCLUSIONS AND RECOMMENDATIONS

10.1 Research Summary

This thesis has addressed the bond performance of the CFRP/steel strengthening system when applied in corroded steel surfaces. Normal Modulus CFRP sheets, steel plates with four different corrosion levels, including non – corroded steel, and two-part epoxy adhesive were used for the experimental study. Two different surface preparation methods were used to study the induced effects on the surface properties of corroded steel. Lab testing was carried out to get a full understanding of the material properties. The effects of the pre-deterioration level of steel, surface preparation, surface roughness characteristics, bonding configurations, short-term and long-term load-carrying capacities, environmental exposure conditions and exposure durations were considered in the analysis. Six different long-term exposure conditions were considered; 01) seawater immersion, 02) accelerated corrosion environment (Dry/Wet condition), 03) tropical environmental condition, distilled water immersion at 04) 3 °C, 05) 40 °C and 06) ambient temperature (25 °C - 30 °C). The failure loads were obtained after 6 months and 12 months of exposure durations. Finally, the research studied the existing theoretical models and bond-slip models were developed.

10.2 Conclusions and recommendations

The research study has enabled to gain a thorough knowledge of the bond behaviour between CFRP and corroded steel elements. In fact, the experimental, analytical, and numerical results proved that CFRP strengthening system can be effectively utilized in corroded steel structures with an understanding of its surface roughness characteristics. The findings of this thesis may provide certain requirements on this subject. Main observations and conclusions are as follows.

1. According to the coupon testing done for the materials, following mechanical properties were obtained. The average modulus of elasticity, average ultimate strength and the average ultimate strain of CFRP fabric were, 175.6 GPa, 1575 MPa and 8980.6 $\mu\epsilon$ respectively. The average tensile strength and its standard deviation of adhesive test

coupons were 30.13 MPa and 16.7 MPa. These measured properties showed some discrepancies with the manufacturer provided material properties and the measured properties were used for the analysis of the test results. The average ultimate tensile strength of steel with corrosion levels A, B, C and D are 583 MPa, 487 MPa, 508 MPa and 513 MPa respectively.

2. Analytical imaging technique was adopted in evaluating quantitative surface roughness properties of corroded and non – corroded steel plates using SEM (Stereoscopic Electron Microscopic) images. According to the surface morphological results, increased profile (R parameters) and aerial (S parameters) roughness parameters were apparent with the increased corrosion levels before subjected to any surface preparation. Thus, this non – destructive surface analysis method can be used effectively to evaluate the surface roughness properties.

3. The surface roughness properties of two different surface preparation methods adopted were evaluated after the surface treatment. The M – 01 method roughened surface in regular manner and the resultant roughness properties increased in the non – corroded steel plates. Yet, the surface roughness decreased with the increased corrosion levels (R_a ; $53.50 \mu\text{m} \rightarrow 45.24 \mu\text{m} \rightarrow 26.90 \mu\text{m} \rightarrow 17.78 \mu\text{m}$) since the inherent pit depths equalized with the new pits induced due to mechanical abrasion and the peaks were cut. The M – 02 method just removed the whole corrosion layer and gave a relatively smoother surface. By this method, surface roughness property of non – corroded steel remained same as before the surface treatment ($3.5 \mu\text{m}$) and for corroded steel R_a value remained in between $14.5 \mu\text{m}$ and $14.8 \mu\text{m}$.

4. The effective bond length of the CFRP/steel double strap joint was determined as 110 mm.

5. Short term bond performance was higher in the CFRP/Steel joints made from highly corroded steel. Increased joint capacities were observed with the increased rust levels and the M-02 prepared CFRP/Steel joints attained higher joint strengths over M-01 prepared specimens. The maximum percentage of bond strength difference between the specimens with these two preparation methods was about 30%.

6. The M-02 prepared specimens with the highest short-term joint strength values showed poor long-term bond performance. The reason was the remaining rust particles

which could not have been removed from the layer removal technique (M-02). Thus, M-01 method showed better bond performance in long-term exposures.

7. CFRP/steel joints prepared with corroded steel and M-01 technique showed greater results in saltwater immersion (SW) and tropical environmental condition.

8. M-01 prepared saltwater (SW) immersed corroded samples (CL (C)), showed about 90% of strength retention after 12 months of conditioning. When the M-02 type was used for the surface preparation, both corroded and non-corroded specimens lost half (50%) of its bond strength. A 24% increment in residual joint strength was observed in the samples with a corroded substrate which were exposed to the tropical environmental condition. Thus, provided with a better surface treatment corroded structures exposed to seawater conditions and tropical environments can be effectively strengthened using CFRP technique.

9. Non – corroded SW specimens indicated a higher joint strength (14%) over distilled water (DW) immersed specimens.

10. After 12 months of exposure duration, both corroded and non-corroded specimens showed a similar bond degradation of about 31% in distilled water immersed specimens at ambient temperature (DW) and about 60% in cyclic condition.

11. The effects of cyclic (Dry/Wet) condition significantly increase the bond strength degradation of CFRP strengthened corroded steel plates and obtained the highest bond degradation in 12 months.

12. The rate of bond degradation was higher in the distilled water immersed specimens at 40 °C when compared to all other exposure conditions irrespective of the pre-corrosion level. In 6 months of exposure duration, the percentage bond strength reduction of these specimens remained to be around 30%.

13. The cold water immersed specimens showed highest residual bond strength capacities in non-corroded specimens. In fact, an increment in the joint strength was observed in cold water immersed, M-01 type specimens made with non-corroded steel (CL-(A)) after 6 months of continuous exposure. However, in the next 6 months, the bond strength reduced by 25%. The cold water immersed specimens showed the highest percentage of residual bond strength of about 82% after 12 months of exposure. The reason was identified as the hardening effect of the adhesive and the FRP matrix.

14. Almost all the long-term exposed specimens failed due to steel/adhesive interface debonding. Slightly corroded edges were visible in DW and HW specimens from 6 months of exposure. This had been aggravated by 12 months of exposure. Hence, providing an intermediate GFRP layer is recommended to lessen this cause since the experimental results showed a significant increment in the joint capacity as well as it satisfies the durability aspects by eliminating the causes for galvanic corrosion.
15. The study suggests a strength reduction factor of 0.7 for long-term performance with the maintenance of proper substrate properties. If the exposure condition is a tropical environment, the study suggests the value of strength reduction factor as 1.0.
16. The composites with heavily corroded and partially treated substrates indicated a low level of strain in the CFRP sheet at 35 mm from the joint, which is less than 25% of strain in other specimens near failure.
17. Special attention should be given on providing adequate bond length in the specimens exposed to long term environmental conditions since the required bond length increases with the exposure duration and environmental condition. In the current study, required bond lengths at one side of the joint in SW condition and DW condition were found to be 160 mm and 170 mm, respectively.
18. It is identified that the effect of long-term joint strength degradation due to interface degradation is approximately 1% of the contribution from adhesive degradation, at a time (t) for DW specimens.
19. The apparent initial slip/maximum slip of the bond shear stress – slip models showed an insignificant effect from the hygrothermal ageing temperature. The initial slip varied between 0.135 mm to 0.174 mm and the maximum slip ranged between 0.3 mm – 0.4 mm, for all specimens. A comparatively narrow range of shear strength variation was observed in NDM1 and DM1 specimens for all exposure conditions.
20. The interfacial fracture energy of CFRP/steel composites is most sensitive to the hot humid environments in comparison with other ageing mechanisms.

10.3 Limitations

- ✓ This research study was conducted using naturally corroded steel plates and therefore the surface roughness was not covering a full range of roughness characteristics. Therefore, accelerated corrosion methods could be adopted so that every range of roughness is accommodated in the study.
- ✓ There was no way of validating the surface roughness parameters obtained from the SEM analysis. If so, the results would have been more reliable.
- ✓ The long-term bond performance was interpreted using the data available for 12 months of period.
- ✓ Materialistic degradation over time with the exposure conditions and stiffness degradation of CFRP strengthened corroded steel joints should also be properly evaluated for a better conclusion of the subject.

10.4 Future research

- ✓ Since only grinding technique was used for surface preparation, other recommended surface preparation techniques such as sand blasting and grit blasting can be used for the surface analysis and bond performance evaluation.
- ✓ The same research study can be continued for a longer duration, more than 12 months, to understand the behaviour of the CFRP/steel joints under different exposure conditions.
- ✓ Different loading conditions such as fatigue loading and impact loading can also be considered for bond strength evaluation.

REFERENCES

- Abanilla, M. A., Li, Y., & Karbhari, V. M. (2006). Durability characterization of wet layup graphite / epoxy composites used in external strengthening, *37*, 200–212. <https://doi.org/10.1016/j.compositesb.2005.05.016>
- Abeygunasekera, S., Gamage, J. C. P. H., & Fawzia, S. (2017). Effects of environmental humidity at installation phase on performance of CFRP strengthen steel I-beam. In *Proceedings of the 8th International Conference on Structural Engineering and Construction Management 2017, ICSECM, Sri Lanka*.
- ACI Committee. (2008). *Guide for the Design and Construction of Externally Bonded FRP Systems*.
- Ahn, J. H., Kainuma, S., Yasuo, F., & Takehiro, I. (2013). Repair method and residual bearing strength evaluation of a locally corroded plate girder at support. *Engineering Failure Analysis*, *33*, 398–418. <https://doi.org/10.1016/j.engfailanal.2013.06.015>
- Al-Mosawe, A., & Al-Mahaidi, R. (2014). Bond characteristics between steel and CFRP laminate under impact loads. In *23rd Australasian Conference on the Mechanics of Structures and Materials 2014* (Vol. I, pp. 489–494).
- Al-Mosawe, A., & Al-Mahaidi, R. (2015). Effect of Impact L Load on the Bond between Steel and CFRP Laminate. *International Journal of Chemical, Molecular, Nuclear, Materials and Metallurgical Engineering*, *9*(1), 84–87.
- Al-Mosawe, A., Al-Mahaidi, R., & Zhao, X.-L. (2016). Experimental and Numerical Study on Strengthening of Steel Members Subjected to Impact Loading Using Ultrahigh Modulus CFRP. *Journal of Composites for Construction*, *20*(6), 04016044. [https://doi.org/10.1061/\(ASCE\)CC.1943-5614.0000703](https://doi.org/10.1061/(ASCE)CC.1943-5614.0000703)
- Al-Mosawe, A., Al-Mahaidi, R., & Zhao, X. (2013). A review of the bond characteristics between steel and cfrp laminate under static and impact loads, *Fourth Asia-Pacific Conference on FRP in Structures (APFIS 2013)* (pp. 11–13).
- Al-Mosawe, A., Al-Mahaidi, R., & Zhao, X. L. (2015). Effect of CFRP properties, on the bond characteristics between steel and CFRP laminate under quasi-static loading. *Construction and Building Materials*, *98*, 489–501. <https://doi.org/10.1016/j.conbuildmat.2015.08.130>
- Al-Shawaf, A., Al-Mahaidi, R., & Zhao, X. (2008). Effect of Elevated Temperature on Bond Behaviour of High Modules CFRP/Steel Double-STRAP Joints. *Australasian Structural Engineering Conference (ASEC)*, *7982*(002), 26–27. <https://doi.org/10.1080/13287982.2009.11465033>
- Al-Zubaidy, H., Al-Mahaidi, R., & Zhao, X. L. (2012). Experimental investigation of bond characteristics between CFRP fabrics and steel plate joints under impact tensile loads. *Composite Structures*, *94*(2), 510–518. <https://doi.org/10.1016/j.compstruct.2011.08.018>
- Al-Zubaidy, H., Zhao, X. L., & Al-Mahaidi, R. (2013). Mechanical characterisation of the dynamic tensile properties of CFRP sheet and adhesive at medium strain rates. *Composite Structures*, *96*, 153–164. <https://doi.org/10.1016/j.compstruct.2012.09.032>
- ANSYS mechanical user's guide. (2013). Retrieved from <https://www.ansys.com>

- Araldite 420 A/B Epoxy Adhesive. (n.d.). Retrieved from <https://www.silmid.com/adhesives/epoxy-adhesives/araldite-420a-b-adhesive-200ml/>
- Ariyachandra, M. R. E. F., Gamage, J. C. P. H., Al-Mahaidi, R., & Kalfat, R. (2017). Effects of surface roughness and bond enhancing techniques on flexural performance of CFRP/concrete composites. *Composite Structures*, *178*, 476–482. <https://doi.org/10.1016/j.compstruct.2017.07.028>
- ASTM. (2003). ASTM D 638 - 02a Standard Test Method for Tensile Properties of Plastics (Vol. 08). West Conshohocken, PA. Retrieved from www.astm.org
- ASTM. (2008). ASTM A 370-08a Standard Test Methods and Definitions for Mechanical Testing of Steel Products. West Conshohocken, PA. Retrieved from www.astm.org
- ASTM D 3039/D 3039M - 00 Standard Test Method for Tensile Properties of Polymer Matrix Composite Materials. (2000) (Vol. 03). West Conshohocken, PA. Retrieved from www.astm.org
- ASTM. (2016). *Standard Test Methods and Definitions for Mechanical Testing of Steel Products 1* (Vol. i). <https://doi.org/10.1520/A0370-15.2>
- Bai, Y., Nguyen, T. C., Zhao, X. L., & Al-Mahaidi, R. (2014). Environment-Assisted Degradation of the Bond between Steel and Carbon-Fiber-Reinforced Polymer. *Journal of Materials in Civil Engineering*, *26*(9), 04014054. [https://doi.org/10.1061/\(ASCE\)MT.1943-5533.0000951](https://doi.org/10.1061/(ASCE)MT.1943-5533.0000951)
- Batuwitage, C., Fawzia, S., Thambiratnam, D., & Al-Mahaidi, R. (2017a). Durability of CFRP strengthened steel plate double-strap joints in accelerated corrosion environments. *Composite Structures*, *160*, 1287–1298. <https://doi.org/10.1016/j.compstruct.2016.10.101>
- Batuwitage, C., Fawzia, S., Thambiratnam, D., & Al-Mahaidi, R. (2017b). Evaluation of bond properties of degraded CFRP-strengthened double strap joints. *Composite Structures*, *173*, 144–155. <https://doi.org/10.1016/j.compstruct.2017.04.015>
- Bocciarelli, M., & Colombi, P. (2013). On the elasto-plastic behavior of continuous steel beams reinforced by bonded CFRP lamina. *Engineering Structures*, *49*, 756–766. <https://doi.org/10.1016/j.engstruct.2012.12.018>
- Bocciarelli, M., Colombi, P., Fava, G., & Poggi, C. (2009a). Fatigue performance of tensile steel members strengthened with CFRP plates. *Composite Structures*, *87*(4), 334–343. <https://doi.org/10.1016/j.compstruct.2008.02.004>
- Bocciarelli, M., Colombi, P., Fava, G., & Poggi, C. (2009b). Prediction of debonding strength of tensile steel / CFRP joints using fracture mechanics and stress based criteria. *Engineering Fracture Mechanics*, *76*(2), 299–313. <https://doi.org/10.1016/j.engfracmech.2008.10.005>
- Borrie, D, Liu, H. B., Zhao, X. L., Raman, R. K. S., & Bai, Y. (2015). Bond durability of fatigued CFRP-steel double-lap joints pre-exposed to marine environment. *Composite Structures*, *131*, 799–809. <https://doi.org/10.1016/j.compstruct.2015.06.021>
- Borrie, D, Zhao, X. L., Raman, R. K. S., & Bai, Y. (2016). Fatigue performance of CFRP patched pre-cracked steel plates after extreme environmental exposure. *Composite Structures*, *153*, 50–59. <https://doi.org/10.1016/j.compstruct.2016.05.092>

- Borrie, Daniel, Raman, R. S., Zhao, X.-L., & Adnan, N. (2014). Quantifying Corrosion between Carbon Fibre Reinforced Polymers (CFRP) and Steel Caused by High Temperature Marine Environments. *Advances in Structural Engineering*, 17(12), 1761–1770. <https://doi.org/10.1260/1369-4332.17.12.1761>
- Bowditch, M. R. (1996). The durability of adhesive joints in the presence of water. *Adhesion and Adhesives*, 16(2), 73–79.
- Buyukozturk, O.; Gunes, O.; Karaca, E. (2004). Progress on understanding debonding problems in reinforced concrete and steel members strengthened using FRP composites. *Construction and Building Materials*, 9–19.
- Cadei, G., Stratford, T., Hollaway, L., & Duckett, W. (2004). *Strengthening metallic structures using externally bonded fiber reinforced polymer*. London, UK.
- Calibur, X.-. (n.d.). X-Wrap C300, High strength carbon fiber fabric for structural strengthening.
- Carpinteri, A; Cornetti, P; Pugno, N. (n.d.). Debonding in FRP strengthened beams: stress assessment versus fracture mechanics approach. In *Dipartimento di Ingegneria Strutturale e Geotecnica, Politecnico di Torino, Turin, Italy*.
- Chandrathilaka, E. R. K., Gamage, J. C. P. H., & Fawzia, S. (2019a). Mechanical characterization of CFRP/steel bond cured and tested at elevated temperature. *Composite Structures*, 207(July 2018), 471–477. <https://doi.org/10.1016/j.compstruct.2018.09.048>
- Chandrathilaka, E. R. K., Gamage, J. C. P. H., & Fawzia, S. (2019b). Numerical modelling of bond shear stress slip behavior of CFRP/steel composites cured and tested at elevated temperature. *Composite Structures*, 212, 1–10. <https://doi.org/10.1016/j.compstruct.2019.01.002>
- Chotickai, P. (2018). Effect of pre-installed corrosion on steel plate-CFRP bond characteristics. *International Journal of Adhesion and Adhesives*, 84(May), 431–437. <https://doi.org/10.1016/j.ijadhadh.2018.05.010>
- Colombi, P, Fava, G., & Sonzogni, L. (2014). Effect of initial damage level and patch configuration on the fatigue behaviour of reinforced steel plates, *Fatigue & Fracture of Engineering Materials & Structures*, 1–11. <https://doi.org/10.1111/ffe.12238>
- Colombi, Pierluigi. (2006). Reinforcement delamination of metallic beams strengthened by FRP strips: Fracture mechanics based approach, *Engineering Fracture Mechanics*, 73, 1980–1995. <https://doi.org/10.1016/j.engfracmech.2006.03.011>
- Colombi, Pierluigi, & Fava, G. (2012). Fatigue behaviour of tensile steel / CFRP joints. *Composite Structures*, 94(8), 2407–2417. <https://doi.org/10.1016/j.compstruct.2012.03.001>
- Colombi, Pierluigi, & Fava, G. (2015). Experimental study on the fatigue behaviour of cracked steel beams repaired with CFRP plates. *Engineering Fracture Mechanics*, 145, 128–142. <https://doi.org/10.1016/j.engfracmech.2015.04.009>
- Colombi, Pierluigi, & Fava, G. (2016). Fatigue crack growth in steel beams strengthened by CFRP strips. *Theoretical and applied fracture mechanic*. <https://doi.org/10.1016/j.tafmec.2016.01.007>

- Colombi, Pierluigi, Fava, G., & Sonzogni, L. (2014). Fatigue behavior of cracked steel beams reinforced by using CFRP materials. *Procedia Engineering*, 74, 388–391. <https://doi.org/10.1016/j.proeng.2014.06.285>
- Colombi, Pierluigi, Fava, G., & Sonzogni, L. (2015). Composites : Part B Fatigue crack growth in CFRP-strengthened steel plates. *Composites Part B*, 72, 87–96. <https://doi.org/10.1016/j.compositesb.2014.11.036>
- Colombi, Pierluigi, & Poggi, C. (2006). An experimental , analytical and numerical study of the static behavior of steel beams reinforced by pultruded CFRP strips, *Composites: Part B*, 37, 64–73. <https://doi.org/10.1016/j.compositesb.2005.03.002>
- da Costa Mattos, H. S., Reis, J. M. L., Paim, L. M., da Silva, M. L. D., Lopes Junior, R., & Perrut, V. A. (2016). Failure analysis of corroded pipelines reinforced with composite repair systems. *Engineering Failure Analysis*, 59, 223–236. <https://doi.org/10.1016/j.engfailanal.2015.10.007>
- Dawood, M. (2014). *Durability of steel components strengthened with fiber-reinforced polymer (FRP) composites. Rehabilitation of Metallic Civil Infrastructure Using Fiber Reinforced Polymer (FRP) Composites: Types Properties and Testing Methods*. Woodhead Publishing Limited. <https://doi.org/10.1533/9780857096654.1.96>
- Dawood, Mina, & Rizkalla, S. (2010). Environmental durability of a CFRP system for strengthening steel structures. *Construction and Building Materials*, 24(9), 1682–1689. <https://doi.org/10.1016/j.conbuildmat.2010.02.023>
- Dehghani, E., Daneshjoo, F., Aghakouchak, A. A., & Khaji, N. (2012). A new bond-slip model for adhesive in CFRP-steel composite systems. *Engineering Structures*, 34, 447–454. <https://doi.org/10.1016/j.engstruct.2011.08.037>
- Deng, J., Jia, Y., & Zheng, H. (2016). Theoretical and experimental study on notched steel beams strengthened with CFRP plate. *Composite Structures*, 136, 450–459. <https://doi.org/10.1016/j.compstruct.2015.10.024>
- Digital Surf. (n.d.). Mountains® SEM software. Retrieved from <https://www.digitalsurf.com/software-solutions/scanning-electron-microscopy/>
- Dodds, N., & Scott, M. (2003). Strengthening a bridge using carbon fibre reinforced plates, (March), 17–19.
- Duncan , B; Crocker, L. (2001). *Review of Tests for Adhesion Strength*. Teddington, Middlesex, UK.
- Elchalakani, M. (2016). Rehabilitation of corroded steel CHS under combined bending and bearing using CFRP. *Journal of Constructional Steel Research*, 125, 26–42. <https://doi.org/10.1016/j.jcsr.2016.06.008>
- Fawzia, S., Zhao, X. L., Al-Mahaidi, R., & Rizkalla, S. (2005). Bond characteristics between cfrp and steel plates in double strap joints. *Advanced Steel Construction*. <https://doi.org/http://dx.doi.org/10.1016/B978-008044637-0/50236-5>
- Fawzia, Sabrina. (2007). *Bond Characteristics between Steel and Carbon Fibre Reinforced Polymer (CFRP) Composites*. Monash University, Victoria, Australia.
- Fawzia, Sabrina, Al-Mahaidi, R., & Zhao, X. L. (2006). Experimental and finite element analysis of a double strap joint between steel plates and normal modulus

CFRP. *Composite Structures*, 75(1–4), 156–162.
<https://doi.org/10.1016/j.compstruct.2006.04.038>

Fawzia, Sabrina, & Kabir, M. H. (2012). A Review on environmental durability of CFRP strengthened system. *Australasian Structural Engineering Conference 2012: The Past, Present and Future of Structural Engineering*, (October 2016), 416.

Fawzia, Sabrina, Zhao, X. L., & Al-Mahaidi, R. (2010). Bond-slip models for double strap joints strengthened by CFRP. *Composite Structures*, 92(9), 2137–2145.
<https://doi.org/10.1016/j.compstruct.2009.09.042>

Fernando, D. (2010). Bond behaviour and debonding failures in cfrp-strengthened steel members. The Hong Kong Polytechnic University, Hung Hom, Kowloon, Hong Kong.

Fernando, D., Teng, J. G., Asce, M., Yu, T., Zhao, X. L., & Asce, F. (2013). Preparation and Characterization of Steel Surfaces for Adhesive Bonding. *Journal of Composites for Construction*, 1–10. [https://doi.org/10.1061/\(ASCE\)CC.1943-5614](https://doi.org/10.1061/(ASCE)CC.1943-5614)

Fernando, D., Yu, T., Teng, J. G., & Zhao, X. L. (2009). CFRP strengthening of rectangular steel tubes subjected to end bearing loads: Effect of adhesive properties and finite element modelling. *Thin-Walled Structures*, 47(10), 1020–1028.
<https://doi.org/10.1016/j.tws.2008.10.008>

Fontana, M. G. (1987). *Corrosion Engineering Mars G. Fontana.Pdf*.

Gamage, J. C. P. H., Al-mahaidi, R., Wong, B., & Ariyachandra, M. R. E. F. (2016). Bond Characteristics of Cfrp-Strengthened Concrete Members Subjected to Cyclic Temperature and Mechanical Stress at Low Humidity. *Composite Structures*.
<https://doi.org/10.1016/j.compstruct.2016.10.131>

Gamage, J. C. P. H., Al-Mahaidi, R., & Wong, M. B. (2006). Bond characteristics of CFRP plated concrete members under elevated temperatures. *Composite Structures*, 75(1–4), 199–205. <https://doi.org/10.1016/j.compstruct.2006.04.068>

Gamage, K., Al-Mahaidi, R., & Wong, B. (2010). Fe modelling of CFRP-concrete interface subjected to cyclic temperature, humidity and mechanical stress. *Composite Structures*, 92(4), 826–834. <https://doi.org/10.1016/j.compstruct.2009.08.036>

Ghafoori, E., Motavalli, M., Botsis, J., Herwig, A., & Galli, M. (2012). Fatigue strengthening of damaged metallic beams using prestressed unbonded and bonded CFRP plates. *International Journal of Fatigue*, 44, 303–315.
<https://doi.org/10.1016/j.ijfatigue.2012.03.006>

Ghafoori, E., Motavalli, M., Nussbaumer, A., Herwig, A., Prinz, G. S., & Fontana, M. (2015a). Design criterion for fatigue strengthening of riveted beams in a 120-year-old railway metallic bridge using pre-stressed CFRP plates. *Composites Part B: Engineering*, 68, 1–13. <https://doi.org/10.1016/j.compositesb.2014.08.026>

Ghafoori, E., Motavalli, M., Nussbaumer, A., Herwig, A., Prinz, G. S., & Fontana, M. (2015b). Determination of minimum CFRP pre-stress levels for fatigue crack prevention in retrofitted metallic beams. *Engineering Structures*, 84, 29–41.
<https://doi.org/10.1016/j.engstruct.2014.11.017>

Ghafoori, E., Schumacher, A., & Motavalli, M. (2012). Fatigue behavior of notched steel beams reinforced with bonded CFRP plates: Determination of prestressing level

for crack arrest. *Engineering Structures*, 45, 270–283. <https://doi.org/10.1016/j.engstruct.2012.06.047>

Ghafoori, Elyas, & Motavalli, M. (2013). Flexural and interfacial behavior of metallic beams strengthened by prestressed bonded plates. *Composite Structures*, 101, 22–34. <https://doi.org/10.1016/j.compstruct.2013.01.021>

Ghafoori, Elyas, & Motavalli, M. (2015). Innovative CFRP-Prestressing System for Strengthening Metallic Structures. *Journal of Composites for Construction*, 19(6), 04015006. [https://doi.org/10.1061/\(ASCE\)CC.1943-5614.0000559](https://doi.org/10.1061/(ASCE)CC.1943-5614.0000559)

Ghafoori, Elyas, Motavalli, M., Zhao, X. L., Nussbaumer, A., & Fontana, M. (2015). Fatigue design criteria for strengthening metallic beams with bonded CFRP plates. *Engineering Structures*, 101, 542–557. <https://doi.org/10.1016/j.engstruct.2015.07.048>

Gholami, M., Sam, A. R. M., Yatim, J. M., & Tahir, M. M. (2013). A review on steel/CFRP strengthening systems focusing environmental performance. *Construction and Building Materials*, 47, 301–310. <https://doi.org/10.1016/j.conbuildmat.2013.04.049>

Gkikas, G., Paipetis, a., Lekatou, a., Barkoula, N. M., Sioulas, D., Canflanca, B., & Florez, S. (2013). Corrosion and environmental degradation of bonded composite repair. *International Journal of Structural Integrity*, 4(1), 67–77. <https://doi.org/10.1108/17579861311303636>

Guidelines for the design and construction of externally bonded FRP systems for strengthening existing structures: Metallic structures - Preliminary Study. (2007). Rome, Italy.

Hart-Smith, L. J. (1973). Adhesive-bonded double lap joints in Technical report NASA CR-112235. Long Beach, California, USA. Retrieved from <https://ntrs.nasa.gov/archive/nasa/casi.ntrs.nasa.gov/19740005082.pdf>

He, J., & Xian, G. (2016). Debonding of CFRP-to-steel joints with CFRP delamination. *Composite Structures*, 153, 12–20. <https://doi.org/10.1016/j.compstruct.2016.05.100>

Heshmati, M., Haghani, R., & Al-Emrani, M. (2015). Environmental durability of adhesively bonded FRP/steel joints in civil engineering applications: State of the art. *Composites Part B: Engineering*, 81, 259–275. <https://doi.org/10.1016/j.compositesb.2015.07.014>

Heshmati, M., Haghani, R., & Al-Emrani, M. (2016). Effects of moisture on the long-term performance of adhesively bonded FRP/steel joints used in bridges. *Composites Part B: Engineering*, 92, 447–462. <https://doi.org/10.1016/j.compositesb.2016.02.021>

Hollaway, L. C., & Cadei, J. (2002). Progress in the technique of upgrading metallic structures with advanced polymer composites, *Progress in Structural Engineering Materials*, 131–148. <https://doi.org/10.1002/pse.112>

HUNTSMAN. (2009). Araldite® 420 A/B Structural Adhesives.

Janssen, M., Zuidema, J., & Wanhill, R. J. H. (2006). *Fracture Mechanics* (2nd Edition).

- Kabir, M. H., Fawzia, S., Chan, T. H. T., & Badawi, M. (2016). Durability of CFRP strengthened steel circular hollow section member exposed to sea water. *Construction and Building Materials*, 118, 216–225. <https://doi.org/10.1016/j.conbuildmat.2016.04.087>
- Kabir, M. H., Fawzia, S., Chan, T. H. T., & Gamage, J. C. P. H. (2016). Comparative durability study of CFRP strengthened tubular steel members under cold weather. *Materials and Structures/Materiaux et Constructions*, 49(5), 1761–1774. <https://doi.org/10.1617/s11527-015-0610-x>
- Kabir, M. H., Fawzia, S., Chan, T. H. T., Gamage, J. C. P. H., & Bai, J. B. (2016). Experimental and numerical investigation of the behaviour of CFRP strengthened CHS beams subjected to bending. *Engineering Structures*, 113, 160–173. <https://doi.org/10.1016/j.engstruct.2016.01.047>
- Kabir, M.H., Fawzia, S., Chan, T. H. T., & Gamage, J. C. P. H. (2013). Effects of cold weather on durability of CFRP strengthened circular hollow steel members. In *Proceedings of the 4th Asia-Pacific Conference on FRP in Structures, APFIS 2013*.
- Kabir, Mohammad Humayun, Fawzia, S., Chan, T. H. T., & Gamage, J. C. P. H. (2014). Durability performance of carbon fibre-reinforced polymer strengthened circular hollow steel members under cold weather. *Australian Journal of Structural Engineering*. <https://doi.org/10.7158/S13-042.2014.15.4>
- Karbhari, V., Chin, J. W., Hunston, D., Benmokrane, B., Juska, T., Morgan, R., ... Reynaud, D. (2003). Durability Gap Analysis for Fiber-Reinforced Polymer Composites in Civil Infrastructure. *Journal of Composites for Construction*, 7(3), 238–247. [https://doi.org/10.1061/\(ASCE\)1090-0268\(2003\)7:3\(238\)](https://doi.org/10.1061/(ASCE)1090-0268(2003)7:3(238))
- Karbhari, V. M., & Shulley, S. B. (2002). Use of Composites for Rehabilitation of Steel Structures—Determination of Bond Durability. *Journal of Materials in Civil Engineering*, 7(4), 239–245. [https://doi.org/10.1061/\(asce\)0899-1561\(1995\)7:4\(239\)](https://doi.org/10.1061/(asce)0899-1561(1995)7:4(239))
- Kayser, J. R., & Nowak, A. S. (1989). Reliability of corroded steel girder bridges. *Structural Safety*, 6(1), 53–63. [https://doi.org/10.1016/0167-4730\(89\)90007-6](https://doi.org/10.1016/0167-4730(89)90007-6)
- Kim, Y. J., Bumadian, I., & Park, J. (2012). Galvanic Current Influencing Interface Deterioration of CFRP Bonded to a Steel Substrate, 1–10. [https://doi.org/10.1061/\(ASCE\)MT](https://doi.org/10.1061/(ASCE)MT)
- Kim, Y. J., Kang, J., Park, J., & Jung, W. (2016). Effect of Corrosion Damage on Service Response of Bridge Girders Strengthened with Posttensioned NSM CFRP Strips, 21(2013), 1–11. [https://doi.org/10.1061/\(ASCE\)BE.1943-5592.0000788](https://doi.org/10.1061/(ASCE)BE.1943-5592.0000788).
- Liu, H. B., & Zhao, X. L. (2010). Effect of fatigue loading on bond strength, *International Journal of Structural Stability and Dynamics*, 10(1), 1-20. <https://doi.org/10.1142/S0219455410003348>
- Liu, H., Xiao, Z., Ā, X. Z., & Al-mahaidi, R. (2009). Thin-Walled Structures Prediction of fatigue life for CFRP-strengthened steel plates. *Thin Walled Structures*, 47(10), 1069–1077. <https://doi.org/10.1016/j.tws.2008.10.011>
- Lucas, F. M., Paulo, J. C., Adams, R. D., & Spelt, J. K. (2009a). International Journal of Adhesion & Adhesives Analytical models of adhesively bonded joints — Part I: Literature survey, 29, 319–330. <https://doi.org/10.1016/j.ijadhadh.2008.06.005>

- Lucas, F. M., Paulo, J. C., Adams, R. D., Wang, A., & Spelt, J. K. (2009b). International Journal of Adhesion & Adhesives Analytical models of adhesively bonded joints — Part II: Comparative study, 29, 331–341. <https://doi.org/10.1016/j.ijadhadh.2008.06.007>
- Luke, S. (2001). The use of Carbon Fibre plates for the strengthening of two metallic bridges of an historic nature in the UK. *FRP Composites in Civil Engineering*, 975–983.
- Mertz, D R, & Gillespie Jr, J. W. (1996). *Rehabilitation of steel bridge girders through the application of advanced composite materials. NCHRP-IDEA Program Project Final Report*. Retrieved from <https://trid.trb.org/view.aspx?id=481482>
- Mertz, Dennis R, Gillespie, J. W., Chajes, M. J., & Sabol, S. A. (2002). The Rehabilitation of Steel Bridge Girders Using Advanced Composite Materials. *IDEA Program: Final Report for NCHRP-IDEA Project 51*, (February), 31.
- Miller, B. T. C., Chajes, M. J., Mertz, D. R., Hastings, J. N., & Member, S. (2001). Strengthening of a Steel Bridge Girder Using CFRP Plates. *Journal of Bridge Engineering*, 6(6), 514–522.
- Moy, S. S. J., & Bloodworth, A. G. (2007). Strengthening a steel bridge with CFRP composites. *Proceedings of the ICE - Structures and Buildings*, 160(2), 81–93. <https://doi.org/10.1680/stbu.2007.160.2.81>
- Nguyen, T. C., Bai, Y., Zhao, X. L., & Al-Mahaidi, R. (2011). Mechanical characterization of steel/CFRP double strap joints at elevated temperatures. *Composite Structures*, 93(6), 1604–1612. <https://doi.org/10.1016/j.compstruct.2011.01.010>
- Nguyen, T. C., Bai, Y., Zhao, X. L., & Al-Mahaidi, R. (2012a). Durability of steel/CFRP double strap joints exposed to sea water, cyclic temperature and humidity. *Composite Structures*, 94(5), 1834–1845. <https://doi.org/10.1016/j.compstruct.2012.01.004>
- Nguyen, T. C., Bai, Y., Zhao, X. L., & Al-Mahaidi, R. (2012b). Effects of ultraviolet radiation and associated elevated temperature on mechanical performance of steel/CFRP double strap joints. *Composite Structures*, 94(12), 3563–3573. <https://doi.org/10.1016/j.compstruct.2012.05.036>
- Perera, U. N. D., & Gamage, J. C. P. H. (2016). Bond Performance of CFRP/Steel Composites: State of the Art Review. In *The 7th International Conference on Sustainable Built Environment (ICSBE)* (pp. 29–38).
- Phan, H. B., Holloway, D. S., & Jiao, H. (2015). An investigation into the effect of roughness conditions and materials on bond strength of CFRP / steel double strap joints. *Australian Journal of Structural Engineering ISSN:*, 16(April), 292–301. <https://doi.org/10.1080/13287982.2015.1092691>
- Phani, K. K., & Bose, N. R. (1987). Temperature Dependence of Hydrothermal Ageing of CSM-Laminate During Water Immersion. *Composites Science and Technology*, 29, 79–87.
- Photiou, N., Holloway, L. C., & Chryssanthopoulos, M. K. (2004). Strengthening Of An Artificially Degraded Steel Beam Utilising A Carbon/Glass Composite System. *Advanced Polymer Composites for Structural Applications in Construction: ACIC*

2004, 20, 274–283. <https://doi.org/10.1016/B978-1-85573-736-5.50030-3>

Rahgozar, R. (2009). Remaining capacity assessment of corrosion damaged beams using minimum curves. *Journal of Constructional Steel Research*, 65(2), 299–307. <https://doi.org/10.1016/j.jcsr.2008.02.004>

Rahgozar, R., & Sharifi, Y. (2011). Remaining Fatigue Life of Corroded Steel Structural Members. *Advances in Structural Engineering*, 14(5), 881–890. <https://doi.org/10.1260/1369-4332.14.5.881>

S. Abeygunasekara, & Amarasinghe, T. I. (2014). Evaluation of Cfrp/Steel Bond Performance Under Tropical Environmental Condition in Sri Lanka. In *SAITM Research Symposium on Engineering Advancements 2014 (SAITM – RSEA 2014)* (Vol. 2014, pp. 39–42).

Sarrado, C; Turon, A; Costa, J; Renart, J. (2015). On the Validity of Linear Elastic Fracture Mechanics Methods to Measure the Fracture Toughness of Adhesive Joints. *International Journal of Solids and Structures*, 1–7.

Sbaat, A., Candidate, D., Scbnercb, D., Candidate, D., Fam, A., & Structures, R. (2003). Retrofit of Steel Structures Using Fiber Reinforced Polymers (FRP): State-of-the-Art, (919).

Schnerch, D; Stanford, K; Sumner, E; Rizkalla, S. (2005). Bond Behavior of CFRP Strengthened Steel Bridges and Structures. In *Proceedings of the International Symposium on Bond Behaviour of FRP in Structures (BBFS 2005)*.

Schnerch, D., Dawood, M., Rizkalla, S., Sumner, E., & Stanford, K. (2005). Bond Behavior of CFRP Strengthened Steel Structures. *Advances in Structural Engineering*. <https://doi.org/10.1260/136943306779369464>

Schnerch, D, Dawood, M., Rizkalla, S., & Sumner, E. (2007). Proposed design guidelines for strengthening of steel bridges with FRP materials, 21, 1001–1010. <https://doi.org/10.1016/j.conbuildmat.2006.03.003>

Schnerch, David, & Rizkalla, S. (2008). Flexural Strengthening of Steel Bridges with High Modulus CFRP Strips. *Journal of Bridge Engineering*, 13(2), 192–201. [https://doi.org/10.1061/\(ASCE\)1084-0702\(2008\)13:2\(192\)](https://doi.org/10.1061/(ASCE)1084-0702(2008)13:2(192))

Shamsuddoha, M., Islam, M. M., Aravinthan, T., Manalo, A., & Lau, K. tak. (2013). Effectiveness of using fibre-reinforced polymer composites for underwater steel pipeline repairs. *Composite Structures*, 100, 40–54. <https://doi.org/10.1016/j.compstruct.2012.12.019>

Stratford, T; Cadei, J; Hollaway, L. (2004). CIRIA C595 - Strengthening Metallic Structures using Externally-Bonded FRP. In *Advanced polymer composites for structural applications in construction: ACIC 2004* (pp. 693–700). Cambridge.

Stratford, T., & Cadei, J. (2006). Elastic analysis of adhesion stresses for the design of a strengthening plate bonded to a beam. *Construction and Building Materials*, 20(1–2), 34–45. <https://doi.org/10.1016/j.conbuildmat.2005.06.041>

Subhani, M., Al-ameri, R., & Al-tamimi, A. (2016). Assessment of bond strength in CFRP retrofitted beams under marine environment. *Composite Structures*, 140, 463–472. <https://doi.org/10.1016/j.compstruct.2016.01.032>

- Tatar, J., & Hamilton, H. R. (2015). Implementation of bond durability in the design of flexural members with externally bonded FRP. *Journal of Composites for Construction*, (June), 04015072. [https://doi.org/10.1061/\(ASCE\)CC](https://doi.org/10.1061/(ASCE)CC)
- Tavakkolizadeh, B. M., & Saadatmanesh, H. (2001). Galvanic corrosion of carbon and steel in aggressive environments. *Journal of Composites for Construction*, (August), 22176, 5(3), 10.1061/(ASCE)1090-0268(2001)5:3(200)
- Teng, J. G., Fernando, D., Yu, T., & Zhao, X. L. (2010). Treatment of Steel Surfaces for Effective Adhesive Bonding. *The 5th International Conference on FRP Composites in Civil Engineering (CICE)*.
- Teng, J. G., Yu, T., & Fernando, D. (2012). Strengthening of steel structures with fiber-reinforced polymer composites. *Journal of Constructional Steel Research*, 78, 131–143. <https://doi.org/10.1016/j.jcsr.2012.06.011>
- Wu, C., Zhao, X., Hui, W., & Al-mahaidi, R. (2012). Thin-Walled Structures Bond characteristics between ultra high modulus CFRP laminates and steel. *Thin Walled Structures*, 51, 147–157. <https://doi.org/10.1016/j.tws.2011.10.010>
- X-Wrap C300 High strength carbon fiber fabric. (n.d.). Retrieved from <https://www.x-calibur.us/files/X-Wrap C300.pdf>
- Xia, S. H., & Teng, J. G. (2005). Behaviour of FRP-to-Steel Bonded Joints. *International Symposium on Bond Behaviour of FRP in Structures (BBFS 2005)*, (BBFS), 411–418.
- Yu, T., Fernando, D., Teng, J. G., & Zhao, X. L. (2012). Experimental study on CFRP-to-steel bonded interfaces. *Composites Part B: Engineering*, 43(5), 2279–2289. <https://doi.org/10.1016/j.compositesb.2012.01.024>
- Zhao, X.-L. (2013). *FRP - Strengthened Metallic Structures*. CRC Press, Taylor and Francis Group.
- Zhao, X. L., & Zhang, L. (2007). State-of-the-art review on FRP strengthened steel structures. *Engineering Structures*, 29(8), 1808–1823. <https://doi.org/10.1016/j.engstruct.2006.10.006>
- Zhou, H., Doroudi, Y., & Fernando, D. (2007). Cyclic bond behaviour of frp-to-steel bonded joints, (October). <https://doi.org/10.14264/uql.2016.408>

APPENDIX A – LIST OF PUBLICATIONS

- Arunothayan Ravendran, J.C.P.H.Gamage and U.N.D.Perera, “Finite Element Analysis of CFRP Strengthened Concrete Beams”, 4th International Symposium on Advances in Civil and Environmental Engineering Practices for Sustainable Development (ACEPS- 2016) at Ruhuna, Sri Lanka
- U.N.D.Perera, J.C.P.H.Gamage, “Bond Performance of CFRP/Steel Composites: State of the Art Review”, 7th International Conference on Sustainable Built Environment (ICSBE2016), Earl Regency Hotel, Kandy, Sri Lanka, 16th – 18th December 2016, pages 29-38.
- U.N.D.Perera, J.C.P.H.Gamage, “Bond Characteristics of Corroded Steel Members Strengthened with Carbon Fibre Reinforced Polymer”, 20th International Conference on Composite Structures, Paris(ICC20), Conservatoire National des Arts et Métiers, 4-7 September 2017
- P.M. Ekanayake, J.C.P.H.Gamage and U.N.D.Perera, “Effects of Span to Bonded Length of CFRP on Flexural Performance of CFRP/Concrete Composites”, 71st RILEM Annual Week & ICACMS 2017, Chennai, India, 3rd – 8th September 2017
- U.N.D.Perera, J.C.P.H.Gamage, “Effects of Bonding Techniques on the Short Term Performance of CFRP Strengthened Corroded Steel Members”, 8th International Conference on Sustainable Built Environment (ICSBE2017), Earl Regency Hotel, Kandy, Sri Lanka
- E.R.K. Chandrathilaka, U.N.D.Perera and J.C.P.H.Gamage, “Bond Slip Models for Corroded Steel – CFRP Double Strap Joints”, 6th International Symposium on Advances in Civil and Environmental Engineering Practices for Sustainable Development (ACEPS-2018),Galle, Sri Lanka.
- Submitted to “Thin-walled Structures” journal (Q1) (Manuscript no. TWST-D-20-00250) Title: Theoretical approach to predict cohesion and interfacial failures of CFRP/steel composites under prolonged exposure to aqueous solutions
- Submitted to “MERCOn 2020” : Manuscript no. 1570633280
Title: Bond-Slip Models of CFRP/Steel Double Strap Joints Subjected to Long Term Exposure of Moisture and Elevated Temperature